I.

MEASUREMENT OF DIAMAGNETIC ANISOTROPY IN SINGLE CRYSTALS.

II.

THE CRYSTAL STRUCTURE OF MONOMETHYLUREA.

Thesis by
Derck Alexander Gordon

In Partial Fulfillment of the Requirements
For the Degree of
Doctor of Philosophy

California Institute of Technology
Pasadena, California

1958

ACKNOWLEDGMENTS.

I wish to express my thanks to Dr. Richard E. Marsh, my research supervisor, for his assistance and advice during my stay at the Institute.

I am indebted to the Allied Chemical and Dye Corporation which granted me a fellowship for the year 1955-6.

ABSTRACT.

I. A method of determining the magnetic anisotropy of single crystals by measuring the torque exerted by a homogeneous magnetic field has been studied. Particular attention was paid to the overcoming of errors in the method of measurement, to the determination of the torsion constants of thin quartz fibers used as torque-measuring devices and to the method of mounting and orienting crystals for use in the investigation. It is believed that the newly devised procedures greatly increase the precision, accuracy and convenience of the measurements.

Measurements of diamagnetic anisotropy in crystals of several simple organic and inorganic compounds and in two protein samples were made and are discussed in terms of crystal and molecular structure.

II. Some time was spent in an effort to determine the crystal structure of monomethylurea using X-ray diffraction data in the literature and a trial structure suggested by the results of diamagnetic anisotropy measurements. A serious error in the published data was discovered, necessitating the rejection of much of the work. The intensities of the hk0, h0ℓ and 0kℓ diffraction maxima were redetermined, and some conclusions about the crystal structure were drawn. Sufficient work has not been done to permit assignment of parameters to the individual atoms.

ERRATA

LOCATION	CHANGE	TO READ
Pg. 5, Eq. 13	$\cdots + \int_{\text{surf.}} (\underset{\sim}{r} \times \underset{\sim}{H})(\underset{\sim}{M} \cdot \underset{\sim}{dS})$	$\cdots + \int_{\text{surf.}} (\underset{\sim}{r} \times \underset{\sim}{\bar{H}})(\underset{\sim}{M} \cdot \underset{\sim}{dS})$
Pg. 28, Table 1	coil compare	coils compared
Pg. 69, Fig. 12, top	--: $\underset{\sim}{C}$ parallel to $\underset{\sim}{H}$	--: $\underset{\sim}{C}^*$ parallel to $\underset{\sim}{H}$
Pg. 69, Fig. 12	Add one more data point exactly on the straight line marked "CCl7", at $H^2 = 407$.	
Pg. 83, bottom	$K_{\parallel}^* - K_{\perp}^* = 2.99 \pm 0.05$	$K_{\parallel}^* - K_{\perp}^* = 2.99 \pm 0.03$
Pg. 83, bottom	$X_{c^*}^* - X_a^* = 1.09 \pm 0.02$	$X_{c^*}^* - X_a^* = 1.09 \pm 0.01$
Pg. 87, middle	$X_c^* - X_b^* = \ldots = 0.43 \pm 0.15$	$X_c^* - X_b^* = \ldots = 0.43 \pm 0.05$
Pg. 87, Table 4, line 1 Pg. 88, line 15	reference 67	reference 49
Pg. 98, Table 9	$\vartheta = 25^\circ$ (observed)	$\psi = 8^\circ$ (observed) ($\vartheta = 26^\circ 42'$)
Pg. 122, Ref. 49	Hencricks	Hendricks
Pg. 142, Prop. 5, line 2	convergen	convergent

TABLE OF CONTENTS.

I. THE MEASUREMENT OF DIAMAGNETIC ANISOTROPY IN SINGLE CRYSTALS.

A. Introduction.

a. Nature of Magnetism.

In this section some properties of magnetic fields and magnetic substances will be outlined briefly in order to present some equations and relations which will be used frequently. For a more thorough discussion of magnetism the reader is referred to texts - for example, to Livens [1], Van Vleck [2], Selwood [3] and Bates [4].

In the absence of electric currents and varying electric fields, a magnetic field in a vacuum is observed to be altered by the introduction of matter. The alteration is attributed to the creation within the matter of magnetic dipoles which in turn are associated with the motion of electrons within the atoms. The contribution to the magnetic field due to a distribution of dipoles is given by:

$$\underset{\sim}{H}_m(x,y,z) = -\int_{\text{vol.}} (\nabla \cdot \underset{\sim}{M})\,\underset{\sim}{R}\,dV + \int_{\text{surf.}} \underset{\sim}{R}(\underset{\sim}{M}\cdot d\underset{\sim}{S}) \qquad (1)$$

($dV = du.dv.dw$ = volume element
$d\underset{\sim}{S}$ = vector area element
$\underset{\sim}{r} = \hat{\underset{\sim}{i}}(x-u) + \hat{\underset{\sim}{j}}(y-v) + \hat{\underset{\sim}{k}}(z-w)$
$\underset{\sim}{M} = \underset{\sim}{M}(u,v,w)$ $\qquad \underset{\sim}{R} = \underset{\sim}{r}/r^3$
$\nabla = \hat{\underset{\sim}{i}}\frac{\partial}{\partial u} + \hat{\underset{\sim}{j}}\frac{\partial}{\partial v} + \hat{\underset{\sim}{k}}\frac{\partial}{\partial w}$)

The vector quantity $\underset{\sim}{M}$ is the "magnetization" or magnetic dipole strength per unit volume and may be regarded as defined by equation 1. This equation may be rewritten in the form of an equivalent differential equation, equation 2, usually written in terms of the "magnetic induction" $\underset{\sim}{B} = \underset{\sim}{H} + 4\pi\underset{\sim}{M}$:

$$\text{Div}\ \underset{\sim}{B} = 0 \qquad (2)$$

Even when combined with the condition on the magnetic field given in equation 3 and the condition that at any surface of discontinuity the

$$\text{Curl}\ \underset{\sim}{H} = 0 \qquad (3)$$

tangential component of the field must be continuous, equation 1 or 2 does not uniquely define $\underset{\sim}{M}$. This is because $\underset{\sim}{M}$ is also dependent on the nature of the substance. It would be impossible to determine the dependence of $\underset{\sim}{M}$ on $\underset{\sim}{H}$, position or direction if the dependence were

not, as generally observed, of a very simple type.

For substances of homogeneous composition, $\underset{\sim}{M}$ is found to depend on $\underset{\sim}{H}$ but not on position; that is, $\underset{\sim}{M}$ does not vary throughout a material object except as $\underset{\sim}{H}$ varies. For substances which are isotropic in composition, that is, lack intrinsic directional differences, $\underset{\sim}{M}$ depends only on the magnitude of $\underset{\sim}{H}$ and not on the direction. For substances in this class, it is invariably found that the magnetization is merely proportional to the field strength:

$$\underset{\sim}{M} = X\underset{\sim}{H} \tag{4}$$

$$\underset{\sim}{B} = (1 + 4\pi X)\underset{\sim}{H} = \mu\underset{\sim}{H} \quad .$$

The constants X and μ are called respectively the "susceptibility" and the "permeability". If X is greater than zero (magnetization parallel to the field), the substance is called "paramagnetic"; if less than zero, it is called "diamagnetic". For paramagnetic substances, the susceptibility is usually of the order of 10^{-5} cgs/cm^3 and is temperature dependent. The susceptibility of diamagnetic substances is usually of the order -10^{-8} cgs/cm^3 and is nearly temperature independent.

Another wide class of substances are those which are homogeneous and anisotropic, that is, $\underset{\sim}{M}$ depends on the direction as well as the magnitude of $\underset{\sim}{H}$. The majority of these substances are crystalline and the intrinsic directional character is related to the crystal lattice. It is found, however, that, except for ferromagnetic substances discussed below, the components of the vector $\underset{\sim}{M}$ are each only linear functions of the components of $\underset{\sim}{H}$. In this case, the susceptibility may be represented by a matrix rather than by a scalar;[5]

$$\underset{\sim}{M} = \mathbb{X}\underset{\sim}{H} \qquad M_i = X_{i,1}H_1 + X_{i,2}H_2 + X_{i,3}H_3 \tag{5}$$

$$i = 1, 2, 3 \quad .$$

For such substances a rectangular coordinate system may be found for the representation of $\underset{\sim}{H}$ such that equation 5 reduces to the simple form in equation 6 in which the matrix, $\mathbb{X}$, has only diagonal ele-

$$M_i = X_iH_i \qquad i = 1, 2, 3 \tag{6}$$

ments. The particular coordinate system is referred to as the "principal magnetic axis" system, and the coefficients X_1, X_2 and X_3 are referred to as "principal susceptibilities". The substance is paramagnetic or diamagnetic depending on whether the principal susceptibilities are greater or less than zero. The difference between two principal susceptibilities will later be referred to as a "principal anisotropy" or sometimes merely as "the anisotropy".

"Ferromagnetic" substances are characterised by the particular dependence of $\underset{\sim}{M}$ on temperature for a given field strength and by the fact that, for field strengths normally obtained in the laboratory, $\underset{\sim}{M}$ within the substance is very much larger than for paramagnetic substances. Furthermore, the relation between $\underset{\sim}{M}$ and $\underset{\sim}{H}$ is more complicated than for paramagnetic substances: at low field strengths $\underset{\sim}{M}$ is not a single valued function of $\underset{\sim}{H}$ and at high field strengths $\underset{\sim}{M}$ becomes constant.

The energy associated with a magnetic field is given by the integral:

$$U = \frac{1}{4\pi} \int_{\text{ALL SPACE}} \left[\int_0^B \underset{\sim}{H} \cdot d\underset{\sim}{B} \right] dV \qquad (7)$$

The magnetization may be discussed in terms of the energy per unit volume, defined by equation 7. The energy in each volume element may be broken into two parts:

$$\Delta U = \Delta U_o + \Delta U_m = \left(\frac{H^2}{8\pi} + \frac{\underset{\sim}{H} \cdot \underset{\sim}{M}}{2} \right) \Delta V \qquad (8)$$

The first part depends only on H^2 which in turn is determined by external sources and the surrounding medium but not by the particular volume element. The second term is determined by the material properties of the volume element of the substance being considered and is therefore of particular interest. For an isotropic homogneeous substance, $\Delta U_m = \frac{1}{2} X H^2$. For an isotropic substance with the magnetic field referred to the principal magnetic axes:

$$\Delta U_m = \frac{1}{2}(X_1 H_1^2 + X_2 H_2^2 + X_3 H_3^2) \qquad (9)$$

In this case, one may speak of an "ellipsoid of susceptibility", an imaginary ellipsoidal surface with axes parallel to the principal magnetic axes of the substance and having semi-axes of length $X_1^{-\frac{1}{2}}$, $X_2^{-\frac{1}{2}}$ and $X_3^{-\frac{1}{2}}$. The ellipsoid has the property that if the length of its radius vector in a given direction is written as $X_o^{-\frac{1}{2}}$, then for a magnetic field, $\underset{\sim}{H}$, having the same direction, $\Delta U_m = \frac{1}{2} X_o H^2$. The quantity X_o may be called the "apparent" susceptibility for the given direction. For an anisotropic crystalline substance it is found that the symmetry of the susceptibility ellipsoid conforms to the point-group symmetry of the crystal class. That is, a two-fold rotation or screw axis of the crystal is a principal axis of the ellipsoid and the cross section perpendicular to the axis is elliptical; a three-fold axis is also a principal axis of the ellipsoid but the cross section is circular ($X_2 = X_3$); for a cubic crystal the ellipsoid is a sphere and the substance is magnetically isotropic[6]. An object composed of a powder of some anisotropic crystalline substance, in which the individual particles are randomly oriented, is found to behave as an isotropic object with average susceptibility $\overline{X}$ given by:

$$\overline{X} = \frac{1}{3}(X_1 + X_2 + X_3) \quad . \tag{10}$$

For ferromagnetic objects, the energy ΔU_m may be expanded in a power series of the components of the magnetic field valid over a particular short range of values of $\underset{\sim}{H}$, or at "saturation" where $\underset{\sim}{M}$ is approximately constant and single-valued. Even powers greater than the second are necessary; consequently one can no longer refer to a susceptibility ellipsoid and the corresponding considerations of crystal symmetry are no longer valid. For example, iron crystals, which are cubic, are not magnetically isotropic[7].

If a sphere or cylinder of isotropic, homogeneous dia- or paramagnetic substance is placed in a magnetic field, initially uniform with strength $\underset{\sim}{H}_o$, the field inside the sphere or cylinder remains uniform and parallel to $\underset{\sim}{H}_o$ but its magnitude is altered, having the value given in equation 11:[8]

$$\text{(11)} \quad \begin{aligned} &\text{a)} \quad H_i = \left(\frac{3}{\mu+2}\right) H_o && \text{sphere} \\ &\text{b)} \quad H_i = \left(\frac{2}{\mu+1}\right) H_o && \text{cylinder, } \underset{\sim}{H}_o \perp \text{ to axis.} \end{aligned}$$

In a nonuniform magnetic field, a paramagnetic object experiences a translational force tending to move it into the region of greatest field strength, while a diamagnetic substance tends to move away from this region. The force is given by:

$$(12) \qquad \underset{\sim}{F} = -\int_{\text{vol.}} \underset{\sim}{H}(\nabla \cdot \underset{\sim}{M})\, dV + \int_{\text{surf.}} \underset{\sim}{\overline{H}}(\underset{\sim}{M} \cdot d\underset{\sim}{S})$$

($\underset{\sim}{\overline{H}}$ = average of interior and exterior field at surface.)

In a uniform field, an isotropic, homogeneous para- or diamagnetic object experiences no translational force but does experience a torque couple unless the object is either cylindrical with H perpendicular to its axis or spherical. The value of the torque for completely general field conditions and types of substances is given by:

$$(13) \qquad \underset{\sim}{L} = -\int_{\text{vol.}} (\nabla \cdot \underset{\sim}{M})(\underset{\sim}{r} \times \underset{\sim}{H})\, dV + \int_{\text{surf.}} (\underset{\sim}{r} \times \underset{\sim}{\overline{H}})(\underset{\sim}{M} \cdot d\underset{\sim}{S})$$

($\underset{\sim}{r}$ = position vector of vol. or surf. element with respect to origin)

An anisotropic substance experiences a torque in a uniform magnetic field even if the object is spherical or cylindrical. The torque for the cases of a sphere and a cylinder may be calculated by the use of equations 11 and 13, equation 11 being applied to the components of $\underset{\sim}{H}_o$ parallel to the principal magnetic axes; the result is given in equation 14. In both cases, the field outside is initially

(14)

$$a) \qquad L = \frac{V}{2}\left(\frac{3H_o}{\mu_1+2}\right)\left(\frac{3H_o}{\mu_2+2}\right)(X_2-X_1)\sin 2\vartheta$$

(Sphere, $\underset{\sim}{H}_o \perp$ to one principal axis and making angle ϑ with X_1 direction)

$$b) \qquad L = \frac{V}{2}\left(\frac{3H_o}{\mu_1+1}\right)\left(\frac{3H_o}{\mu_2+1}\right)(X_2-X_1)\sin 2\vartheta$$

(Cylinder, $\underset{\sim}{H}_o \perp$ axis of rotation which is also a principal axis; $\underset{\sim}{H}_o$ makes angle ϑ with X_1)

uniform, with strength H_o, and directed as noted. The field strength inside the object is still uniform, as in the case for isotropic sub-

stances, but is no longer parallel to the original field. For paramagnetic and diamagnetic substances, the difference between μ_1 or μ_2 and unity may be neglected in equation 14 without appreciable error.

b. Magnetic Susceptibilities [2]:

A charged particle (mass = m, charge = e esu.) undergoing a periodic motion about a fixed point gives rise to a magnetic field which at large distances is identical to that of a magnetic dipole of moment $\underset{\sim}{\mu} = (e/2mc)\underset{\sim}{P}$, where $\underset{\sim}{P}$ is the time-average angular momentum of the particle and c is the velocity of light. A system of n charged particles moving about a fixed point in an electrostatic field whose strength is a function of radial distance only undergoes, according to Newtonian mechanics, a motion which, to a first approximation, is unchanged by the introduction of a magnetic field except for the addition of the constant amount $\underset{\sim}{w} = -(e/2mc)\underset{\sim}{H}$ to the angular velocity of each particle. That is, the angular momentum vector of the unperturbed system precesses with angular velocity $\underset{\sim}{w}$ about the direction of the magnetic field. The corresponding addition to the angular momentum of the entire system is $\Delta\underset{\sim}{P} = \mathbb{I}\underset{\sim}{w}$, where $\mathbb{I}$ is the time-average moment-of-inertia matrix of the system. The total magnetic moment of such a system of particles (equal masses and charges) is then:

$$(15) \qquad \underset{\sim}{\mu}_{tot.} = \frac{e}{2mc}\sum_{i}^{n}\underset{\sim}{P}_i + \frac{e}{2mc}\mathbb{I}\underset{\sim}{w} = \sum_{i}^{n}\underset{\sim}{\mu}_i - \frac{e^2\mathbb{I}}{4m^2c^2}\underset{\sim}{H}.$$

If the time-average distribution of particles about the center is spherically symmetric, then $\mathbb{I}$ becomes the scalar quantity:

$$(16) \qquad I = m\left(\sum_{i}^{n}\overline{\rho_i^2}\right) = \frac{2m}{3}\left(\sum_{i}^{n}\overline{r_i^2}\right).$$

where r_i is the distance of the i-th particle from the origin, ρ_i is the perpendicular distance of the i-th particle from an axis passing through the origin and parallel to $\underset{\sim}{w}$, and where the averages are

time averages.

In a system of such model atoms the condition of each model atom will be disturbed by collisions and it may be expected that the average component parallel to the field of the magnetic moments will be determined by the thermal agitation. When calculations involving statistical mechanics are applied to this total system it is necessary to use some knowledge of atomic mechanics, since only discrete values of angular momentum are allowed; without this "quantization" there would be no net average moment. It is also necessary to add the angular momentum due to electron spin and to restrict the components of the angular momentum parallel to $\underset{\sim}{H}$ to discrete values. When Boltzmann statistics are then applied to the population of the energy levels corresponding to various angular momentum states, the method of summation and the exact result depend on the number of angular momentum states and on the ratio of their energy, in the magnetic field, to the thermal energy, RT. The resulting molar magnetization** (for N systems) is of the general form:

$$\underset{\sim}{M^*} = \frac{C\,\mu_B^2\,\underset{\sim}{H}}{RT} - \frac{Ne^2\,\underset{\sim}{H}}{6mc^2}\sum_i^n \overline{r_i^2} \qquad (17)$$

(N = Avogadro's number, T = absolute temp., r_i = angstroms, μ_B = Bohr magneton)

$$= + \frac{0.375\,C}{T}\underset{\sim}{H} - 2.83\times10^{-6}\underset{\sim}{H}\sum_i^n \overline{r_i^2}$$

The corresponding molar susceptibility is then $X^* = M^*/H$.

This result fits the experimental findings with real atoms fairly closely. The constant C is determined by the net angular momentum of the system. If the net angular momentum is not zero, then C is of the order of magnitude one, and the first term is therefore much larger than the second. This state corresponds to paramagnetic substances for which the magnetization is parallel to the field and the susceptibility is observed to be proportional to 1/T, at least for

---

**The magnitization per mole, $\underset{\sim}{M^*}$, and the susceptibility per mole, X^*, will be used frequently. They may be converted to the corresponding quantities per unit volume by dividing by the gram formula weight and multiplying by the density.

temperatures far above absolute zero and for magnetic fields normally encountered in the laboratory. The state for which C equals zero (no net orbital or spin angular momentum) corresponds to diamagnetic substances in which the susceptibility is found to be negative, temperature independent and smaller than for paramagnetic substances.

When this general treatment is applied to molecules, there is a slight addition to the average paramagnetic susceptibility if the molecule is allowed to rotate. In the diamagnetic term, the summation is carried out over all electrons in the molecule, r_i being the distance from the i-th electron to the atom nucleus about which it moves. These results may also be derived with the aid of quantum mechanics.

To interpret the diamagnetic susceptibility of molecules, one may imagine the atoms placed one atop the other (without disturbing the motion of the electrons) so that all the electronic motions have a common center. The time-average moment of inertia of this system of electrons determines (equation 18) the diamagnetic susceptibility.

(18) $$\chi^* = -\left(\frac{Ne^2}{4m^2c^2}\right)\mathrm{I}$$

If the symmetry of the molecule is such that the moment of inertia of the above imaginary electron distribution is a matrix, then the molecule is magnetically anisotropic, as discussed above,(Pg.3). The distribution of electrons around the nucleii of atoms is such that a few electrons farthest from the nucleus contribute most of the diamagnetism. These electrons, the valence electrons, are involved in chemical reactions and in covalent bonds. The diamagnetic anisotropy of a molecule is therefore a measure of the unequal spreading out in various directions of the valence electrons.

Since the diamagnetic susceptibility is so intimately connected with the state of the valence electrons, it has been used as a means of investigating the bonding in molecules. An extensive investigation of many diamagnetic substances led Pascal [9] to conclude that the average susceptibility is an additive property. That is, to every atom could be assigned a "Pascal constant" such that the average susceptibility of a molecule was approximately equal to the sum of the

Pascal constants of the atoms involved. It was also necessary to add "constitutive corrections" to account for variations observed when certain atoms are involved in different types of covalent bonds.

The average susceptibilities of organic compounds calculated by use of the Pascal constants frequently agree with the observed values within 1%. However, large deviations (10%) are sometimes found. These deviations have been attributed to the fact that the covalent bonds are of a type different from the type supposed. Attempts have been made to determine the correct electronic structures of such molecules either by juggling the "constitutive corrections" or by making corrections for partial ionic character of some of the atoms [9,10]. The deviation of calculated and observed susceptibilities has also been attributed to the anisotropy of the molecule and used as a method of determining the principal molecular anisotropies [11].

Measurements of principal diamagnetic susceptibilities of ions and molecules have been used to investigate their electronic structures. Most notable success has been obtained in interpreting the anomalously large anisotropy of aromatic and polynuclear hydrocarbons, such as benzene, naphthalene, anthracene, etc. which contain networks of conjugated double bonds. In most substances, the principal molecular susceptibilities vary only about 10% from their average value whereas in these latter molecules the susceptibility perpendicular to the plane of the conjugated ring or network is found to be several times the susceptibility parallel to the plane. A quantitative theory has been proposed by Pauling [12] to account for this anisotropy. He treats the molecules as conducting networks in which electrons (two per double bond) may move freely. An electric current is assumed to be induced in the network by the rising external magnetic field. Kirchhoff's laws of electricity [13] are used, assuming an electrical resistance in each circuit proportional to the circuit's length, to determine the division of the current among the various branches. The magnetic moments of such a network is the sum of the magnetic moments of each current circuit which, in turn, is proportional to the product of the current times the area of the circuit [14]. Relative magnetic moments so calculated are compared with the moment for benzene obtained by the same method. The absolute magnetic moment of benzene

is calculated by use of equations 15 and 16, assuming that six electrons (n = 6) move in a circular orbit, of radius ρ = 1.39A, circumscribed about the hexagon formed by the six carbon nucleii. The principal anisotropy calculated for benzene (magnetically uniaxial because of the hexagonal symmetry) is 49×10^{-6} cgs/mole, which may be compared with the experimental result obtained by Raman and Krishnan[15,16] from magneto-optical measurements (see below, pg. 13) of 54×10^{-6} cgs. per mole. Pauling has made caclulations of the principal susceptibilities of 15 planar aromatic and conjugated polynuclear hydrocarbons, making an allowance for a decrease in the susceptibilities of the aromatic carbon atoms due to the effective loss of the electrons free to move in the network. The values calculated for the difference between the susceptibilities perpendicular to the molecular planes and the average susceptibilities parallel to the planes agree, in all but two cases, within 10% with the experimental data available at the time. More recently, extensive quantum mechanical calculations have been applied to benzene, naphthalene and anthracene giving susceptibilities somewhat different from those calculated by Pauling. The predicted value for anthracene was, however, too large by a factor of two[17].

Other sources of magnetic anisotropy of a much smaller magnitude have also been noted[18,19,20]. For example, long-chain saturated hydrocarbons have greater diamagnetism (more negative susceptibility) parallel to the chain than perpendicular to it, suggesting a tendency of the nucleii to draw together with a spreading out radially of the electrons. Distinct anisotropy is also associated with substances containing double bonds even when they do not form conjugated rings.

The principal diamagnetic susceptibilities and the orientation of the principal magnetic axes of a crystal may be calculated by summing χ^* for each of the molecules in the unit cell, taking into account their different orientations. Conversely, principal molecular susceptibilities may be calculated from those of the crystal, provided the crystal structure is known and the unit cell does not have too much symmetry. The details of this latter calculation may best be illustrated by examples in section D. The vast majority of determin-

ations of principal molecular susceptibilities or anisotropies reported in the literature were made in this way. In addition to being used to investigate the electronic structure of molecules, measurements of the magnetic anisotropies of crystals may occasionally be used as an aid in crystal structure determinations by suggesting the orientation of molecular groups known to confer anisotropy on the molecule.

c. Plan of the Work.

The work described in this thesis was originally begun as an investigation of the diamagnetic anisotropy of some proteins. The molecular structures proposed [21] for these substances, involving peptide chains either coiled in helices, or linked together into sheets by hydrogen bonds, imply a distinct anisotropy. The purpose was to correlate the anisotropy measurements with existing data on magnetic anisotropy and to determine whether the magnitudes and signs of the anisotropies were consistent with the proposed helical or sheet-like structures.

Since the equipment for the measurements on protein samples would also be suitable for measuring the anisotropy of crystals, it seemed appropriate to obtain additional data for the correlation by making some original measurements on crystals of simple organic compounds for which crystal structures were known. Much work has been done in the past along the line of qualitatively correlating crystal anisotropy with molecular structure. However, in the 15 or 20 years since magnetic anisotropy of crystals was last actively studied, many new crystal structures have been worked out, lending added interest to the proposed measurements on crystals. It was therefore planned to make a number of new measurements of diamagnetic anisotropy on some organic crystals and, further, to study the possibility of determining quantitatively the contribution to the principal molecular anisotropies of certain structural features such as C=C and C=O double bonds, carboxyl groups, etc.

Since the principal anisotropies of the crystals to be investigated were, in general, only small fractions of their average diamag-

netic susceptibilities, it was desired to expend some effort to improve the precision and accuracy in their measurement. It was desired to use a method of absolute rather than relative measurement and consequently it was necessary to refine the various auxiliary calibrations to obtain the necessary accuracy. The main part of the experimental work was devoted to these latter tasks and only a few new measurements of crystal anisotropy were made.

Part I of this thesis deals with measurements of diamagnetic anisotropy of single crystals. In addition to the introduction, section A, part I is divided into other sections, devoted to various aspects of the work, as follows: section B, detailed description of the method used and of the auxiliary calibrations; section C, discussion of the cause and the elimination of certain errors in the anisotropy measurements; section D, tabulation of new measurements and discussion of them in terms of crystal and molecular structure; section E, conclusion.

d. Measurement of Magnetic Anisotropy.

In principle, any phenomenon involving the principal magnetic susceptibilities or anisotropies of molecules may be used in their determination; the methods which have been actually employed are discussed here. The methods generally involve the measurement of susceptibilities or anisotropies of crystals using forces or torques exerted by magnetic fields, followed by the calculation of the corresponding molecular quantities from a knowledge of the crystal structure. Molecular anisotropies may be determined directly, in some cases, from observation of certain magneto-optical properties of liquids and gases.

Measurement of principal susceptibilities of crystals;

1) In a method devised by Jackson [22], a crystal is suspended in an inhomogeneous magnetic field such that the direction of the field is always parallel to a principal axis, but decreases in magnitude in a direction perpendicular to the axis. The translational force act-

ing on the crystal is measured and the susceptibility in the direction of the field is calculated by use of equation 12. This method is suitable for measuring changes in principal susceptibilities, as for example with changing temperature, when the same specimen is used throughout the experiment and is constantly in the same position with respect to the magnet. The method is not suitable for accurate measurement of the principal susceptibility if small crystals are used because of the difficulty in measuring accurately the field gradient across a small distance. To obtain crystals in the form of long rods extended along the various principal axes would in general be very difficult.

2) In a method devised by Rabi [23] a small crystal is attached to a fine quartz fiber (low resistance to torsion and bending) and suspended in a bath of liquid whose susceptibility may be varied. The bath is in a region of inhomogeneous field near the poles of a magnet. One principal axis of the crystal is set vertical and the crystal is allowed to turn only around this axis. The direction of algebraically greatest susceptibility in the plane perpendicular to the vertical axis will line up parallel to the magnetic field and a horizontal translational force, due to the field inhomogeneity, will act on the crystal. The susceptibility of the surrounding liquid is altered by addition of other substances until the crystal no longer experiences the translational force. The susceptibility of the liquid is then equal to the susceptibility of the crystal in the direction of the magnetic field. The susceptibility of the liquid may sometimes be calculated, or can be determined directly by the Gouy method [24]. The susceptibility of the liquid may be determined by present methods to an accuracy of about $\pm 0.1 \times 10^{-6}$ cgs/mole; hence if a small difference between two principal susceptibilites, of the order of 1×10^{-6} cgs per mole, is sought, this method may not be sufficiently accurate.

Magneto-optical measurements:

Raman and Krishnan [15,16] have used Cotton-Mouton constants and the depolarization factors to calculate the principal molecular anisotropies of benzene and of the nitrate ion. The Cotton-Mouton effect is the ability of a magnetic field to make the refractive index of a liquid or gas different for the directions parallel and perpendicular to the field. The Cotton-Mouton constant is the difference

in refractive indices measured parallel and perpendicular to the magnetic field divided by the square of the field strength and by the wave length of the light. The depolarization of linearly polarized light involves the scattering of an incident linearly polarized light ray by a liquid or gas with the conversion of some of the energy into light polarized at right angles to the direction of polarization of the incident ray, the depolarization factor being the ratio of the intensities of the two components of polarization after scattering at right angles. Theories have been proposed to relate both of these quantities to the principal electric and magnetic susceptibilities of the molecules. If the molecules in the sample have sufficient symmetry that they have only two distinct magnetic and electric susceptibilities (uniaxial), then the Cotton Mouton constant, the depolarization factor, the average magnetic susceptibility and the refractive index (in absence of magnetic field) may be combined to calculate the difference in the two principal molecular magnetic susceptibilities. However, two theories have been proposed to account for the depolarization factor of liquids, and the calculated value of the molecular anisotropy depends on which theory is used. Furthermore, the Cotton-Mouton effect and the depolarization effect are small for weakly anisotropic substances and not accurately measured.

Measurement of principal anisotropies of crystals:

The methods discussed here were developed and extensively used by Krishnan [25]. They involve the use of the torque exerted by a homogeneous magnetic field on an anisotropic crystal. The crystal is first attached to a quartz fiber or other torque measuring device and suspended such that one principal axis is vertical. In the homogeneous magnetic field the horizontal principal axis of algebraically greatest susceptibility lines up parallel to the magnetic field. One of the following three variations is then used.

1) A definite torque is applied to the crystal by twisting the quartz fiber through a given angle. The crystal turns until the torque exerted by the magnetic field cancels that due to the fiber. The angle through which the crystal turns is measured and equation 13 is used to calculate the principal anisotropy. The angle through which the crystal turns may be measured with a mirror and light ray in the manner in which the angle of rotation of a galvanometer coil

is measured. This rather difficult measurement is avoided in the next two variations.

2) The crystal may be caused to undergo small torsional oscillations about the vertical axis. The periods of oscillation in the presence and absence of the magnetic field, T_1 and T_o respectively, are then measured. The amplitude, ϑ, of the oscillation is made small enough that $\sin 2\vartheta$ may be set equal to 2ϑ. The principal anisotropy may then be calculated from the relation:

$$X_1 - X_2 = \frac{K}{VH^2}\left(\frac{T_o^2 - T_1^2}{T_1^2}\right)$$

where K is the torsion constant of the fiber and V is the volume of the sample. The difficulties in this method are connected with the measurement of the period of oscillation. Unless the crystal is rather large, the periods of oscillation are too short for accurate measurement without elaborate equipment. Furthermore, the oscillation is strongly damped because of the viscosity of air.

3) It is noted that in a magnetic field of given strength there is a maximum torque which the field can sustain against that applied by the quartz fiber. This maximum torque occurs when one principal axis makes an angle of very nearly 45° with the direction of the magnetic field. When a greater torque is exerted by the quartz fiber by twisting it further, the crystal suddenly begins to spin and, because of its kinetic energy, does not stop until the fiber has unwound. The principal anisotropy may then be calculated by use of equation 13. This method appeared to offer the greatest accuracy in measurement of anisotropies of all magnitudes with a minimum of subsidiary observations and calibrations. It is also suitable for use with small crystals in the range of a few milligrams in weight - a size readily obtainable in the laboratory. Finally, it required relatively inexpensive equipment, most of which was already available as the result of the work of other researchers. Consequently, this method was adopted for the work reported below.

In the next two sections, this last method, the method of "maximum torque", will be discussed at length.

B. Measurement of Magnetic Anisotropy by the "Maximum Torque" Method.

a. General Equation.

Consider a sphere (volume V, mass m) of anisotropic diamagnetic or paramagnetic substance (gram formula weight W) immersed in a homogeneous magnetic field, $\underset{\sim}{H}$. The torque acting on the sphere is given by equation 13. The magnetic field inside the sphere is uniform but is slightly different in direction and magnitude from that outside initially. For a sphere of anisotropic substance the relation between interior and exterior field is more complicated than that for an isotropic substance (equation 11a) and enters into the torque calculation, in general, in a way more complicated than in equation 14a. However, for the work to be described the values of X_1, X_2 and X_3 are always small compared to unity and the alteration in the magnetic field is negligible. Hence, the field strength inside the sphere will be assumed to be equal in magnitude and direction to that outside; the error introduced by this assumption involves only powers of X_1, X_2 and X_3 greater than the first. Integration of equation 13 then gives for the total torque acting on the sphere:

$$(19) \qquad \underset{\sim}{L} = V(\underset{\sim}{M} \times \underset{\sim}{H}) \qquad \text{(use volume susceptibilities } X_{1,2,3})$$

$$\underset{\sim}{L} = (m/W)(\underset{\sim}{M}^* \times \underset{\sim}{H}) \qquad \text{(use molar susceptibilities } X^*_{1,2,3}).$$

Let vectors $\hat{\underset{\sim}{1}}$, $\hat{\underset{\sim}{2}}$, $\hat{\underset{\sim}{3}}$ be the principal magnetic axes of the sphere. They are mutually orthogonal unit vectors attached to the sphere and forming a coordinate system in which only the diagonal elements X^*_1, X^*_2, X^*_3 of the magnetic susceptibility (per mole) matrix, χ^*, are not zero. Let $\hat{\underset{\sim}{i}}$, $\hat{\underset{\sim}{j}}$, $\hat{\underset{\sim}{k}}$ be three other unit vectors forming an orthogonal coordinate system fixed in space with the $\hat{\underset{\sim}{k}}$ axis vertical (see figure 1). Let $\sum$ be the plane containing the $\hat{\underset{\sim}{i}}$ and $\hat{\underset{\sim}{j}}$ axes and $\prod$ be the plane containing the $\hat{\underset{\sim}{1}}$ and $\hat{\underset{\sim}{2}}$ axes. Let ψ, φ and ϑ be Eulerian angles defining the orientation of the 1-2-3 coordinate system with respect to the i-j-k system. In a given case, ψ and φ will be fixed and ϑ will be variable, corresponding to rotation of the sphere about the $\hat{\underset{\sim}{k}}$ axis. Let the magnetic field, $\underset{\sim}{H}$, have the direction of the $\hat{\underset{\sim}{i}}$ axis. The torque tending to turn the sphere about the $\hat{\underset{\sim}{k}}$ axis is given by equation 20.

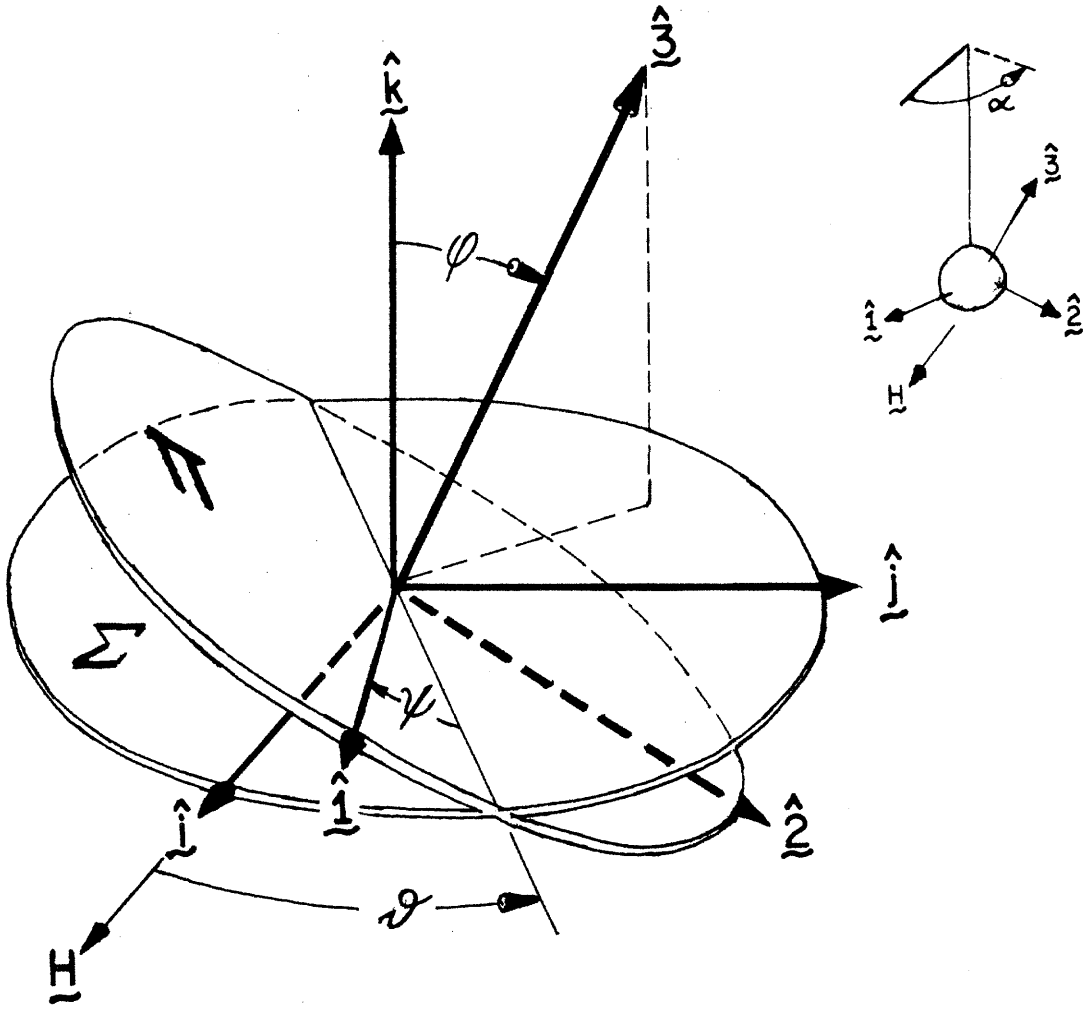

FIGURE 1. RELATION BETWEEN STATIONARY AXES AND PRINCIPAL AXES.

$$
\begin{aligned}
L_1 &= (mH^2/2W)(A\cdot \mathrm{Sin}2\vartheta + B\cdot \mathrm{Cos}2\vartheta) \\
A &= X_1^*(\mathrm{Cos}^2\varphi\cdot \mathrm{Sin}^2\psi - \mathrm{Cos}^2\psi) + X_2^*(\mathrm{Cos}^2\varphi\cdot \mathrm{Cos}^2\psi - \mathrm{Sin}^2\psi) \\
&\quad + X_3^*\mathrm{Sin}^2\varphi \qquad (20) \\
B &= (X_1^* - X_2^*)\cdot \mathrm{Cos}\,\varphi\cdot \mathrm{Sin}2\psi
\end{aligned}
$$

H = magnetic field strength outside sphere.

W = gram formula weight of substance

m = mass of crystal sphere

Let the sphere be suspended by an untwisted quartz fiber of torsion constant K. Let the initial angular position of the sphere, $\vartheta = \vartheta_0$, be the position in which the magnetic torque L_1 is zero. Then:

$$\text{Tan}2\vartheta_0 = -\frac{B}{A} \qquad (21)$$

Let the free end of the fiber be twisted through angle α, measured positively in the same direction as ϑ. The quartz fiber then exerts a torque on the sphere about the $\hat{k}$ axis given by:

$$L_2 = K(\alpha - \vartheta + \vartheta_0) \qquad (22)$$

The total torque tending to turn the sphere about the $\hat{k}$ axis, ℓ, is the sum of L_1 and L_2. If ℓ is positive, the sphere tends to turn in the direction of increasing ϑ; if negative, in the direction of decreasing ϑ. In order to be in stable equilibrium under both torques, not only must ℓ vanish but also the partial derivative of ℓ with respect to ϑ, keeping α constant, must be less than zero.

$$\left(\frac{\partial \ell}{\partial \vartheta}\right)_\alpha = -K + (mH^2/W)(A\cdot\text{Cos}2\vartheta - B\cdot\text{Sin}2\vartheta) \leq 0 \qquad (23)$$

If the sphere is initially in equilibrium ($\ell = 0$) and if α is increased (quartz fiber twisted) the sphere will turn (increasing ϑ) in order to reduce the net torque ℓ to zero. As ϑ increases, a point will be reached at which the derivative in equation 23 will become zero (critical equilibrium). A further slight increase in ϑ will make the derivative positive, since L_1 is beginning to decrease, and a positive torque will act on the sphere tending to make ϑ still larger. Consequently, the sphere will begin to spin, kinetic energy preventing it from being stopped when L_1 again begins to increase, until the fiber is unwound and air viscosity stops the oscillations.

The values of α and ϑ at this critical equilibrium point will be called α_{max} and ϑ_{cr}. At this point the quartz fiber is exerting the maximum torque which can be sustained by the magnetic field. Hence the designation of the method.

(24) $$\left(\frac{\partial \ell}{\partial \vartheta}\right)_{\alpha}\Big|_{\alpha_{max},\vartheta_{cr}} = 0, \qquad \ell(\alpha_{max}, \vartheta_{cr}) = 0$$

$$\mathrm{Tan}2\,\vartheta_{cr} = \frac{B + 2A(\alpha_{max} - \vartheta_{cr} + \vartheta_o)}{-A + 2B(\alpha_{max} - \vartheta_{cr} + \vartheta_o)}$$

Before considering special cases, it may be pointed out that for a particular orientation (ψ and φ) of the crystal sphere the magnetic-torque free stable equilibrium position ($L_1=0$, $\ell=0$), ϑ_o, is that in which the direction of algebraically largest susceptibility in the plane perpendicular to the axis of rotation is parallel to the magnetic field. This may be understood without resorting to equation 20 merely from a consideration of the conservation of energy in a cyclic process in which the crystal is brought into the field, rotated 90°, and then taken out.

First Special Case: Principal axis parallel to axis of rotation.

Let the principal axis $\hat{\underset{\sim}{3}}$ be parallel to the axis of rotation $\hat{\underset{\sim}{k}}$ so that the angle φ is zero. Formal rearrangement of equation 20 gives for the total torque:

(25)
$$\ell = K(\alpha - \vartheta + \vartheta_o) - (mH^2/2W)(X_1^* - X_2^*)\cdot \mathrm{Sin}2(\vartheta - \psi)$$
$$\text{let} \quad \psi = 0$$
$$\text{let} \quad D = (mH^2/2W)(X_1^* - X_2^*) > 0 \quad .$$

Since in this case ϑ is not defined, it will now be defined as the angle between the field direction ($\hat{\underset{\sim}{i}}$) and the $\hat{\underset{\sim}{1}}$ axis, making ψ zero. Clearly, the magnetic torque L_1 vanishes, and stable equilibrium is possible either for $\vartheta_o = 0$ (if $X_1^* > X_2^*$ algebraically, as will be assumed for convenience) or for $\vartheta_o = \pi/2$ (if $X_2^* < X_1^*$):

(26) $$\ell = K(\alpha - \vartheta) - D\cdot \mathrm{Sin}2\vartheta = 0 \text{ at equilibrium} \quad .$$

Using the relations in equations 23, 24 it is seen that the value of ϑ_{cr} is given by:

(27)
$$\mathrm{Cos}2\vartheta_{cr} = -\frac{K}{2D} \qquad (K,D \text{ both} > 0) \qquad \text{or}$$
$$\mathrm{Tan}2\vartheta_{cr} = -2(\alpha_{max} - \vartheta_{cr}) \quad .$$

Hence the value for critical equilibrium is between 45° and 90°, depending on the torsion constant, field strength, mass, anisotropy and gram formula weight of the substance. Practically, however, D is large compared to K so little error is incurred in assuming $\vartheta_{cr}=45^\circ$. If, however, one were to carry out the measurements with a short, stout quartz fiber for which K were fairly large, then either ϑ_{cr} would have to be measured or equation 27 would have to be substituted into equation 26 to eliminate $\mathrm{Sin}2\vartheta_{cr}$. Such a method would have the advantage of making the torsion apparatus more rugged and the quartz fiber possibly less subject to aging effects, but would make the computation of the anisotropy more difficult and would reduce the precision with which α_{max} could be measured. Using the second form of equation 27, it is seen that if α_{max} is greater than 4π radians (two turns), less than 0.1% error is made in calculating $\mathrm{Sin}2\vartheta_{cr}$ by assuming that ϑ_{cr} is exactly 45°.

If the principal magnetic axis $\hat{3}$ is parallel to the axis of rotation, and α_{max} is large enough to set ϑ_{cr} equal to $\pi/4$, then the magnetic anisotropy is given by:

$$(X_1^* - X_2^*) = \frac{2KW(\alpha_{max} - \frac{\pi}{4})}{mH^2} - E$$

$$E = \varphi^2(X_1^*.\mathrm{Sin}^2\psi + X_2^*.\mathrm{Cos}^2\psi - X_3^*) \qquad (28)$$

$$|E| \leq |\varphi^2(\Delta X^*_{max})| \quad .$$

The term E is an estimate of the error introduced if φ is slightly different from zero; the quantity ΔX^*_{max} is the numerically largest anisotropy. If φ is 2° (0.035 radians) and ΔX^*_{max} is 10×10^{-6} cgs/mole, then $|E| \leq 0.01\times10^{-6}$ cgs/mole.

Second Special Case: Axis of rotation perpendicular to a principal axis.

In this case, φ is not necessarily zero but ψ is. Let the axis of rotation be somewhere between the $\hat{2}$ and $\hat{3}$ principal axes and perpendicular to the $\hat{1}$ axis. Then from equation 20:

$$\begin{aligned} l &= K(\alpha - \vartheta + \vartheta_o) - (mH^2/2W)\left[X_2^*\mathrm{Cos}^2\varphi + X_3^*\mathrm{Sin}^2\varphi - X_1^*\right]\mathrm{Sin}2\vartheta \\ &= K(\alpha - \vartheta + \vartheta_o) - D'\mathrm{Sin}2\vartheta \end{aligned} \qquad (29)$$

The value of ϑ_{cr} is determined by equation 24 and in this case

again reduces to the form in equation 27 (with D replaced by D'); likewise, if α_{max} is greater than two turns, ϑ_{cr} may be set equal to $(2n+1)\pi/4$ with negligible error.

Equation 30 gives the anisotropy in the plane perpendicular to the axis of rotation. The term E is an estimate of the amount of

$$(X_2^* \mathrm{Cos}^2\varphi + X_3^* \mathrm{Sin}^2\varphi - X_1^*) = \frac{2KW(\alpha_{max} - \frac{\pi}{4})}{mH^2 \, \mathrm{Sin}2\vartheta_{cr}} - E \tag{30}$$

$$E = \Delta\varphi(X_3^* - X_2^*)\,\mathrm{Sin}2\varphi + \psi^2(X_1^* - X_2^*)(1 + \mathrm{Cos}^2\varphi)$$

$$|E| \leq |(\Delta\varphi + 2\psi^2)(\Delta X_{max}^*)|$$

error incurred if there is a slight error, $\Delta\varphi$, in φ, and if the axis of rotation is not exactly perpendicular to the $\hat{\underset{\sim}{1}}$ principal axis (ψ slightly different from zero). Note that the error depends on the first power of $\Delta\varphi$ and on $\mathrm{Sin}2\varphi$ and not on $(\Delta\varphi)^2$ alone as in the first special case. For $\Delta\varphi = \pm 1^\circ$ (0.017 radians) and $\Delta X_{max}^* = 5\times10^{-6}$, an error $|E| \leq 0.1\times10^{-6}$ cgs/mole would be caused. For φ between 3° and 10°, small errors in alining the crystal can make ψ considerable so that for accurate calculations a reasonable estimate of ψ should be obtained and used. For φ less than 3°, the calculations in the first special case may be used.

If the magnetic-torque free ($L_1=0$) stable equilibrium position, ϑ_o, corresponds to the $\hat{\underset{\sim}{1}}$ principal axis parallel to the field ($\vartheta_o=0$) then $\vartheta_{cr} = 45^\circ$ and $\mathrm{Sin}2\vartheta_{cr} = +1$, but if the $\hat{\underset{\sim}{1}}$ principal axis is perpendicular to the field ($\vartheta_o = 90^\circ$), then $\vartheta_{cr} = 135^\circ$ and $\mathrm{Sin}2\vartheta_{cr} = -1$.

It is generally convenient to make a second anisotropy measurement with the same mode of suspension, but with φ changed by 90°. In case the value of φ is not known, or only approximately known, a third anisotropy measurement is made using the known principal axis ($\hat{\underset{\sim}{1}}$) as axis of rotation. From the three measurements, the three principal anisotropies as well as the angle φ may be calculated as shown in equation 31:

$$\left.\begin{aligned} (X_3^* - X_2^*) &= a \\ X_2^*\mathrm{Cos}^2\varphi + X_3^*\mathrm{Sin}^2\varphi - X_1^* &= b \\ X_2^*\mathrm{Sin}^2\varphi + X_3^*\mathrm{Cos}^2\varphi - X_1^* &= c \end{aligned}\right\} \quad \begin{aligned} (X_3^* - X_1^*) &= \tfrac{1}{2}(a+b+c) \\ (X_2^* - X_1^*) &= \tfrac{1}{2}(b+c-a) \\ \mathrm{Cos}2\varphi &= (c-b)/a. \end{aligned} \tag{31}$$

From this it appears that to obtain the maximum precision in the determination of φ the experiment should be arranged so that φ is as nearly equal to 45° as convenient since for this angle the first derivative of $\cos 2\varphi$ is a maximum and an error in the ratio (c-b)/a would cause a minimum error in φ. However, the maximization of this derivative is offset by the fact that the probable error in the difference (c-b) is also maximized, according to equation 30. For a comparison of practical examples, see the work on glycine in section D.

b. Equipment.

The torsion apparatus, magnet and other accessories are shown schematically in figure 2. The "torsion head" and steel box were designed and built at the Institute and used by Hoyer[26]. The other features of the apparatus are mainly new.

Since α_{max} may range up to 300 turns, turning the torsion head by hand and counting the turns mentally are impractical. Therefore the torsion head is turned though a system of speed-reducing pulleys by a variable-speed electric motor. A cam (not shown in fig. 2) is attached to the graduated scale and, once per revolution, operates a microswitch and a solenoid-operated mechanical counter; the counter is not, however, synchronised with the scale zero. The maximum speed of rotation of the torsion head, 30 rpm., is determined by the reaction time of the counter. As the crystal approaches ϑ_{cr}, the speed is reduced to 5 rpm. The delay in stopping the rotation of the torsion head after the crystal begins to spin causes α_{max} to be exceeded by about 10°; this error was generally negligible.

The glass tube around the full length of the quartz fiber forms an absolutely effective draft shield. Detachable caps of various diameters are available in order to accomodate crystals of various dimensions and permit the smallest possible pole gap with a given crystal. A microscope cover-slide is used to close the bottom of

FIG. 2 APPARATUS FOR MAGNETIC ANISOTROPY MEASUREMENT.

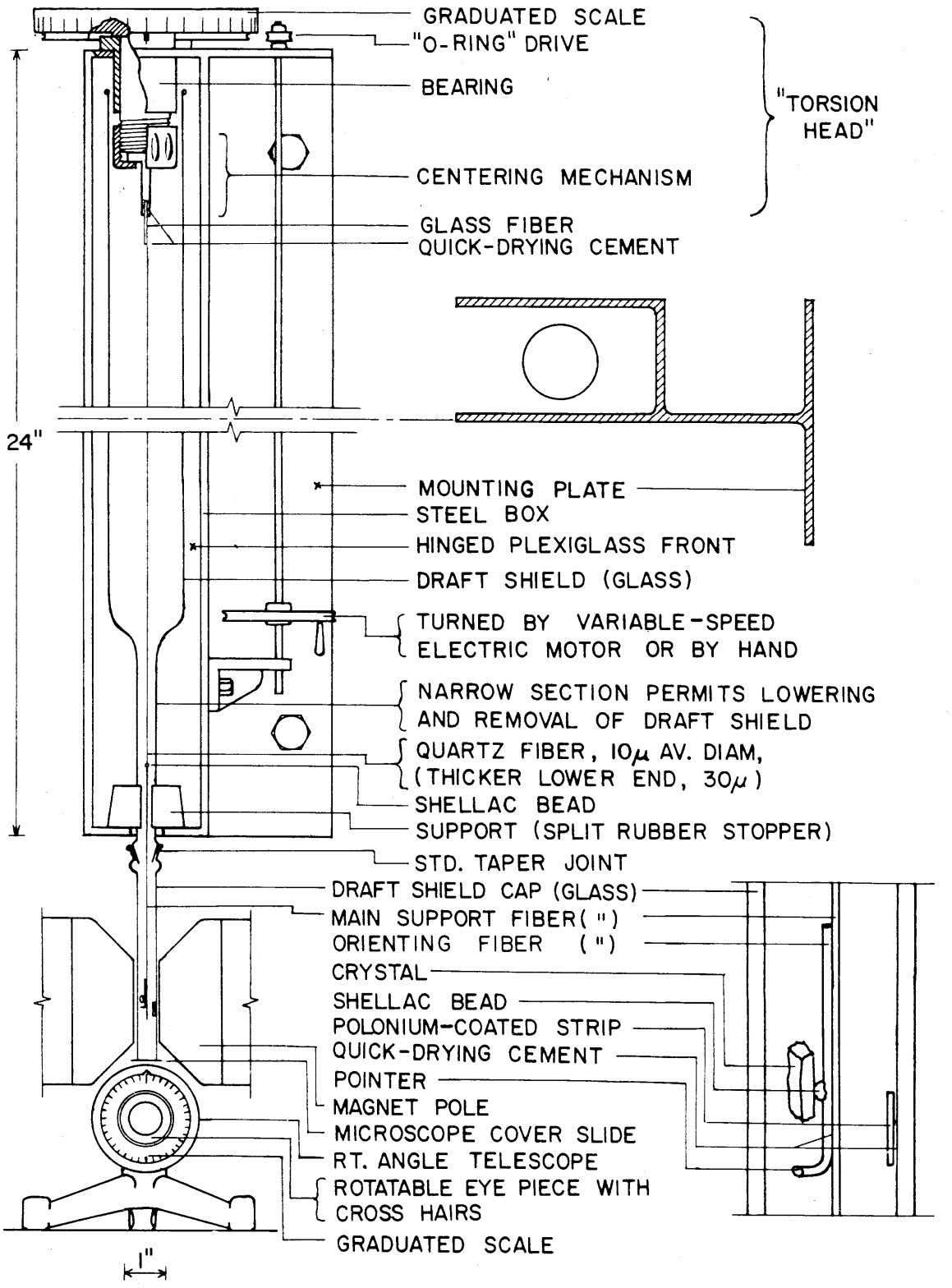

the cap in order to make it optically clear for observing the position of the crystal. The cap causes negligible magnetic shielding.

The centering mechanism is used to bring the axis of rotation of the torsion head into coincidence with the length of the quartz fiber. By adjusting the mechanism so that the fiber is slightly off the axis, the corresponding circular motion of the crystal, occurring as the torsion head is turned, verifies that the crystal and suspension do not touch the draft shield walls.

The telescope is used to determine the initial orientation, ϑ_0, of the crystal in the field and to determine ϑ_{cr}. The eyepiece and cross-hairs may be rotated and a graduated scale attached to the eyepiece has 2° divisions for measuring the angle of rotation. The crystal is seen through a 45° prism attached to the telescope; the focus is fixed at about 5 cm. from the prism (see also fig. 8).

The magnet, which has 4-inch diameter poles, was manufactured by Varian Associates (Palo Alto, California). Field strengths up to 24 kilogauss, for an 8 mm. pole gap and truncated-conical pole pieces, may be attained continuously. The use of low-current, high-voltage windings and a combined A-C rectifier and voltage stabilizer helps to counteract field strength changes due to heating of the coils and variations in line-voltage. The homogeneity of the magnetic field produced was measured with a search coil; for the narrow pole gaps, truncated-conical pole pieces and high field strengths used, the field was constant within 0.1% over a region 1 cm. in diameter near the center of the gap, constant within 1% over a region 3 cm. in diameter, and decreased monotonically in all radial directions from a point slightly above the center of the gap.

The glass fiber attached to the upper end of the quartz fiber and the thickening at the lower end of the fiber are designed to permit the fiber to be attached to things (supports, torsion pendulum, etc.) without changing the torsion constant after calibration. The glass fiber at the bottom, the "main support fiber", is for the attachment of crystals. By making this glass fiber fairly long and stout (one-half mm. diameter) and by attaching the crystals near the bottom, it is assured that it will hang vertically whatever size crystal is attached; if the center of gravity of the crystal were not

close to the glass fiber, the fiber might not otherwise hang vertically, causing an error in φ.

c. Magnetic Field Measurements.

Field strength measurements were made with search coils and a ballistic galvanometer[27]. The coils were home-made since they were required to be not over 8 mm. thick and to have a small cross

FIGURE 3. SEARCH COIL AND HOLDER.

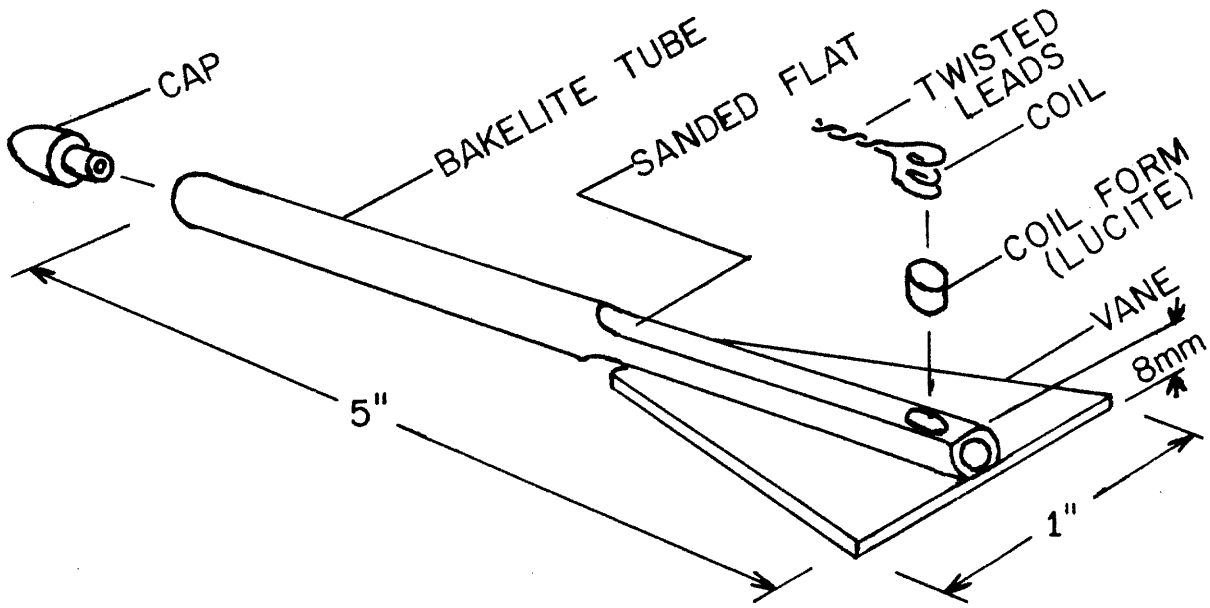

section for a given amount of inductance so that the average field over small regions of the pole gap could be measured. Coils with different inductances were constructed for use in different ranges of field strengths (see figure 3). The vane attached to the coils allows them to be held in a fixed orientation in the field by being placed against a pole face.

Field measurements with a search coil require that the coil be removed from the magnetic field to a place of zero magnetic field in a time short compared to the period of oscillation of the galvanometer coil. This was not difficult to arrange since the major change

in field strength occurred just at the edge of the pole gap; at a distance of one foot from the center of the gap, the field was always less than 10 gauss. The period of oscillation of the galvanometer used was 27 seconds. Experiments showed that the movement of the galvanometer coil was independent of the rate at which the search coil was manually removed from the pole gap over a wide range of rates. Turning the coil through 90°, which greatly reduces the magnetic flux through the coil, was combined with the withdrawal motion to insure accurate galvanometer readings.

An accuracy of at least ±0.5% in the field strength measurements, somewhat better than is normally obtained with search coils, was desired. First, the search coils were designed to make the gal-

FIGURE 4. TYPICAL DEVIATION OF GALVANOMETER READING WITH INITIAL POSITION AND DIRECTION OF MOTION OF HAIR-LINE.

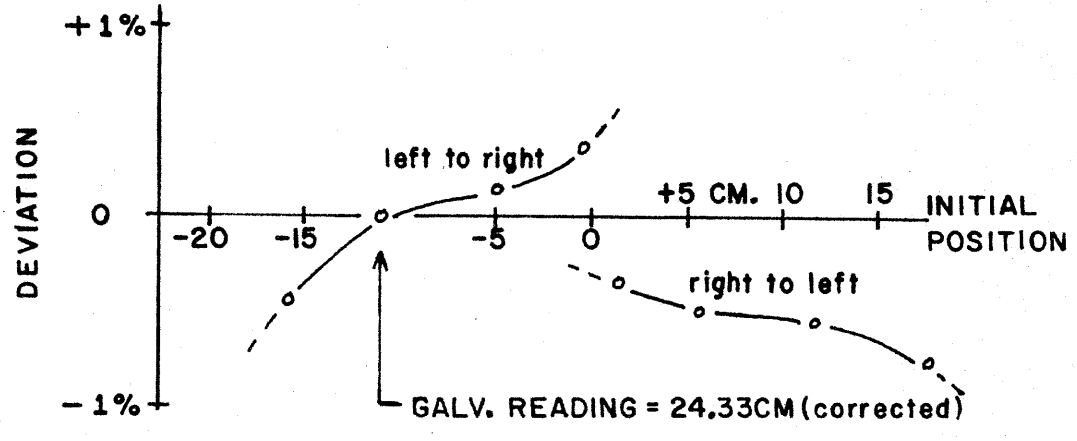

vanometer readings large, from 10 to 40 cm., and capable of being observed with an accuracy of 0.1% or better. A correction for the use of a straight scale rather than a curved scale was necessary and was always made; for a displacement of the hair-line by 20 cm. (from scale zero) the correction is -0.26 cm. Next, the reproducibility of the measurement of a fixed field strength was studied. Experiments showed a slight variation of the galvanometer reading, of the order of a few tenths of one percent, depending on the initial position and direction of displacement of the hair line (see, for example, figure 4). The magnitude of the dependence was too large to

be attributed to a misalinement** of the scale and was attributed to nonuniformity in the field of the permanent magnet in the galvanometer. It was not practical to use the galvanometer with the hair-line always in the same initial position on the scale since the sharpness of the focus of the hair-line changed as it moved; a circular scale, which would eliminate this difficulty, was not available.

Therefore, the use of the galvanometer was standardized as follows: (1) the displacement of the hair-line was always made in the same direction; (2) the initial and final positions of the hair-line were always, as nearly as practical, equally distant from, and on opposite sides of zero; (3) for the measurement of a particular field strength, a search coil was always used such that the initial and final hair-line position was in the middle range of the scale, from 10 to 20 cm. from zero; (4) whenever possible, in a series of measurements, only one search coil was used. By use of this standard procedure: (1) the variation of the galvanometer reading with initial position and direction of motion of the hair-line was eliminated; (2) the influence of the variation in calibration of the galvanometer with initial position was reduced; (3) the error due to misalinement of the scale was minimized; (4) the correction for the use of the straight scale was reduced by a factor of 4 and its calculation (from a graph) made simpler; (5) the hair-line was always in sharp focus so that its position could be estimated to the nearest 0.02 cm., and the focus never required readjustment between measurements; (6) the galvanometer readings were always suitably large; (7) finally, when only one search coil was used in a series of measurements, the results were always consistent.

Whenever field strength measurements were made the average of three observations was usually taken. Under the above conditions, the measurement of a fixed field with a given coil was reproducible with an average deviation of $\pm$0.05 cm. or less. The standard procedure was used in the calibration of the equipment and throughout the

---

** For proper alinement, the plane containing the scale zero and the axis of rotation of the galvanometer coil (the support wire) must be perpendicular to the scale.

magnetic anisotropy measurements. The precautions, although tedious, were acknowledged by the smallness of the amount of scatter of the data points in the anisotropy measurements (see appendix).

The combination of search-coil and galvanometer was calibrated as a unit since the absolute calibration of neither the galvanometer (0.11 microcoulombs/cm) nor of the search coils was known with sufficient accuracy. The calibrating was done with the aid of a magnet whose field strength was measured by the method of nuclear magnetic resonance[28]. Two search coils were so calibrated and the other coils were compared with these. (Since the standard magnet was not equipped to measure field strengths outside the range of about 3 to 5 kilogauss, it was not possible to calibrate every coil directly.) The calibration data are contained in table 1. To minimize read-

TABLE 1.

CALIBRATION OF SEARCH COILS.

Coil Designation	$\frac{\text{gauss}}{\text{cm}}$**	$\frac{\text{gauss}}{\text{microcoulomb}}$	Remarks
A	333.7 ± 2.0 *	3030	Calibrated against standard magnet.
B	96.7 ± 0.1	880	
C	39.0	354	Calculated using ratio C/B
D	18.2	16.5	" " " D/B
E	13.2	12.0	" " " E/B
F	$938 \pm 5.$	8530	" " " F/B

Coil Compare	Ratio	Remarks
B/A	3.442 ± 0.009	Average of many observations at several field strengths.
A/F	2.818 ± 0.004	
C/B	2.48	Approximate.
D/C	2.14	"
E/D	1.38	"

**When used with galvanometer, Chem.Stock #4700, with distance of 100.0cm between galvanometer coil support wire and scale; calibration of galvanometer, 0.11 microcoulombs/cm. Galvanometer readings must be corrected for use of straight scale.

* Higher average deviation for A than for B is mainly due to use of smaller galvanometer readings. Calibration of B was taken as standard.

justment of the equipment after calibration, the galvanometer and scale were clamped to a board. The distance from the scale to the galvanometer coil support wire (100.0 cm.) and the alinement of the scale were rechecked periodically.

Since search coil "F" was used almost exclusively for the magnetic anisotropy measurements, the uncertainty of $\pm$0.5% in its absolute calibration caused an uncertainty of $\pm$1% in the values of the anisotropies (proportional to H^2) reported in section D. Judging from the smallness of the scatter in the magnetic anisotropy data, the precision of the measurement of H^2 was about $\pm$0.3% which was better than expected.

d. Weighing of Crystals.

The preparation of individual crystal specimens is described in section D. Once obtained, the crystals were cleaved to remove occlusions and other imperfections. From the available samples, those in the range of 0.2 to 40 mg. were used. The lower limit is that mass which can be measured on a semi-microbalance with a reproducibility of 1%; the upper limit is set by the dimensions of the pole gap and draft shield cap, and by the maximum torque which the quartz fiber can safely exert without danger of breaking. Large crystals are necessary when small anisotropies are to be measured in order that the anisotropy torque will be greater than that due to other sources discussed in section C; the practical upper limit is determined by the ability of the substance to form large perfect crystals. For some substances, however, crystals even as large as 0.2 mg. are hard to obtain.

The chief difficulty encountered in the use of the semi-microbalance was the random variation during each weighing of the initial and final rest points. These variations are probably connected with local temperature changes and with building vibration. To obtain a precision of better than $\pm$10 micrograms, it was necessary to make repeated determinations alternatively of the initial and final rest points.

e. Mounting and Orienting of Crystals.

Only crystals with monoclinic or higher symmetry were used in the investigations reported here. The method of calculating the magnetic anisotropy of these crystals falls into one or the other of the two special cases discussed above, pgs. 19-22. The method of locating the principal axes and calculating the principal anisotropies of a triclinic crystal can be derived from equation 20.

Tetragonal crystals were mounted with an arbitrary direction perpendicular to the crystallographic 4-fold axis as axis of rotation. Orthorhombic crystals were mounted with crystallographic axes as axes of rotation. Monoclinic crystals were treated under the second special case: the known principal axis is the 2-fold crystallographic axis, $\underset{\sim}{b}$; the two arbitrary axes of rotation perpendicular to the known principal axis were chosen for convenience to be a crystallographic axis ($\underset{\sim}{a}$ or $\underset{\sim}{c}$) and the corresponding reciprocal axis ($\underset{\sim}{a}^*$ or $\underset{\sim}{c}^*$).

The crystal to be investigated was first attached to a short, thin (2 x 0.01cm) bent glass fiber called the "orienting fiber" (see figure 2). The short (1 mm) bend acted as a pointer to locate the position of the crystallographic axes when observing a suspended crystal through the right-angle telescope; it also formed a convenient handle for holding the fiber. For reasons discussed in section C, the glass fibers used within the magnetic field were prepared from stock glass rod (pyrex) which had been thoroughly washed with hydrofluoric acid, to remove surface impurities, before the fibers were drawn. A thermoplastic cement (shellac, beeswax, apiezon tar, etc.) was used to attach the crystal to the orienting fiber because it was usually necessary either to change the orientation of the crystal or to detach and remount it. The cement used was chosen after a consideration of the melting point of the crystal. An electrically heated wire was used to soften the cement; a low power binocular microscope was of considerable aid in watching this operation.

During the mounting operation the crystal was adjusted to have the desired rotation axis approximately parallel to the glass fiber. The axis was located on the basis of crystal habit, cleavage, optical interference patterns in convergent polarized light, or by some other method. Thereafter, the orienting fiber was attached to a goni-

ometer head of the usual type used in X-ray crystallographic work (shown in figure 6). Goniometric measurements and Laue photographs were then used to adjust the goniometer head so that the desired crystal axis was accurately parallel to the axis of rotation of the goniometer head. Observed interfacial angles were compared with angles calculated from the unit cell dimensions (in a few cases in which observed and calculated angles did not agree within 10 minutes, there was usually an error in the indexing of the crystal faces). Goniometric measurements were not suitable for crystals whose faces were rough or absent.

With Laue photographs symmetry axes and mirror planes are easily identified. When checking the orientation of monoclinic crystals, however, it was necessary to be able to identify the Laue photographs taken parallel to the $\underset{\sim}{a}$, $\underset{\sim}{c}$, $\underset{\sim}{a}^*$ and $\underset{\sim}{c}^*$ axes which have no other distinguishing feature than that they are parallel to a mirror plane. To do this, the appearance of the Laue photograph was calculated from a gnomonic projection of the reciprocal lattice[29]. For convenience, a gnomonic projection ruler was constructed so that the projection and the corresponding Laue photograph could be drawn on a single 8½x11" sheet of paper (see for example, figure 5). In addition to unambiguously identifying the $\underset{\sim}{a}$, $\underset{\sim}{c}$, $\underset{\sim}{a}^*$ and $\underset{\sim}{c}^*$ axes when other available crystallographic data were insufficient, the gnomonic projections were also an aid in calculating the amount of misalinement when trying to set one of these axes accurately parallel to the axis of rotation of the goniometer head. The great sensitivity of the location and intensity of the diffraction spots on a Laue photograph to slight changes in the orientation of the crystal made it possible to determine the crystal orientation with a precision of $\pm$15 minutes.

When the crystal orientation had been checked with Laue photographs, necessary adjustments were calculated. The reflection of light from the glass orienting fiber permitted the optical goniometer to be used for making these adjustments accurately. If after these adjustments the glass fiber was not within 1° of parallel to the axis of rotation of the goniometer head (and the desired rotation axis of the crystal), the goniometer head was transferred to the holder shown in figure 6. The translating mechanisms of the goniometer head were then used as a micro-manipulator for the transferring of the

FIG. 5 TYPICAL GNOMONIC PROJECTION OF A RECIPROCAL LATTICE AND CORRESPONDING LAUE REPRESENTATION.

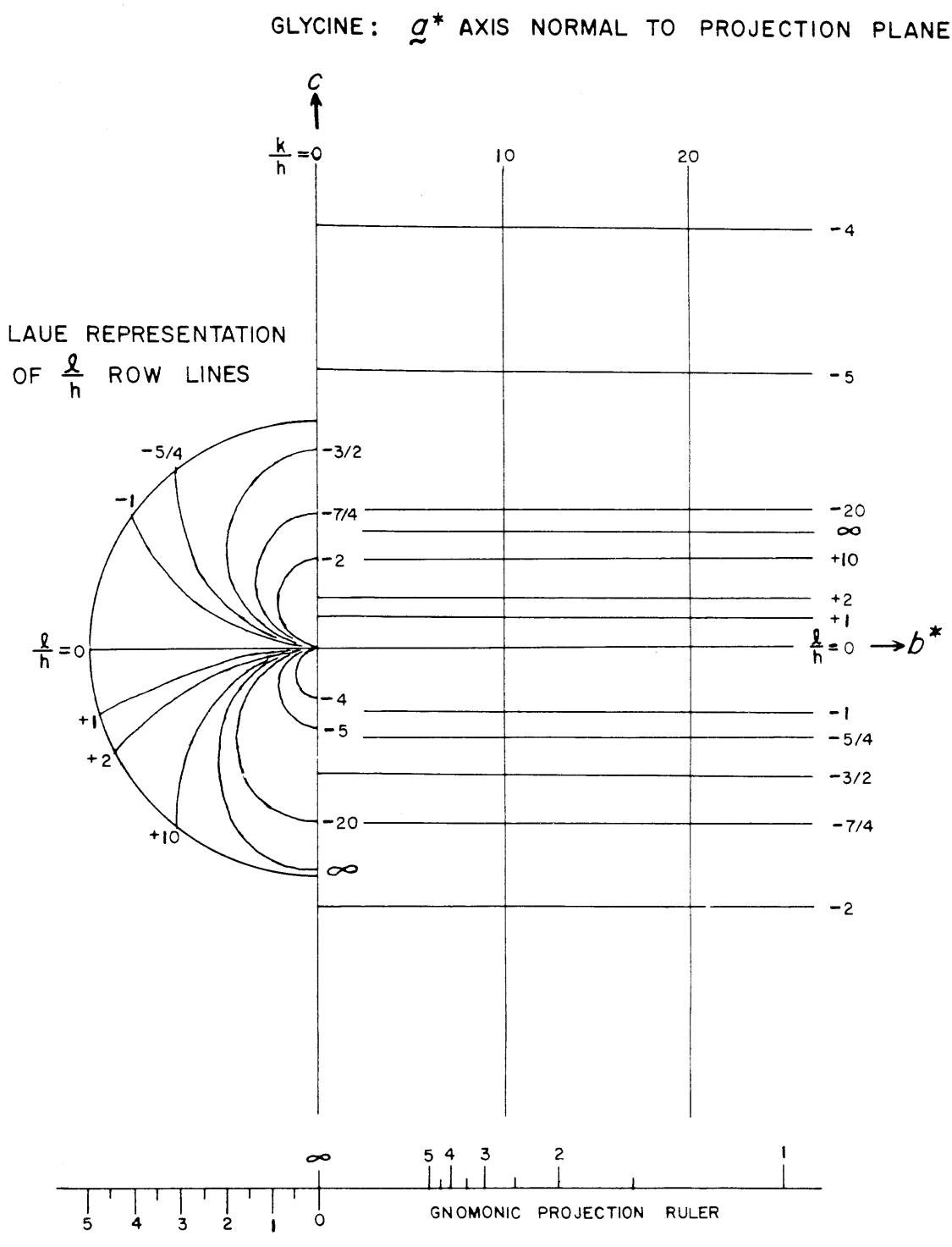

FIG. 6 CRYSTAL-ORIENTING APPARATUS.

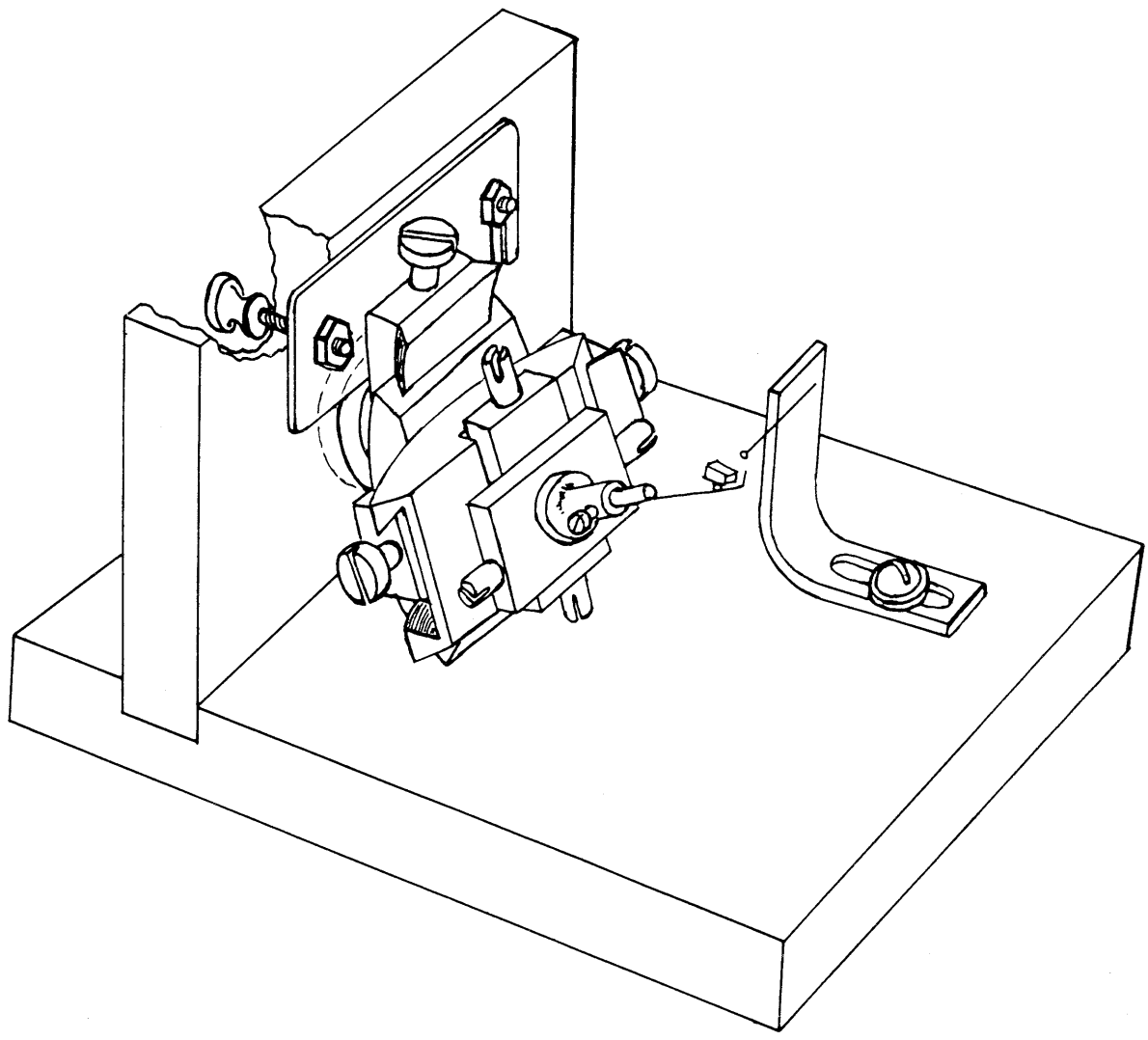

crystal to another glass fiber fixed to the holder. Once the crystal had been transferred, the goniometer head was removed from the holder and the orienting fiber set accurately parallel to the axis of rotation of the goniometer head by use of the optical goniometer, as described above. The crystal was then transferred back to the orienting fiber by the same method.

During the transferring operation there was some difficulty in melting one cement bead and not the other. This difficulty was reduced by reducing the size of the electrically heated wire and by operating it at the lowest possible temperature. In most cases, however, the change in the orientation of the crystal was 20 minutes or less.

After remounting the crystal on the goniometer head and rechecking its orientation with Laue photographs or by goniometric observations, it was usually found that the crystal was alined within the desired accuracy (1°). Lack of good alinement at this stage may be attributed to inaccurate adjustment of the goniometer head prior to the transfer. The inaccuracy may be due to: (1) imperfections in the crystal which made the Laue photographs difficult to interpret; (2) the approximate nature of the calculation from the Laue photographs of the adjustments to be made; (3) alinement of the crystal by goniometric observations in a case in which there is a slight difference between the axes located goniometrically and the axes located by Laue photographs. If the alinement is not within the desired accuracy, the process of adjustment, detaching, transferring and remounting may be repeated. Despite occasional difficulty in the transferring operation, this systematic method of orienting the crystals is far superior to a trial-and-error method.

When making the final check on the orientation of the crystal, the glass orienting fiber was set parallel to the axis of rotation of the goniometer head while the Laue photographs were being made. The Laue photographs could then be used to calculate the direction and amount of misorientation of the desired axis of rotation. For very precise magnetic anisotropy measurements, it would be easier to estimate the angles φ (or the error in φ) and ψ from the final Laue photographs than to orient the crystal with an error less than

20 minutes.

Laue photographs also serve to detect errors in interpretation of the visual crystallographic properties and to detect twinned crystals and imperfect crystals. Every crystal used in the magnetic anisotropy measurements reported here was oriented and checked by this procedure.

Whenever a further check on the assignment of axes is necessary, as was the case with monomethylurea for which two of the (orthorhombic) axes are of almost equal length, the goniometer head and crystal may be placed in a precession camera or Weissenberg camera to obtain intensity data for comparison with published data.

After final adjustment and checking of the orientation of the crystal, the orientation of the "pointer" (figure 2) with respect to the crystal axes was noted. The orienting fiber was then removed from the goniometer head and attached to the "main support fiber" of the torsion apparatus (figure 2). Only a drop of non-volatile oil or of cement diluted with volatile solvent (nitrocellulose in acetone, rosin in benzene, sodium silicate in water, etc.) is necessary for a firm bond, the surface tension of the liquid being sufficient to pull the two glass fibers accurately parallel. The choice of cement is determined by the solubility of the crystal in the solvent. The orienting fiber can later be detached without disturbing the orientation of the crystal by dissolving the cement with solvent. It was preferred to use a new specimen for measurement of the anisotropy about a different axis rather than to reorient a specimen which had been used once.

f. Quartz Fiber Preparation and Properties.

Quartz (actually silica glass) fibers are characterized by remarkable strength and nearly perfect elasticity. A literature survey on their preparation, properties and uses is available[30]. The tensile strength of 35-40 Kg/mm^2 (48000-55000 lb/in^2) of a 100-micron diameter fiber exceeds that of many metals. The tensile strength in-

creases slowly with decreasing diameter down to 10 microns and then increases very rapidly; a fiber of 3 microns diameter may have a tensile strength 10 times that of a 100 micron fiber[30,34]. A quartz fiber of 10 microns diameter can withstand a torsional strain of about 20 turns per centimeter of length and a tension up to 15 grams weight and stretches about 3% before breaking[31,34]. The elastic properties of quartz fibers are reported to be independent of the stress right up to the point of failure[34].

Extensive investigations of the mechanical properties of quartz fibers have been made by Reinkober[31-33]. He found a great uncertainty in the elastic and strength constants. The uncertainty arose partly from the difficulty in accurately determining the diammeters of the fibers and partly from uncontrollable or unknown variables. The strength constants, such as the tensile strength, seemed to be dependent on age, minute flaws and surface impurities and on the presence of adsorbed liquids and gases. The latter dependence was indicated by the fact that the tensile strength of fibers was found to be different when they were tested in vacuum, in dry air, and in air containing the vapors of water or other liquids. On the other hand, the elastic constants, such as the torsion modulus F,

$$F = \frac{2 L K}{\pi G r^4} \tag{32}$$

L = length
r = radius
K = torsion constant
G = gravity constant (converts dynes to gram-weight)

seemed to be unaffected by these variables[32,33]. However, the measurements were mainly of a statistical nature and only relatively large variations in strength and elastic constants could be detected.

It was hoped that the torsion constants of quartz fibers to be used in the torsion apparatus could be determined with an accuracy of $\pm 0.1\%$. The fibers to be used would be subjected to rough handling, exposed to all atmospheric changes, not protected from dust and used over long periods of time. Further, they were to be calibrated while under high vacuum (see below, h.) but used to make torque measurements while exposed to air. Hence there was some doubt as to the permanence of the torsion constant calibration. The results of the

statistical observations above were not encouraging. For example, the effect of age on the torsion modulus (and therefore on the torsion constant) was determined by testing many fibers of various ages rather than individual fibers over long periods of time; although no age effect was noted, a change in torsion constant of the order of 10% per year or less could not have been detected. One result, however, seems definite : the torsion constant of a fiber is unchanged when measured in air, in high vacuum, or in high vacuum after baking the fiber for two hours at 300°C (under high vacuum) and cooling to room temperature[33]. In this case, individual fibers were carried through all three tests; however, the precision of individual torsion constant determinations was ±1% and hence it can not be concluded that the effect of adsorbed gases and vapors is negligible for the work anticipated. It was found incidently in this latter investigation that the temperature coefficient of the torsion modulus (and torsion constant) was +0.00010 per degree centigrade, and that temperature changes had no permanent effect on the torsion modulus. However, once prepared, the quartz fibers were not to be exposed to strong heating since fusing of dust particles into the surface of the fiber would definitely weaken them and change their elastic properties.

A few experiments were made during this work to determine the effect of tension and total torsional stress on the torsion constant and to determine the change in the torsion constants of individual fibers over long periods of time. The results are discussed below (page 50).

Several methods of preparing quartz fibers are known[34]. The simplest method and the one used here was the following: short, stout (100 microns x 10 cm.) fibers are first drawn from a stock rod; the stout fibers are then elongated by holding them in a high-velocity oxygen-illuminating gas flame and allowing the friction of the flame gases to pull the heat-softened quartz into a fiber of a few microns diameter and many feet in length. To get a suitable fiber of desired thickness and length (40 cm), many fibers had to be prepared and examined. Variations in thickness of the fibers or curling of the fibers did not prevent them from hanging straight under slight tension

or otherwise adversely affect their use as torque-measuring devices.

The thickness of the fibers was judged by laying them on a long glass slide and observing them under a microscope having a measuring reticle with a smallest division of 3.5 microns. Since fibers with torsion constants varying over a wide range, 10^{-5} to 10^{-3} cm-dynes per radian (diameters between 6 and 16 microns for a 40 cm length), were usable, an acceptable fiber could be judged after only a very little experience.

The fibers selected were ones which had one end thicker than the average, say 30 to 40 microns diameter. This thickness did not prevent the end from being flexible, but was thick enough so that the contribution to the total torsion constant of one or two millimeters of length was negligible. Hence, when the torsion pendulum used for the torsion constant determination (see g.), or the "main support fiber" were attached to the quartz fiber, a variation of the position of attachment by a millimeter (0.2% of the total length) would not change the torsion constant. The other end of the quartz fiber was permanently glued to a short glass fiber (3 x 0.01cm) for convenience in attaching the quartz fiber to various supports.

g. Construction of Torsion Pendulum for Determination of Torsion Constants.

The torsion constant of a quartz fiber may be calculated from the moment of inertia and period of oscillation of a torsion pendulum suspended by the fiber.

The selection of a torsion pendulum is based on its total mass, period of oscillation, ease of construction, the ease and precision of the determination of its moment of inertia and on the precision of available measuring equipment. The mass must be far less than the maximum safe load (less than 1g. for a 10 micron diameter fiber) and it must be large enough so that no appreciable percentage change occurs with changing amounts of adsorbed moisture. In any event, the mass had to be large compared to 2 micrograms which is the minimum mass measurable with the available semimicrobalance. The period of oscillation of the pendulum had to be large compared to 0.002

minutes (or 0.1 second), the minimum time interval measurable with available timers, and preferably of the order of a few minutes; as discussed below, precision in the measurement of the period of oscillation cannot be indefinitely increased by making the period longer or by timing larger numbers of periods. The linear dimensions must be much greater than the minimum measurable length which, with the available travelling microscope, was 0.001 cm. Large dimensions are usually precluded by concomitant large mass. Finally, the pendulum should be structurally strong and resistant to corrosion.

Two convenient choices are a circular microscope-slide cover-glass suspended from an edge and a length of wire suspended from its center. The cover slide has a mass of about 0.1g. and a radius of about 1 cm; its moment of inertia is about 0.025 g-cm^2. The period of oscillation with a quartz fiber of torsion constant 10^{-4} cm-dynes per radian would then be 100 seconds. The uniformity of thickness of the glass might be checked by the use of optical flats and interference patterns. Its diameter would have to be measured and averaged for many directions to insure that it was circular. Since it would be very nearly symmetric about its axis of rotation it would presumably not wobble. It could be silvered for use with optical and electronic timing devices.

The second choice was preferred because of its high ratio of moment of inertia to mass. For the same moment of inertia as the glass disk above, a wire of convenient length need only weigh 20 to 30 milligrams. Since the dependence of the torsion constant on total linear stress was not investigated by Reinkober[31-33], a pendulum of weight about equal to the weight that would always be on the fiber was desired, at least initially. When properly constructed, the pendulum may be treated as a linear mass distribution and only its mass and length need be accurately measured. Since it can be conveniently made 3 to 5 cm long, the percentage uncertainty in its dimension can be made smaller than for a disk of equal moment. Slight asymmetry in its construction, however, may cause it to wobble. Also, the uniformity of thickness and density of the wire cannot be verified except by determining the period of oscillation of several similarly constructed pendulums when attached to the same fiber; the

net effect of such variations might then be expected to cancel out.

Chromel wire was chosen in preference to copper, platinum, aluminum or iron because of its stiffness, resistance to corrosion, resistance to mercury vapor (used in the vacuum pump discussed below in h.), non-magnetic character and availability in the desired sizes. An estimate of its coefficient of thermal expansion is $+10^{-5}/^{\circ}C$ (average of that of chromium and nickel). An arbitrary length was cut and straightened by rolling between two plates of glass; the ends were sanded to make them flat and square. The uniformity of thickness was checked by cursory observation under a microscope.

FIGURE 7. SKETCH OF TORSION PENDULUM.

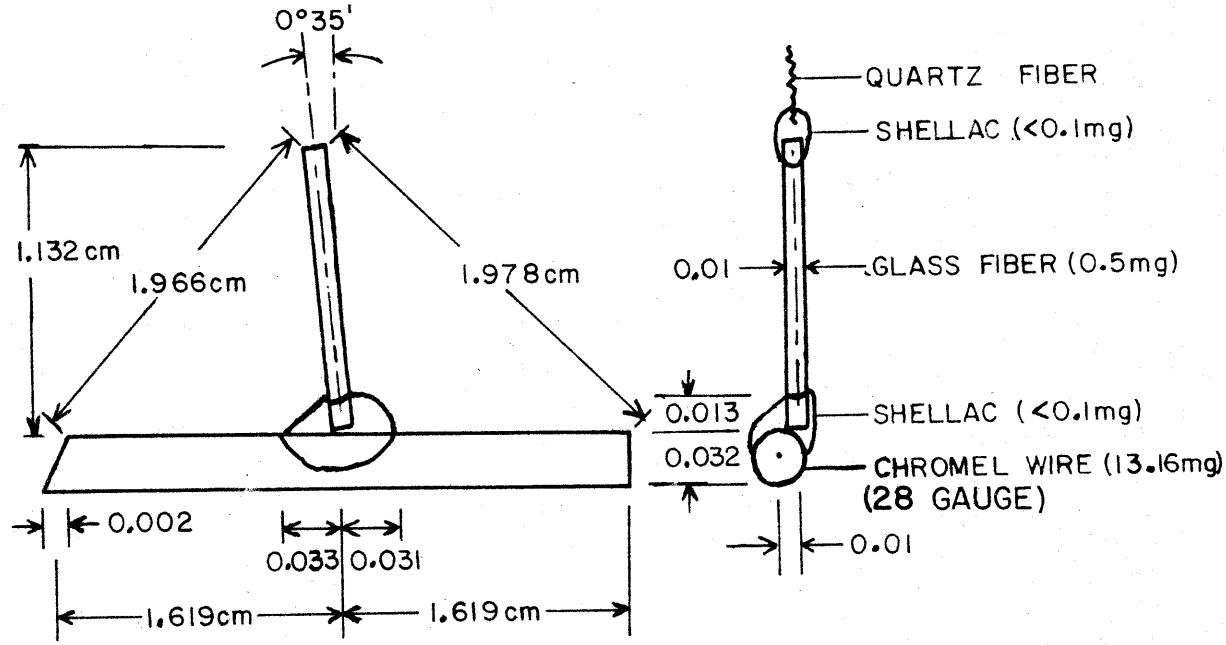

A short glass fiber (about 1 x 0.01 cm) was attached to the wire at its center with a bead of shellac, forming a "T" (see figure 7); the quartz fiber was to be attached to the free end of the glass fiber. Since the center of gravity of the pendulum was far below the point of attachment, it was assured that the wire would always be horizontal, no matter how the quartz fiber was attached.

The mass of the wire, 13.16 ± 0.005 milligrams, was determined with a semi-microbalance. The mass was determined several times and at intervals of several months, and found to be unchanged despite

handling and washing with organic solvents. The dimensions of the T-shaped pendulum were measured with a travelling microscope. The length of the wire (3.238 ± 0.002 cm), position of attachment of glass fiber, length of glass fiber, distance of free end of the glass fiber from each end of the wire, diameters of the wire and glass fiber, dimensions of shellac beads, and distance of axis of fiber from axis of wire were determined. Each measurement was repeated several times and averaged. Although the measuring instrument was graduated for estimation of the nearest micron, the average deviation of the various measurements ranged from 6 to 14 microns.

The moment of inertia of a right-cylindrical rod having mass M, length L and radius R, and rotating about an axis perpendicular to and intersecting the cylinder axis is:

$$I = M\left[\frac{R^2}{4} + \frac{L^2}{12}\right] \quad . \tag{33}$$

Assuming that the wire satisfied the above conditions, and neglecting the contribution of the other parts of the pendulum and the term involving the radius, the moment of inertia of the pendulum calculated from equation 33 was 0.01150 ± 0.00002 g-cm^2. Corrections were then made for the fact that the true axis of rotation (through point of attachment of quartz fiber and center of gravity) does not intersect the axis of the wire, for variations in the position of attachment of the quartz fiber, for the contribution of the glass fiber and the shellac beads, for the omission of the term involving R in equation 33, and for an irregularity in one end of the wire. The two largest errors were both of order of magnitude 1×10^{-6} g-cm^2 and had opposite signs; hence all corrections were negligible.

Since the torsion pendulum was not a truly symmetric rigid body, some consideration was given this approximation. If the pendulum were supported at its center of gravity by the quartz fiber and caused to rotate, the torque exerted on the pendulum by the fiber would have fixed direction but time-dependent magnitude. The angular velocity, $\underset{\sim}{w}$, of the object is related to the torque, $\underset{\sim}{L}$, by the relation $\underset{\sim}{L} = d(\mathbb{I}\underset{\sim}{w})/dt$, where $\mathbb{I}$ is the inertia matrix. Since the direction of $\underset{\sim}{L}$ is fixed, the direction and magnitude of $\underset{\sim}{w}$ would vary

in a highly complicated manner; physically speaking, the pendulum would turn and tumble irregularly. The fact that the quartz fiber is actually attached at some distance from the center of gravity means that gravity will exert a torque on the pendulum tending to hold a fixed axis (point of attachment of quartz fiber to center of gravity) parallel to the quartz fiber ($\underset{\sim}{L}$). Instead of tumbling, the pendulum will rotate more or less smoothly about the quartz fiber but will wobble. The wobble may be expected to be small because of the near symmetry of the pendulum. The wobble will decrease the moment of inertia of the wire by a factor $\mathrm{Cos}^2\varphi$, where φ is the average angle between the glass fiber and the axis of rotation. The decrease in moment of the wire will be compensated slightly by the increased moment of the glass fiber. Consider a small periodic wobble taking place only in the plane of the T-shaped pendulum and such that $\varphi = \varphi_{max}.\mathrm{Sin}\omega t$. The average value of $\mathrm{Sin}^2\varphi$, for small φ_{max}, is the average value of $(\varphi_{max}.\mathrm{Sin}\,\omega t)^2$, or $\frac{1}{2}\varphi^2_{max}$. If φ_{max} is 2° (0.035 radians), then the decrease in the moment of inertia of the wire is 0.06% and is about 20% compensated by the increased moment of the glass fiber. For the case in which the free end of the glass fiber moves in a tiny circle about the axis of rotation with constant velocity, so that φ_{max} is 2°, the moment of inertia of the wire is again decreased by 0.06% but is about one-third compensated by the increased moment of the glass fiber.

h. Determination of the Period of Oscillation.

With the pendulum just described it was found impossible to carry out oscillation observations at atmospheric pressure, at least with quartz fibers with torsion constants in the range $1\text{-}100\times10^{-5}$ cgs. because the viscosity of the air caused the oscillation to be overdamped. Even at pressures of about 1 micron the damping was about 80% per period. Other workers have used similarly constructed pendulums to calibrate fibers of comparable torsion constants by observing the period of oscillation in air. Rogers[35] was able to meas- the period of oscillation of a horizontal wire suspended at its cen-

ter (I = 0.001265 cgs.; period = 30.0 seconds; torsion constant, K = 5.55×10^{-5} cgs.**) and then to duplicate within 3% the value reported by Krishnan[36] for naphthalene crystals (perpendicular to b axis). Krishnan used a torsion pendulum consisting of a glass disk but does not give an estimate of either the moment of inertia or of the torsion constant. It is possible that for different values of K/I or for large total energy stored in the pendulum, the damping may be sufficiently overcome to permit accurate observations of the period. Experiments discussed below show that electrostatic forces can overcome air damping to give an erroneously short period and excessively large torsion constants; presumably, Hoyer[37] encountered some of these difficulties. Most of the other workers in this field calibrated quartz fibers by use of a crystal of "known" magnetic anisotropy.

The oscillation experiments were consequently carried out in a vacuum chamber as shown in figure 8; the lowest pressure attainable was conservatively estimated at 10^{-5} mm. Oscillation was started by picking up the compact, rigidly-clamped apparatus and giving it a small circular motion to cause the pendulum to swing around, lying flat against the chamber wall as it did so, and thus twist the fiber. The apparatus was then tilted and set down so that the suspended pendulum lay against the wall; this stopped the pendulum from vibrating and prevented the fiber from unwinding. The apparatus was then slowly set upright so that the pendulum began to rotate with little swinging***. When the apparatus was fully upright any swinging could be stopped by applying slight pressure to the top of the vacuum chamber in such a way as to cause the support to move out of phase with the swinging. Thus, pure torsional oscillations of practically any amplitude (even up to 200 revolutions) could be induced without, at least initially, any wobbling or vibrating of the pendulum. A small spontaneous wobble always developed, however, after the pendu-

---

**The value 5.73×10^{-5} given by Rogers is evidently the result of an erroneous calculation.

***A mechanical device constructed of bent wires and operated externally by means of a magnet was originally placed inside the chamber to start the oscillation. After the effect of electrostatic forces was discovered, it was removed for fear it might interfere with the oscillation.

FIG. 8 APPARATUS FOR DETERMINING TORSION CONSTANTS OF QUARTZ FIBERS

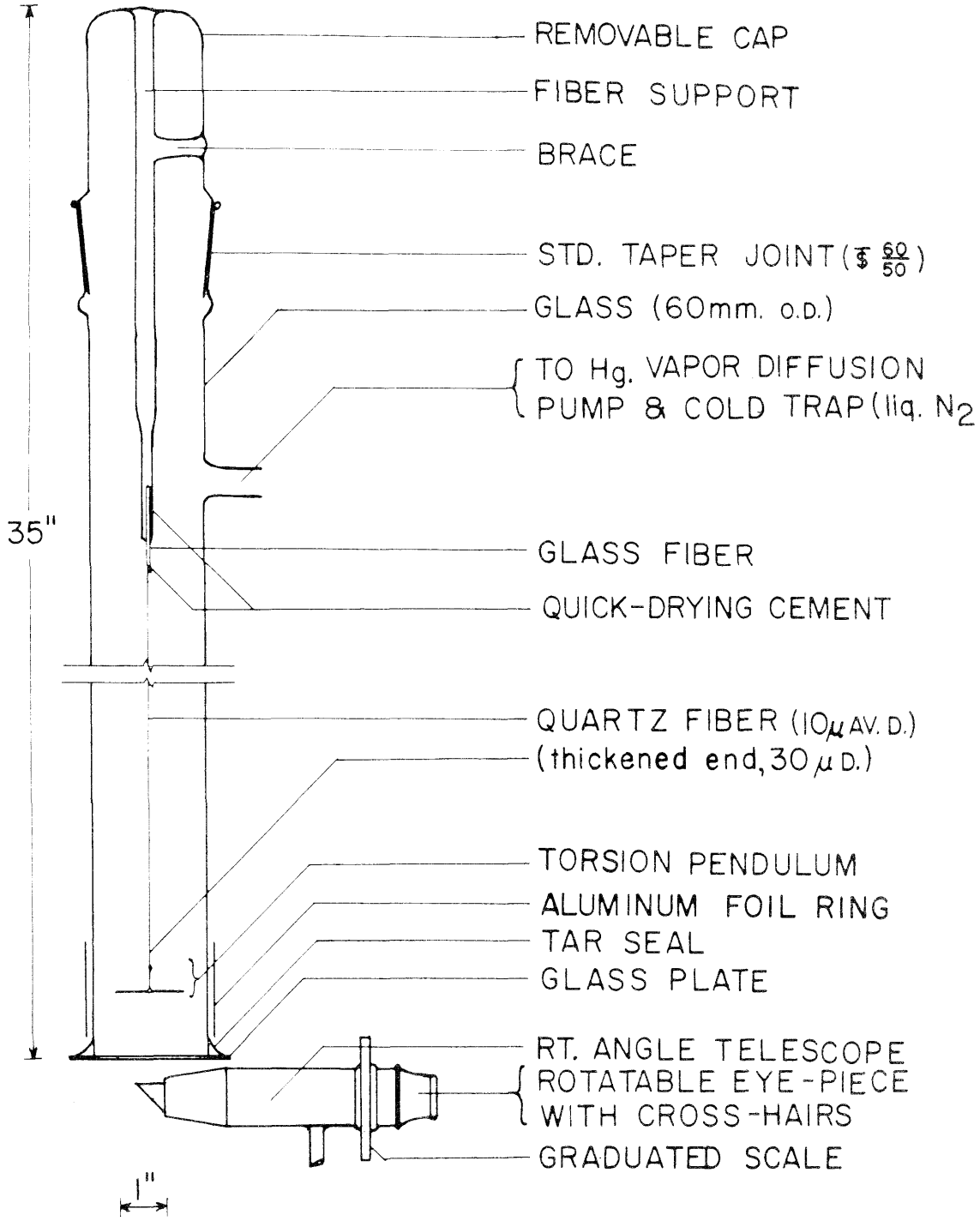

lum had made a few torsional cycles. The wobble then induced a small swinging which had to be stopped occasionally, by the method described above, as it interfered with the observation.

The damping of the oscillation was considerably reduced by the high vacuum. Within a few minutes after the diffusion pump began to operate the damping dropped below 1% per period; the damping usually reached its minimum value, 0.1% per period, after 12 hours. The usual precautions for the operation of high-vacuum systems[38] were observed. Since the viscosity of a gas at these low pressures increases with molecular weight, the vacuum chamber was first filled with helium before evacuation; this procedure also helped to remove residual CO_2 and water vapor which might otherwise condense in the liquid-nitrogen cold-trap.

A new source of error was then observed. When the amplitude of the pendulum was small (total energy small) the pendulum was noted to turn erratically with a considerably shortened period (by a factor of 2 or 3). The pendulum was also strongly influenced by objects, such as a finger, outside the vacuum chamber. The influence was obviously not magnetic and was not due to uneven molecular bombardment since a flame brought near the chamber wall had no particular effect. The influence was undoubtedly due to electrostatic fields since it could be considerably reduced by wrapping a strip of aluminum foil around the outside of the chamber; the pendulum was then no longer affected by outside objects but its period was still erratic for low amplitudes (less than 2 revolutions). Consequently, the period was always observed for amplitudes greater than 2 revolutions and usually from 10 to 30 revolutions. With large amplitudes and large angular velocities it was hoped that the time-average influence of the electrostatic forces was zero. The electrostatic forces did not disappear after several days under vacuum or even after months at atmospheric pressure. A small radioactive source consisting of a polonium-coated silver strip ("Staticmaster", Nuclear Products Co., El Monte, California), was placed on the bottom of the vacuum chamber but did not noticeably reduce the electrostatic effect.

The pendulum was observed though the clear bottom of the vac-

uum chamber using the right-angle telescope described previously (page 24). The cross-hairs were used both in the timing and in the measurement of the damping. The timer was driven by a synchronous electric motor and was started and stopped by pressing a button. (This type of timing device was found to be more accurate than ordinary mechanical stop-watches since the latter were usually out of adjustment!) The timer was graduated in intervals of 0.01 minutes and 0.001 minutes could be estimated. The reaction time of the observer proved to be the main source of error in the timing, but it is believed that the errors in starting and stopping the timer tended to cancel each other out. By timing the oscillation over several periods, the influence of this error was reduced.

As a reference point for timing the oscillation one could use the instant at which the pendulum stops and reverses its direction. This choice has the advantage that the period so obtained is independent of the damping. Observing the reversing point is made difficult, however, by the slowness of the movement near this point, particularly if the moment of inertia is large and the torsion constant and amplitude small, and by the unpredictability of the angular position ϑ at which the pendulum will stop. For timing based on visual observations it is preferable to use the instant at which the moving pendulum passes a marker at a given angular position, $\vartheta = C$. To use this method it is necessary, when the amplitude is greater than one revolution, that the observer be able to distinguish between $\vartheta = C$ and $\vartheta = C \pm 2N\pi$; that is, either the motion must be slow enough that each revolution can be counted or, if this is not possible, the decrease in amplitude with each period must be known with sufficient accuracy that it is only necessary to count the turns between the reversing point and $\vartheta = C$. Except for the special case $C = 0$ (fiber completely unwound), the interval between successive occurrences of $\vartheta = C$ is dependent on the damping. To obtain the true period, T, of the undamped oscillation by this method one may use the knowledge of the amount of damping either: (1) to calculate the amount by which the marker should be moved (C decreased) during each period so that the time interval between successive coincidences of pendulum and marker will be the true period; (2) calculate a cor-

rection to be added to this time interval, the marker remaining fixed. In practice it was convenient to use the marker (one of the cross-hairs in the telescope) to keep track also of the decrease in amplitude with each period; consequently, altering the position of the marker was undesirable.

The method of timing adopted used the fixed marker and a calculated correction. The mathematical analysis of the motion of the torsion pendulum will be presented in order to clarify both the method and the derivation of the correction.

The torsion pendulum is treated as a harmonic oscillator with damping proportional to its angular velocity. The differential equation of motion is equation 34 and the general solution of the equation is given by equation 35:

(34) $$I\ddot{\vartheta} + a\dot{\vartheta} = -K\vartheta$$

I = moment of inertia
ϑ = angular position
K = torsion constant (>0)
a = damping coefficient (≥ 0)
(dots indicate time derivatives)

(35) $$\vartheta = A.EXP(-at/2I).Cos(\omega t + d)$$

A, d = constants of integration.

where $$\omega^2 = (K/I) - (a/2I)^2$$

The form of the solution corresponding to a pendulum initially ($t=0$) at rest ($\dot{\vartheta} = 0$) at angular position $\vartheta = A_o$ is:

(36) $$\vartheta = (A_o/Cos\ d).EXP(-kt/T).Cos(\frac{2\pi t}{T} + d) \qquad \vartheta(t=0) = A_o$$

$$\dot{\vartheta} = -(A_o/T.Cos\ d).EXP(-kt/T) \times \left[k.Cos(\frac{2\pi t}{T} + d) + 2\ Sin(\frac{2\pi t}{T} + d)\right] \qquad \dot{\vartheta}(t=0) = 0$$

where d = phase angle = $\arctan(-k/2\pi)$
and k = logarithmic decrement = $aT/2I$
T = period = $2\pi/\omega$
} definitions

Equations 37 and 38 state that the timer is started at time t' and

when ϑ has decreased to $\vartheta = C$, and is then stopped at time $t'+nT-t''$ (the reading on the timer is $nT-t''$), after n full cycles, just as

$$(37) \qquad C = (A_o/\text{Cos } d).\text{EXP}(-kt/T).\text{Cos}\left(\frac{2\pi t'}{T} + d\right)$$

$$(38) \qquad C = (A_o/\text{Cos } d).\text{EXP}\left[-k(t'+nT-t'')/T\right].\text{Cos}\left[\frac{2\pi}{T}(t'+nT-t'') + d\right]$$

the pendulum crosses $\vartheta = c$. The quantity t'' is the error due to the fact that the timer was not stopped after an exact integral number of periods, but a bit too soon because of the damping. Equations 37 and 38 may be solved for t'' after making certain assumptions about the size of t'' and nk in order that the exponential term may be represented by the first two terms of the power series, and that t''/T may be treated as a differential in the cosine term. Equation 39

$$(39) \quad 0 \leq t''/T \leq 0.01: \qquad \text{Cos}\left[\frac{2\pi}{T}(t'-t'') + d\right] \cong \left(1 - t''\frac{d}{dt'}\right)\text{Cos}\left(\frac{2\pi t'}{T} + d\right)$$

$$= \text{Cos}\left(\frac{2\pi t'}{T} + d\right) + \frac{2\pi t''}{T}.\text{Sin}\left(\frac{2\pi t'}{T} + d\right)$$

$$0 \leq nk \leq 0.1: \qquad \text{EXP}\left[-k(nT-t'')/T\right] \cong 1 - nk \qquad (kt''/T \leq 0.01k, \text{ negligible})$$

$$0 \leq t'/T \leq \frac{1}{4}: \qquad 1 \geq \text{EXP}(-kt'/T) \cong 1 - (kt'/T) \geq 1 - 0.025$$

$$\text{Cos}^2 d = 1 + (k/2)^2 \qquad \text{(exact; from equation 36)}$$

[Substitute into equations 37, 38 and eliminate $\text{Cos}\left(\frac{2\pi t'}{T} + d\right)$]

outlines the solution and lists the approximations to be used. From the solution, equation 40, t'' may be calculated with an error less

$$(40) \qquad t'' = \frac{n\,k\,T}{2\pi\sqrt{(A_o/C)^2 - 1}}$$

than $\pm 10\%$. For example, if $n = 10$ periods, $k = 1.1 \times 10^{-3}$ ($nk < 0.01$), $A_o = 20$ revolutions, $C = 10$ revolutions and the final reading on the timer is $nT-t'' = 10.000 \pm 0.002$ minutes $\cong nT$, then t'' is 0.0010 minutes, the true period is $T = 1.0001 \pm 0.0002$ minutes, and $t''/T = 0.001$ (< 0.01).

As C approaches zero, t" vanishes as would be expected since $\vartheta = 0$ is the only definite value of ϑ for which the time $t(\vartheta)$ (see equation 35) is not affected by the damping. Incidently, as C approaches zero the angular velocity of the pendulum approaches a a maximum and the instant at which the pendulum crosses the hair-line is most sharply defined.

This method was used in connection with the simple correction, equation 40, with complete success. The restrictions (equation 39) that $0 \leq nk \leq 0.1$ and $0 \leq t''/T \leq 0.01$ limited the precision obtainable by limiting the number, n, of periods which could be averaged. In practice, the value of k was sufficiently small in all cases that the desired precision in T, $\pm 0.1\%$, was readily attained. If it had been desired to use larger values of n than were permitted by the restrictions, then it would have been necessary to use equations 37 and 38 to calculate t" more exactly. It is not always possible to make C arbitrarily close to zero to reduce t" and to simplify the calculation since the angular velocity of the pendulum may become so high that the turns cannot be counted.

It was found experimentally that the average deviation in the corrected duration of n periods (nT) was only a few thousandths of a minute. Apparently, in spite of the errors due to electrostatic forces and wobbling of the pendulum, the main errors were those due to operation of the timer and estimating the nearest thousandths of a minute. Experiments showed that if the instant of reversal of direction of the pendulum were used for timing, the uncertainty of visual observation would cause an average deviation upwards of 10 times this amount. The lowest average deviation in period, T, so far obtained is $\pm 0.015\%$ ($T = 1.3495 \pm 0.0002$ minutes, an average of 10 observations with n = 10-20, $k = 1\text{-}7 \times 10^{-3}$, $A_o/C = 3\text{-}4$). With a more symmetrical pendulum, a vacuum chamber of larger diameter (reducing electrostatic forces) and an electronic timer, the average deviation could probably be reduced to $\pm 0.001\%$ or less. However, the precision in the measurement of T using only the simple equipment was far greater than necessary for the magnetic anisotropy measurements.

No variation of the period of oscillation was noted from the first observation, less than an hour after the diffusion pump began

to operate, until the last observation, sometimes several days later. This seems to confirm the fact that the torsion constant is not affected by adsorbed layers of air or moisture. Further, it was observed that the period of oscillation was always independent of the amplitude provided, as noted above, the amplitude was greater than two turns. In one early experiment this dependence was examined over the range of amplitudes from 11 to about 200 turns; any change in period must have been less than the average deviation of 0.1% for all the observations. The damping constant was also found to be independent, within experimental error, of the amplitude (a distinction from metal wires[39]). The dependence of torsion constant on total linear tension was cursorily investigated by attaching a length of wire 2cm. long and weighing 17 mg. to the pendulum. The wire was attached with a small hook so that the wire hung parallel to the glass fiber and close to the axis of rotation; hence, the mass of the pendulum was doubled without significant increase in moment of inertia. No significant change in the period of oscillation was noted in this early experiment; the experiment was not repeated. Any change in torsion constant with tension is undoubtedly much less than 0.1% change for a doubling of the tension.

The "internal viscosity" of quartz fibers can be estimated from the damping of the pendulum[34,39]. The value of the viscosity coeffieient in terms of the pendulum experiment is given by:

$$(41) \qquad \eta = \frac{2aL}{\pi r^4} = \frac{4ILk}{\pi r^4 T} \quad ^{**}$$

L = length of fiber
r = radius .

Using the lowest value of k observed in this work and estimates or typical values of the other quantities ($k = 1\times10^{-3}$, $I = 0.01150$ g-cm^2, $T = 100$ sec., $L = 40$ cm, $r = 3\times10^{-4}$ cm), the internal viscosity is calculated to be $\eta = 1\times10^{9}$ cgs., which is about 1000 times the value given by Strong[34] and is about equal to that for an ordinary metal such as nickel. Either the observed damping is entirely due to the

**The expression given in references 34 and 39 differs by a factor of 2 since it uses the logarithmic decrement of only one-half of a period.

viscosity of the residual gas, or the "approximate" value of η given by Strong is over-optimistic.

The torsion constant is calculated from the expression in equation 35. This equation may be rewritten in terms of the period and the logarithmic decrement:

(42) $$K = \frac{(4\pi^2 - k^2) I}{T^2}, \qquad k < 2\pi \quad .$$

From this it is seen that if k = 0.1, it affects K by only $\frac{1}{40}$% and for the values actually observed (0.01 to 0.001) it is entirely negligible in this work.

i. Aging of Quartz Fibers.

Finally, an attempt was made to detect the influence of age on the torsion constant of individual fibers. Three experiments were made: (1) A fiber with pendulum attached was suspended in the vacuum chamber and the torsion constant was determined. The measurement was repeated one month and two months later. The fiber and pendulum were allowed to hang in the air-filled chamber in the interim. During each month the torsion constant decreased about 0.065% (0.8% per year). (2) A second quartz fiber was left suspended, with pendulum attached, in the air-filled chamber for a whole year after first determining its torsion constant. At the end of this time the torsion constant was found to have decreased 0.6%. (3) The fiber used for the collecting of most of the magnetic anisotropy data was also retested a full year after its first calibration. In this time it had been exposed to the open air under varying atmospheric conditions and varying stresses, but under a more or less average tension of 30 mg. Its torsion constant had also decreased, but only by 0.12%. Each fiber was freshly prepared when first calibrated. The conclusion is that there is a definite decrease in the torsion constants of quartz fibers with age, at least when they are under prolonged tension. The decrease is probably due to an elongation of the fiber

by plastic flow. For accurate work with quartz-fiber torque-measuring devices the fiber should be recalibrated periodically and the tension removed when the fiber is not in use.

Except for the fiber mentioned above which lasted over a year, the quartz fibers used for the magnetic anisotropy measurements lasted only one or two months before being broken. It is therefore concluded that the error in the magnetic anisotropy measurements to be reported, due to aging of the quartz fiber, is less than or equal to 0.1%.

C. Errors in the Anisotropy Measurements.

a. Introduction.

The errors to be discussed are in addition to those in weighing and orienting the crystals, in calibrating the quartz fiber and in measuring the magnetic field. They deal with stray forces and torques which act on a crystal suspended in a magnetic field, namely:

1. Air drafts and mechanical vibrations.
2. Torque due to ferromagnetic impurities.
3. Electrostatic forces.
4. "Asymmetry torque" dependent on the shape of the crystal.
5. Torque due to field inhomogeneity.

The methods of eliminating, correcting for, or estimating the magnitudes of the effects of these forces will be described. Since the experiments undertaken to define these sources of error were large in number and unsystematic, they cannot be described in detail. The second source of error listed above proved to be the most serious and required a revision of the experimental procedured used by Krishnan. The revised procedure is described at the end of section C after discussing the results of actual measurements in terms of the effects of the various sources of error and their elimination.

b. Air Drafts and Mechanical Vibrations.

The draft shield shown in figure 2 (section B) was found to be completely effective. The torsion apparatus was fastened to a structural wall of the building and mechanical vibrations were found to be negligible. No motion in a suspended crystal attributable to either of these causes was ever detected. Several times the possibility that drafts or vibrations might cause a crystal to prematurely exceed ϑ_{cr} was tested by suspending a crystal in a magnetic field and twisting the quartz fiber to within 5 or 10 degrees of α_{max}; in some cases α_{max} exceeded 100 revolutions. Under these conditions no crystal was ever observed to begin to spin spontaneously. Whenever the crystal did begin to spin, the torsion head was always simultaneously in motion in the same direction.

c. Ferromagnetic Impurities.

It was discovered before any anisotropy measurements had been made that the magnetic field exerted a considerable torque, of order of magnitude 10^{-4} to 10^{-3} cm-dynes at 10 kilogauss, on the main supsport fiber alone with nothing attached. Since this range of torques overlapped the range (10^{-4} to 10^{-2}cm-dynes) of torques reasonably expected to be encountered in diamagnetic anisotropy measurements, the nature of this added torque was investigated extensively. The torque on the glass fibers was noted even when a short length was suspended entirely within the most homogeneous part of the magnetic field. Under these conditions there could be no appreciable effect due to inhomogeneity of the field or to asymmetry of the object. Although in the absence of a magnetic field the glass fibers turned smoothly as the torsion head was turned, when the magnetic field was turned on they appeared to behave like an anisotropic crystal; they had two positions of equilibrium approximately 180° apart and ϑ_{cr} was generally in the range 45° to 90°. The torque varied greatly with the different glass fibers.

The possibility of ferromagnetic surface impurities was at first rejected when it was found that washing the fibers with strong mineral acids including hydrofluoric acid did not eliminate the

torque. The possibility of an intrinsic anisotropy of the glass induced by drawing the fibers was considered even though the observed anisotropy was in the plane perpendicular to the direction of drawing which would be expected to be isotropic. Glasses from various sources and of various kinds were tried (including sodium phosphate and sodium borate glasses) and various drawing and heat-treating techniques were tried without conclusively demonstrating a method of reducing or eliminating the anisotropy.

The presence of ferromagnetic surface impurities was then reinvestigated. An experiment to determine the dependence of the apparent anisotropy on field strength showed α_{max} to be proportional to $H^{1/2}$ over the range 0-8½ kilogauss; that is, the torque tended toward a constant value at high field strengths. Such a phenomenon cannot be attributed to any ordinary paramagnetic or diamagnetic anisotropy. It is, however, the effect observed with ferromagnetic objects with either intrinsic or shape anisotropy[40]. It was then found that the anisotropy of the glass fibers was decidedly reduced, but not eliminated, if the glass rods from which the fibers were drawn were cleaned and washed with hydrofluoric acid before the fibers were drawn. Finally, in an experiment in which a fairly isotropic glass fiber was purposely allowed to hang suspended in open air (draft shield cap removed) for a day, it was found after this time that its apparent anisotropy had increased. These results are interpreted as meaning that the apparent anisotropy of the glass fibers is caused by bits of ferromagnetic dust which have settled on the fiber or were fused into the fiber during the drawing. Since the magnetic torque acting on a ferromagnetic crystals may be many millions of times greater than on a diamgnetic crystal of the same mass, it may be reasoned that the observed anisotropy of the fibers could be caused by a few particles of iron of about 0.001 micrograms in mass (approximately one-half micron in diameter). The increase in the anisotropy in the experiment described above can only be ascribed to the settling of a dust particle on its surface (another incident of this nature will be described on page 74). The fact that the anisotropy of the fibers was unaffected by acids, including hydrofluoric, is attributed to the fusing of the impurities deeply

enough into the glass so that they were not removed by superficial washing. Attempts to detect hysteresis due to "hard" ferromagnetic impurities were inconclusive.

The conclusion that ferromagnetic impurities are present is further strengthened by the reports of workers in related fields. Constant and Formwalt[41] investigated the existence of volume-distributions of ferromagnetic impurities in various isotropic nonferromagnetic substances, mostly metals. Their technique was different from that used above; they essentially measured the torque exerted by a homogeneous magnetic field (up to 1000 gauss) as a function of angular position of the test object. Their results are given in terms of the calculated magnetic dipole moment per unit volume, I, of the specimen. The torque exerted by a uniform field on a dipole is $IVH \cdot \mathrm{Sin}\vartheta$, where V is the volume of the specimen and ϑ is the angle between the dipole axis and the direction of the field, $\underset{\sim}{H}$. By their technique they were able to detect both "hard" and "soft" ferromagnetic components. They could detect a volume-moment as small as $I = 2 \times 10^{-7}$ cgs; the volume-moments they ordinarily encountered were in the range 10^{-4} to 10^{-6} cgs. The volume-moment was determined only after the specimens had been etched with acid to remove surface impurities and a constant moment had been obtained. Constant and Formwalt do not give an estimate of the contribution of surface impurities but say only that a "sharp drop" in the observed moment occurred when the surface was dissolved away. They were unable, however, to detect a volume-magnetic-moment in either soft glass or pyrex. An estimate of the magnetic moment actually observed in the present work with (pyrex) glass fibers (torque $\cong 10^{-3}$ cm-dynes; $H \cong 10^{5}$ gauss; volume $\cong 10^{-3}$ cm^3; $\mathrm{Sin}\vartheta = \mathrm{Sin}45^{\circ} = 0.7$ **) is $I = 10^{-5}$ cgs, which is considerably above the minimum detectably by Constant and Formwalt; the observed moment is therefore undoubtedly due to <u>surface</u> impurities only.

The effect of ferromagnetic impurities on measurements of magnetic susceptibilities has been considered by Bates[42].

** Since the observed torque was more nearly proportional to $\mathrm{Sin}2\vartheta$, the impurities did not behave as dipoles. This calculation is merely for illustration.

Selwood[43] reports observations of a weak magnetic anisotropy in glass fibers in a plane containing the fiber axis and compares the anisotropy of magnesium sodium silicate glass and nickel sodium silicate glass. The higher observed anisotropy of the nickel glass was attributed to an effect on the spin-orbital coupling of the electrons in the nickel atoms produced by crystalline electrostatic fields made asymmetric by the drawing procedure. In view of the observations on ferromagnetic impurities discussed above, this conclusion appears doubtful; it is certain that no such effect produced the apparent anisotropy of glass fibers discussed above.

The magnitude and variability of the effect of ferromagnetic impurities, the inability to estimate their amount or to remove them, and the suspicion that they may be present on or in the crystals to be tested as well as on the glass fibers demanded that they be considered. The following analysis was made.

The dependence of the observed torque, due to ferromagnetic impurities, on field strength and angular position is approximately:

$$L_f = F H^{1/2} \sin 2(\vartheta - \vartheta_f) \qquad (43)$$

For fixed angular position the torque increases about proportional to $H^{1/2}$, at least below 10 kilogauss, and at higher field strengths becomes nearly constant. For fixed field strength, the ferromagnetic impurities apparently behave like a second anisotropic crystal attached to the specimen under investigation; the parameter ϑ_f reflects the fact that the torques due to ferromagnetic impurities and to crystal anisotropy need not act in phase. The dependence of α on ϑ for an anisotropic crystal containing ferromagnetic impurities would then be:

$$\alpha - (\vartheta - \vartheta_0) = A H^2 \sin 2\vartheta + F H^{1/2} \sin 2(\vartheta - \vartheta_f) \qquad (44)$$

$$\alpha(\vartheta_0) = 0 \qquad \text{(see figure 9)}$$

The right half of equation 44 is a periodic function of ϑ, with period π. For fairly large values of α (several revolutions) the term $(\vartheta - \vartheta_0)$ on the left will have negligible effect on ϑ_{cr}

FIG. 9 EFFECT OF FERROMAGNETIC IMPURITIES.

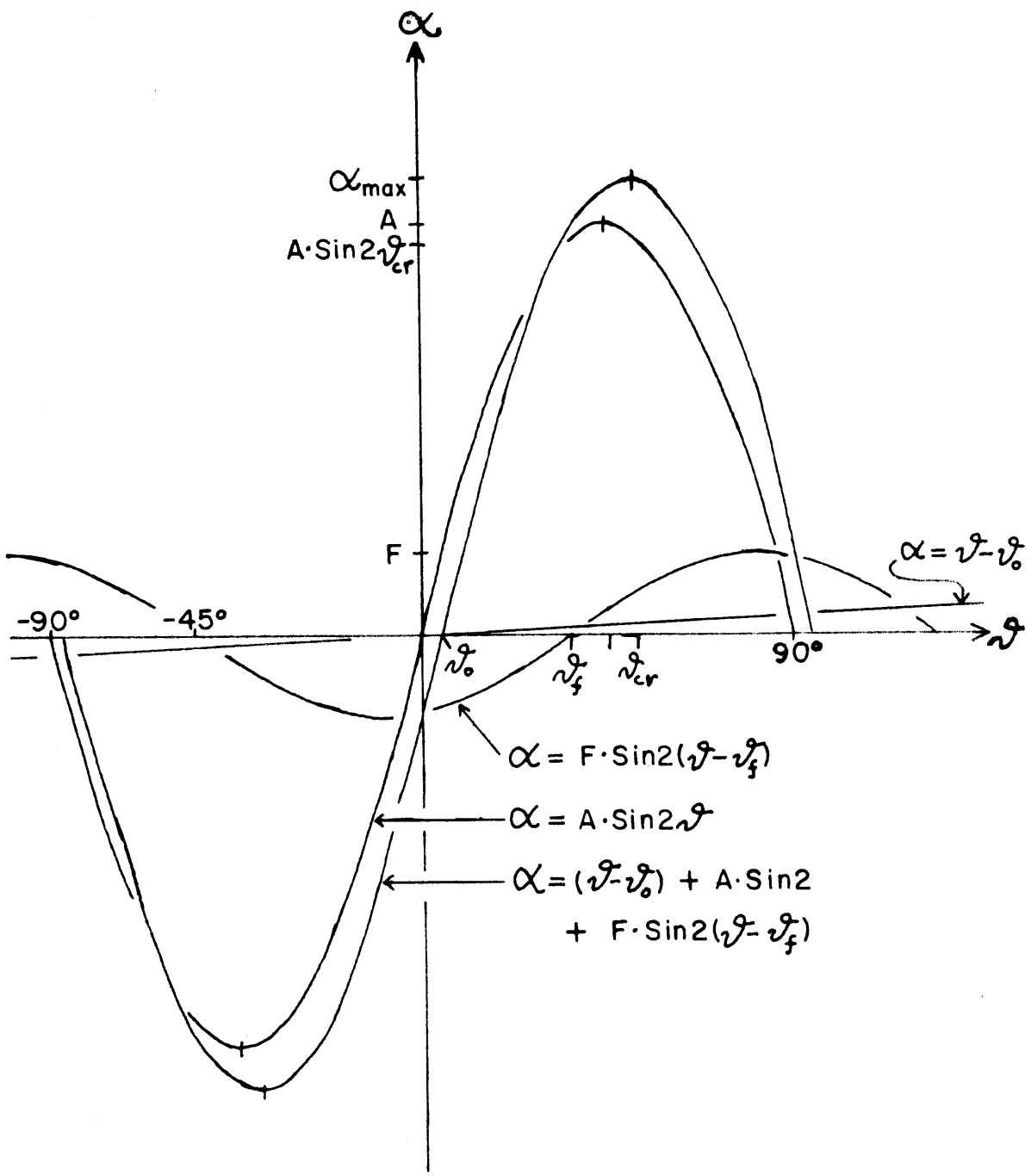

which will therefore still occur at intervals of $\pi/2$; hence, for opposite directions of rotation, α_{max} will differ by about $2\vartheta_o$, that is, by less than 90^o.

At sufficiently high field strengths the torque due to crystal anisotropy (proportional to H^2) will far exceed that of the ferromagnetic impurities. Under this condition, ϑ_{cr} will be determined by the crystal anisotropy and will not differ appreciably from 45^o (special cases 1 and 2, section B). If the empirical relation, equation 44, is correct, then when $(\alpha_{max} - \pi/4)$ is plotted against H^2 over a short range of values of H^2, for both directions of rotation of the torsion head and both initial equilibrium positions of the crystal, two straight lines with equal slopes, separated only slightly ($\Delta\alpha_{max} = 2\vartheta_o$), should be obtained. Extrapolation of the straight lines to $H^2 = 0$ should in general give intercepts $(\alpha_o - \pi/4)$ different from zero and with equal probability of having positive or negative values. The magnetic anisotropy may be calculated from the slope of the straight lines, $A \cdot \mathrm{Sin}2\vartheta_{cr} \cong A$.

At lower field strengths it may occur that L_f is still practically independent of the field strength but no longer small compared to the torque due to crystal anisotropy. Then ϑ_{cr} will be determined to some extent by the ferromagnetic impurities and will no longer be at $45^o \pm (N\pi/2)$. The magnetic anisotropy calculated from the slope of the straight lines $(\alpha_{max} - \pi/4)$ vs. H^2 will be too large if the factor $\mathrm{Sin}2\vartheta_{cr}$ is not evaluated and used. Graphical analysis (see figure 9) suggests that $FH^{1/2}$ may be a considerable fraction of AH^2 with only slight effect on $\mathrm{Sin}2\vartheta_{cr}$. Since ϑ_{cr} will be slightly dependent on field strength, a slightly curved line rather than a straight line would be obtained when plotting the data; fitting a straight line to the data points would introduce new errors.

For still lower field strengths, where the ferromagnetic torque becomes strongly field-dependent and of the same order of magnitude as the torque due to crystal anisotropy, chaos will occur. The contribution of ferromagnetic impurities will vary from sample to sample and ϑ_{cr} as well as L_f will be field-strength-dependent. When $(\alpha_{max} - \pi/4)$ is plotted against H^2 for both initial positions and directions of rotation, the data points will be scattered about the

correct straight line, perhaps widely. If the ferromagnetic impurities act out of phase with the crystal anisotropy the data points may lie far below the line; if they act in phase the data points may lie far above the line. The effect of ferromagnetic impurities on ϑ_o, the initial position of the crystal, will generally cause negligible error since this quantity appears in the calculations only in the difference $(\alpha_{max} - \vartheta_{cr} - \vartheta_o)$.

The ratio of the contributions of crystal anisotropy and ferromagnetic impurities will depend on the size and anisotropy of the crystal. For highly anisotropic substances ($\Delta X^* > 100 \times 10^{-6}$ cgs/mole), such as anisotropic paramagnetic substances or conjugated polynuclear hydrocarbons, it may be expected that the error caused by ferromagnetic impurities will be small, even at fairly low field strengths, for crystals larger than 0.5 milligrams.

In the literature on magnetic anisotropy measurements, references to the precision of the measurements are exceedingly few, and seldom is enough information (such as crystal size, or largest value of α_{max} and the torsion constant) given to judge whether ferromagnetic impurities were a source of error. However, there is no report of field strengths in excess of 10 kilogauss being used, most measurements being made in the range 4 to 8 kilogauss and many simply by observing α_{max} at a single field strength. The reason that ferromagnetic impurities have not been noticed earlier is probably that whenever tests were made to determine whether a torque was exerted on an isotropic object, they were always under conditions such that any torque observed could be attributed to some other effect, such as field inhomogeneity.

In view of the magnitude of the ferromagnetic torque it was feared, in spite of apparent success of other workers, that the deviation in anisotropy measurements with different samples might be as much as $\pm 10 \times 10^{-6}$ cgs/mole, that is, 100 times larger than was wanted. Hope for more reliable results lay in the use of high field strengths. Consequently, a series of experiments on weakly anisotropic $KClO_3$ crystals was carried out to verify the conclusions of the previous paragraphs. The results of these experiments will be discussed below.

d. Electrostatic Forces.

The magnitude of the error caused by electrostatic charges was initially passed off as negligible. Later observations forced a revision of this opinion. Indeed, perhaps the only suggestion of low reproducibility in a measurement of magnetic anisotropy to be found in the literature is undoubtedly due to this effect[44].

Electrostatic charges seem to reside on the glass walls of the draft shield or on the crystal. Their presence is evidenced by their ability to exert a torque, commonly 2×10^{-4} cm-dynes and occasionally as large as 10×10^{-4} cm-dynes, in the absence of a magnetic field (magnet poles depolarized and withdrawn). In the worst cases, the suspended specimens were affected by objects outside the draft shield. The influence of the electrostatic charges seemed to be greater on unionized organic substances than on ionic inorganic substances and also greater on specimens which were large and nearly touched the walls of the draft shield than on smaller specimens. The electrostatic torque probably also depended on the shape of the crystal and on the geometry of the mounting.

The potential energy of the crystal due to the electrostatic charges was usually observed to have only a single minimum at a more or less definite angular position but occasionally had a less pronounced minimum about 180° away. An empirical function roughly approximating the behavior of the electrostatic torque is:

$$L_e = E \cdot \mathrm{Sin}(\vartheta - \vartheta_e) \qquad (45)$$

Using this approximation and assuming no other stray torques are acting, it is predicted that if α_{max} were determined at fixed field strength for both directions of rotation and both initial equilibrium position of the crystal, four slightly different values would be obtained. If the torque function remained about constant then plotting $(\alpha_{max} - \pi/4)$ against H^2 should give four parallel non-coincident straight lines; if the electrostatic torque varied randomly with time then the data points would be scattered about one (or four) straight lines(s). If the electrostatic torque were so strong that there were uncertainty about whether or not the quartz

fiber were completely unwound initially, as was practically never observed, then the data points might be scattered widely about the straight line(s).

For weakly anisotropic substances and/or small specimens, any uncertainty or scatter in the data is undesirable. Lining the inside of the draft-shield cap with aluminum foil did not eliminate the electrostatic effect. A tiny radioactive source, in the form of a strip (2x5 mm) of silver (diamagnetic) coated on one side with polonium, was then placed inside the draft-shield cap in the proximity of the crystal. This radioactive source is a commercial product devised for just such problems and was mentioned in section B (page 45). The radioactivity did not eliminate the electrostatic effect entirely and its effectiveness has not been thoroughly tested since it was introduced only after most of the magnetic anisotropy measurements had been made. However, in the three cases in which it was used (see below, page 75), there was noted only very little torque at zero magnetic field and also a decrease in the scatter of the data points ($\alpha_{max} - \pi/4$) vs. H^2 about straight lines.

e. Asymmetry Torque.

Consider a rectangular prism of anisotropic substance with cross section as shown in figure 10. The dimensions of the plate are $L_1 x L_2 x L_3$ and the areas of the faces are A_1, A_2 and A_3. The plate is placed in a magnetic field which was initially uniform with direction parallel to A_3 (parallel to plane of paper).

The field inside and outside the plate will be referred to orthogonal axes parallel to the edges of the plate. For convenience, it will be assumed that these coordinate axes are identical with the principal magnetic axes of the substance. For a plate sufficiently thin ($L_2 \simeq 0$) and broad (L_1, L_3, A_2 large) the component H_1' of the field inside the plate is unaffected by the polarization charges on the two faces A_1 and may be taken equal to $H_1 = H \cdot \cos\vartheta$, the corresponding component outside the plate. The component H_2' of the field inside the plate and perpendicular to the broad faces A_2 may

be considered equal to the sum of the corresponding component outside the plate and the contribution, $4\pi\sigma_2$, due to the polarization charge density σ_2 on the faces A_2. Since the interior field is parallel to the faces A_3, no polarization charge is induced on them to affect the calculations. The surface charge densities, σ_1 on A_1 and σ_2 on A_2, are equal to the components of the magnetization, $\underset{\sim}{M} = X_1\underset{\sim}{H}_1' + X_2\underset{\sim}{H}_2'$, normal to the faces; hence $\sigma_1 = X_1H_1' = X_1H_1$, and $\sigma_2 = X_2H_2' = X_2H_2/\mu_2$, where $\mu_2 = 1 + 4\pi X_2$.

The torque acting on the plate may be calculated by use of equation 13. Since H and M are constant inside the plate, $\nabla\cdot\underset{\sim}{M} = 0$

FIGURE 10.

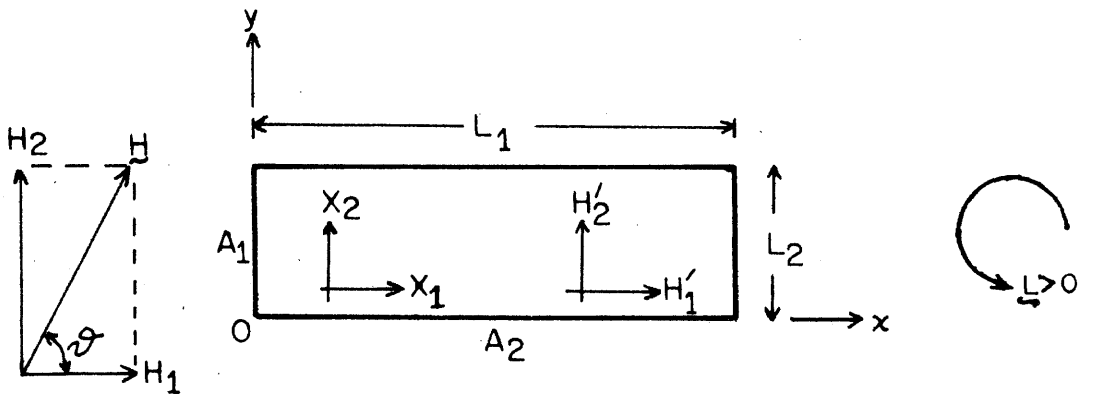

and the first integral in equation 13 vanishes; the second integral is the interaction of magnetic polarization charges on the surface with the tangential field, the effect of the normal field component vanishing. The torque L is caused by two pairs of equal but oppositely directed parallel forces, $H_1\sigma_2A_2$ and $H_2\sigma_1A_1$, separated by distances L_2 and L_1 respectively; such a set of forces forms a torque-couple which is independent of the location of the axis of rotation. The approximation is being made here that the variation in H_1 and H_1' near the edges of the plate is negligible.

$$(46) \qquad L = -H_1L_2A_2(X_2H_2/\mu_2) + H_2L_1A_1(X_2H_2)$$

$$= (H^2V/2\mu_2)(X_1 - X_2 + 4\pi X_1X_2)\,\mathrm{Sin}2\vartheta$$

$$(V = L_1A_1 = L_2A_2;\quad \rho = m/V = \text{density};\quad X = \rho X^*/W)$$

$$L = (H^2 m/2W\mu_2)(X_1^* - X_2^* + 4\pi\rho X_1^* X_2^*/W)\ \mathrm{Sin}2\vartheta$$

The torque-couple acting on the plate, tending to turn it about an axis perpendicular to A_3, is then given by equation 46. The part of the torque which depends on the difference $(X_1^*-X_2^*)$ is the contribution of magnetic anisotropy which it is desired to measure; the term involving the product $X_1^*X_2^*$ is the error caused by the non-spherical shape. The largest value of $4\pi\rho X_1^* X_2^*/W$ encountered in this work (anthracene) was 1.9×10^{-9}cgs. The precision desired in the determination of $(X_1^*-X_2^*)$ was $\pm10^{-7}$cgs. The conclusion is that for the range of susceptibilities encountered in this work asymmetry torque caused negligible error.

If the principal magnetic axes of the substance (figure 10) were in a completely general configuration, the expression for the asymmetry torque would be more complicated but the conclusion would be unchanged.

A similar calculation can be more or less easily made for other simple shapes. For the limiting cases of oblate and prolate ellipsoids of revolution[45] in which the oblate ellipsoid approaches a disk or the prolate ellipsoid approaches a needle, the torque in a uniform field, for an isotropic substance, is $(2\pi VH^2X^2/\mu)\mathrm{Sin}2\vartheta$, a value identical with that derived from equation 46 for an isotropic plate. The asymmetry torque decreases from this value as the object becomes more spherical.

f. Field Inhomogeneity.

Again consider a rectangular plate of anisotropic substance with dimensions and orientation of principal axes as shown in figure 10. Let the magnetic field be parallel to A_3 (plane of the paper) but no longer constant; in particular, let the components of the field have initially the simple linear dependence on position given in equation 47. The field defined by equation 47 is the simplest non-constant field such that Curl $\underset{\sim}{H} = 0$, that is, such that no electric currents are present in the region.

$$H_1 = H_o\left[\mathrm{Cos}\vartheta + a(x\mathrm{Sin}2\vartheta - y\mathrm{Cos}2\vartheta)\right]$$

$$H_2 = H_o\left[\mathrm{Sin}\vartheta - a(x\mathrm{Cos}2\vartheta + y\mathrm{Sin}2\vartheta)\right]$$

(47)

$$\mathrm{Curl}\ \underset{\sim}{H} = 0$$

$$\mathrm{Div}\ \underset{\sim}{M} = a(X_1 - X_2)H_o\mathrm{Sin}2\vartheta$$

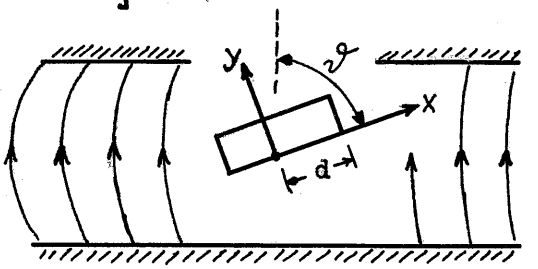

The torque exerted by the field about an axis parallel to L_3 (perpendicular to the plane of the paper) and lying in a face A_2 will be calculated using the most general form of equation 13. Let the origin of the x-y coordinate system (fig. 10) be shifted by a distance L_1-d $(0 \leq d \leq L_1)$ along the x-axis and let the axis of rotation pass through x=0, y=0. The previous remarks concerning the field strength inside and outside the plate still apply, as a reasonable approximation, but since the difference between exterior and interior field gives rise only to negligibly small terms involving the product X_1X_2, the difference will be neglected in this calculation. Finally, the dimension L_2 will not, as previously, be assumed infinitesimal compared to L_1. The calculation is outlined in equation 48.

$$L = aH_o(X_2 - X_1)\mathrm{Sin}2\vartheta \int_0^{L_2}\int_{d-L_1}^{d} (xH_2 - yH_1)L_3\,dx\,dy$$

$$+ X_2 \int_{d-L_1}^{d} (xH_2 - L_2H_1)H_2L_3\,dx\Big|_{y=L_2} + X_1 \int_0^{L_2} (dH_2 - yH_1)H_1L_3\,dy\Big|_{x=d} \tag{48}$$

$$+ X_1 \int_0^{L_2} \left[yH_1 + (L_1 - d)H_2\right]H_1L_3\,dy\Big|_{x=d-L_1} - X_2 \int_{d-L_1}^{d} xH_2^2L_3\,dx\Big|_{y=0}$$

In carrying out the integration indicated in equation 48, it will be assumed that the constant "a", which is the measure of the field inhomogeneity, is small enough that terms involving a^2 may be neglected. The result of the calculation, after converting to molar susceptibilities is:

$$L = (mH_o^2/2W)\left[\left\{(X_1^*-X_2^*) + a(2d-L_1)(3X_1^*-2X_2^*)\sin\vartheta - aL_2(2X_1^*-3X_2^*)\cos\vartheta\right\}\sin 2\vartheta - a(2d-L_1)(2X_1^*-X_2^*)\cos\vartheta + aL_2(X_1^*-2X_2^*)\sin\vartheta\right] . \quad (49)$$

Let D be the largest value, for all ϑ, of the fractional change in the field strength across a distance equal to the larger of the two dimensions L_1 and L_2. Let X^*_{max} be the principal susceptibility, X_1^* or X_2^*, having the larger absolute value. Then the maximum value of either $a(2d-L_1)$ or aL_2 is D, and the maximum values of $3X_1^*-2X_2^*$ and $2X_1^*-X_2^*$ are less than $3X^*_{max}$ and $2X^*_{max}$ respectively. The values of X^*_{max} encountered in this present work ranged mainly from -30 to -50×10^{-6} cgs/mole. A reasonable estimate of D for the size of crystal used, based on cursory measurements of the variation in field strength between the magnet poles, is $D = 0.001$. Hence, each of the terms in equation 49 involving the field inhomogeneity are of the order of magnitude 0.1×10^{-6} cgs/mole, the range to which it was originally desired to restrict all errors.

When DX^*_{max} is small compared to $X_1^*-X_2^*$, ϑ_{cr} will be determined mainly by the crystal anisotropy and will not differ appreciably from $45^\circ \pm N\frac{\pi}{2}$. The field inhomogeneity will cause an apparent variation in the anisotropy for different directions of rotation and different initial equilibrium positions. Hence, if $\frac{2KW}{m}(\alpha_{max}-\pi/4)$ vs. H^2 were plotted for both initial positions and both directions of rotation, four straight lines with slightly different slopes would be obtained. However, the terms in equation 49 which involve the field inhomogeneity would cancel out on averaging the four slopes, giving the true anisotropy. This conclusion remains valid if the principal axes in figure 10 are in a completely general orientation and is believed to be at least approximately true for a crystal of more

general shape.

The type of field inhomogeneity assumed in this illustrative example is believed to be a good approximation whenever the fluctuations in field strength are not too rapid and whenever a sufficiently small crystal is used.

g. Summary.

In equation 50, the torque due to crystal anisotropy is combined with empirical relations for the effects of the asymmetry torque, field inhomogeneity, ferromagnetic impurities and electrostatic forces, assuming a completely general shape for the crystal.

$$L = \frac{mH^2}{2W}\left[\left\{(X_1^*-X_2^*) - S\left(\frac{4\pi\rho}{W}X_1^*X_2^*\right) + 3DX^*_{max}G_1(\vartheta)\right\}\mathrm{Sin}2\vartheta + 2DX^*_{max}G_2(\vartheta)\right] + FH^{1/2}\mathrm{Sin}2(\vartheta - \vartheta_f) + E\,\mathrm{Sin}(\vartheta - \vartheta_e) \qquad (50)$$

The parameter S takes values in the range $0 \leq S \leq 1$. The functions $G_1(\vartheta)$ and $G_2(\vartheta)$ are periodic (period 2π), of the order of magnitude of unity, and such that $G_1(\vartheta+\pi) \cong -G_1(\vartheta)$ and $G_2(\vartheta+\pi) \cong -G_2(\vartheta)$.

h. Experimental Observations.

A series of measurements over a wide range of field strengths, from 3 to 21 kilogauss, was carried out on crystals of weakly anisotropic $KClO_3$ (monoclinic). The crystals were weighed, mounted and attached to the torsion apparatus as described in section B. The b

axis was the axis of rotation**. The three crystals used weighed about 7 mg.; the torsion constant of the quartz fiber was 2.300×10^{-5} cm-dynes/radian. The observed values of $\frac{2KW}{m}(\alpha_{max} - \pi/4)$ are plotted against H^2 in figures 11 and 12 where the units of α_{max} are radians*** and those of field strength are kilogauss; the slope of a straight line on such a graph is numerically equal to the anisotropy involved, the factor 10^{-6} being omitted.

In figure 11 all the data points are referred to the same origin and, for clarity, the points are not labeled to distinguish between different samples or directions of rotation. Through the origin is drawn a straight line with a slope of 1.09 (see below); it is seen that this line is approximately the one which would have been fitted to the data points either visually or by a least-square averaging process. The data points are scattered about this line quite widely even at high field strengths. The slopes of straight lines drawn connecting the various data points with the origin range from 0.5 to 4.0 cgs. and if measurements had been confined to field strengths less than 10 kilogauss ($H^2 < 100$), deciding on the correct slope would be mainly a matter of guessing. At low field strengths, even though some of the points are quite near the line, there is a set of four points which deviate widely from the line. The curved arrow indicates that the observations on a single specimen represented by these four points were continued to higher field strengths. The manner in which the function $(\alpha_{max} - \pi/4)$ vs. H^2 changed in this region for the particular specimen, also indicated by the arrow, is precisely the type of behavior predicted for the case in which ferromagnetic impurities interfere strongly. It is felt that the data in figure 11 confirm the previous conclusions concerning the effects of ferromagnetic impurities at low field strengths and justify the use of the higher field strengths.

** The specimens were later discovered to be twinned by reflection on (001), resulting in nearly perfect orthorhombic symmetry instead of the true monoclinic symmetry. This fact does not affect the conclusions made here and is discussed more fully in section D.

***An impression of the size of α_{max} may be obtained by imagining the crystal to be suspended by a fiber of torsion constant $1/(4000\pi) = 7.96 \times 10^{-5}$ cgs, a value well within the range actually used; then α_{max} may be imagined to be plotted in units of revolutions per millimole along the vertical axis. The crystals used here and in later experiments ranged about one-tenth millimole in size.

FIG. 11 MAGNETIC ANISOTROPY DATA FOR $KClO_3$.

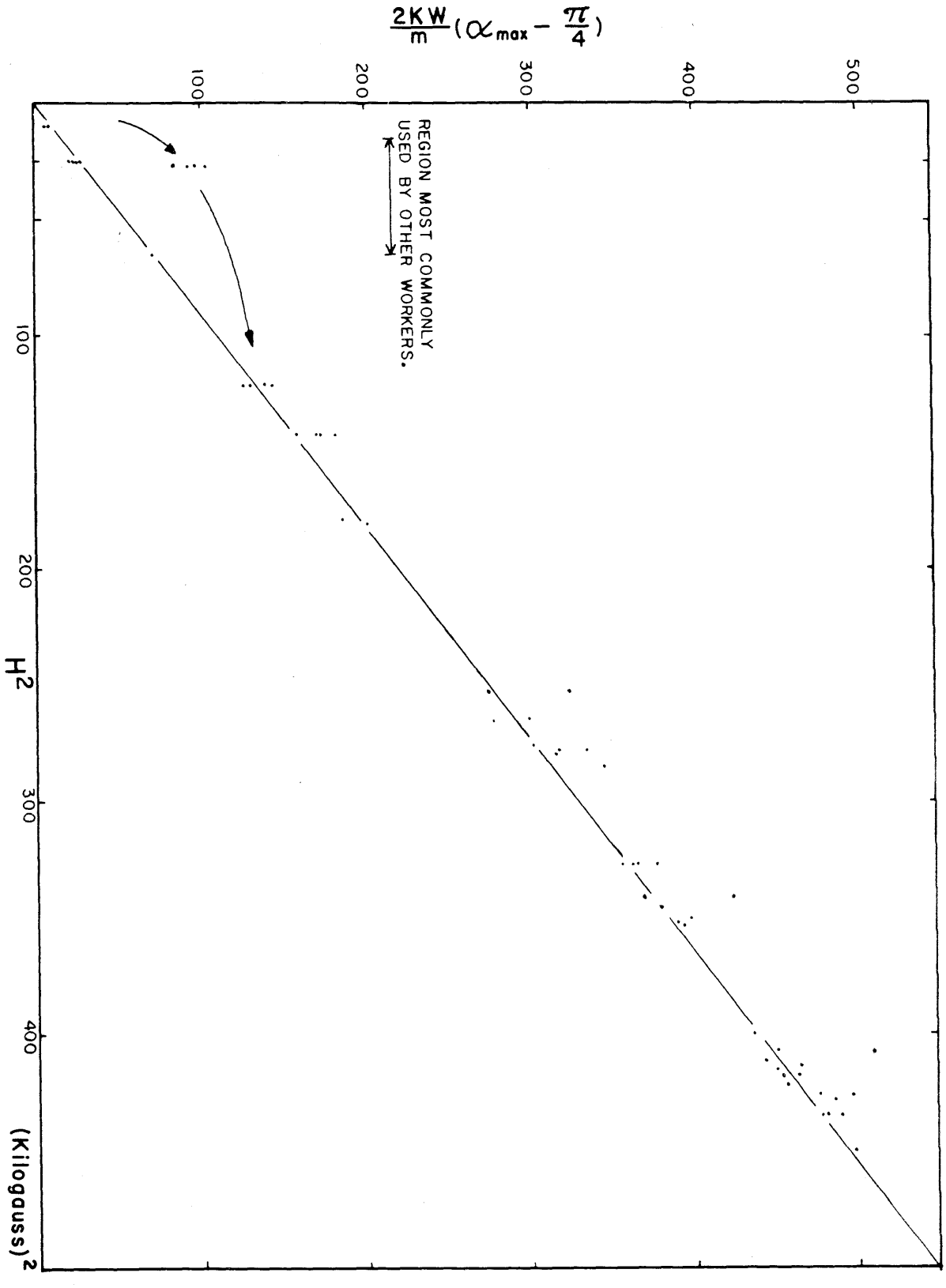

FIG. 12 MAGNETIC ANISOTROPY DATA FOR $KClO_3$.

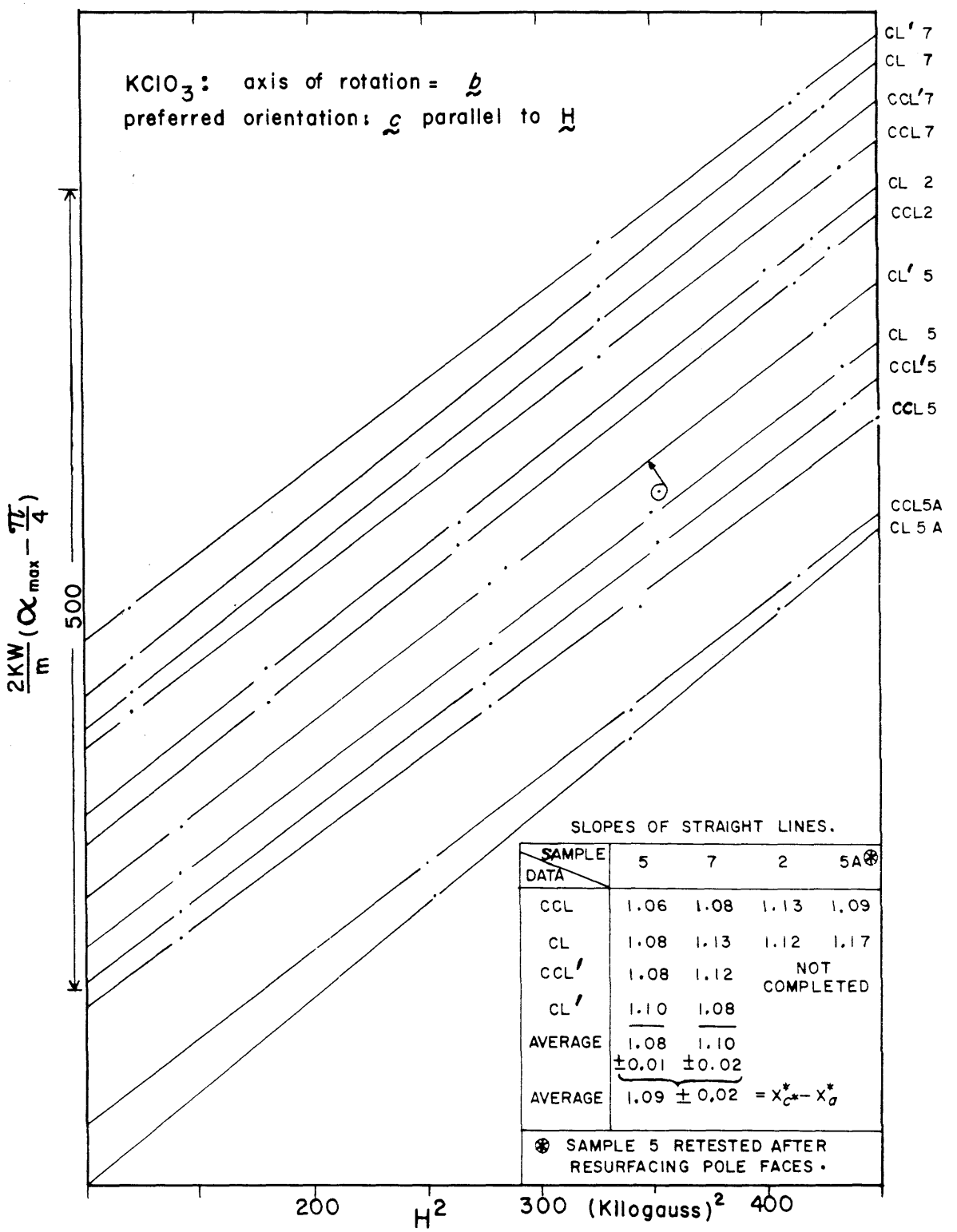

SLOPES OF STRAIGHT LINES.

SAMPLE / DATA	5	7	2	5A⊛
CCL	1.06	1.08	1.13	1.09
CL	1.08	1.13	1.12	1.17
CCL′	1.08	1.12	NOT COMPLETED	
CL′	1.10	1.08		
AVERAGE	1.08 ±0.01	1.10 ±0.02		
AVERAGE	1.09 ± 0.02		$= X^*_{c^*} - X^*_a$	

⊛ SAMPLE 5 RETESTED AFTER RESURFACING POLE FACES.

In figure 12, the data between 10 and 21 kilogauss are plotted again. The points corresponding to different samples, directions of rotation and initial positions are separated by moving the origin arbitrarily along the vertical coordinate axis so that straight lines may be fitted to the data points and labeled without crowding. The designations CL, CCL, CL' and CCL', followed by a number, are used to identify each line according to direction of rotation (clockwise or counterclockwise), initial equilibrium position and sample number. Although the data points seem quite scattered in figure 11, in figure 12 it is seen that they fit the separate straight lines very closely. One data point (indicated by a circle with an arrow pointing to its proper location) deviates widely from the assigned straight line; since such deviations are not general, a mistake in reading the turn counter is believed to have occurred. Smaller deviations are probably due to uncertainy in the field strengths measurements and to fluctuations in the electrostatic torque. The straight lines do not in general extrapolate through the origin. The table attached to figure 12 gives the numerical value of the slope of each line. The average slope for the two completed sets of measurements, 1.09 $\pm$0.02 ($\times 10^{-6}$) cgs., is taken as the correct value of the anisotropy involved.

Observations of the initial equilibrium positions and of ϑ_{cr} showed that above 5 kilogauss they remained constant within 2° but varied considerably at lower field strengths, changing as much as 20°-30° at 1 kilogauss. This fact also agrees with the predictions of the effects of ferromagnetic impurities at low field strengths.

The reproducibility of α_{max} at constant field strength and for given initial position and direction of rotation was also tested several times. To do this the magnet was moved away after each observation to allow the quartz fiber to unwind completely and then moved back. By so doing, no uncertainty in the readjustment of the field strength was incurred as would have been if the magnet had been turned off. The magnet** was mounted on a cart on rails to facilitate this movement, and a back-stop insured that it was always

** A different magnet from that previously described (section B) was used here and for part of the work on glycine and KNO_3 to be discussed in section D.

returned to its original position. It was then found that when no other effects (such as electrical heating of the magnet coils) caused the field to change, α_{max} was reproducible to within a few degrees out of a total of 30 or more revolutions, that is, to better than 0.1%. The reproducibility of α_{max} indicates that either the electrostatic forces remained fairly constant or, if random, they were quite small in this case.

The measurements labeled 5A in figure 12 were a repetition of measurements on sample 5 made after resurfacing the pole faces in an attempt to reduce the field inhomogeneity. In the absence of conclusive evidence, the slight change in the slopes of the lines was tentatively attributed to a change in the field inhomogeneity.

After each measurement it was necessary to make sure that the quartz fiber was completely unwound. The usual test was to turn the torsion head one full turn after the magnet had been turned off and to check that the crystal also turned one full turn in the same direction. It was noted in this process that when the crystal turned in absence of the magnetic field, it oscillated with a period of only a few seconds and the motion was strongly damped by air viscosity; if the initial amplitude were one turn, the oscillation ceased within 30 seconds. As in the case of the torsion pendulum used to calibrate the quartz fiber, the period of oscillation was undoubtedly strongly affected by electrostatic fields. The period is shortened in presence of the field, making its measurement still more difficult. Presumably, crystals of several tenths of a gram in mass would be necessary to obtain moments of inertia and rotational energies large enough to overcome air damping and give a conveniently measurable period. This is mentioned in connection with the discussion in section A (pages 14-15) of the measurement of magnetic anisotropy by observation of the period of oscillation of a crystal within and in absence of a magnetic field.

With the encouragement of the results with $KClO_3$, it was felt worth-while to make further tests with crystals of several other substances, namely KNO_3, KHC_2O_4, glycine, urea, monomethylurea, thiourea and anthracene, and with two protein samples. The measurements were generally made only over the range 15 to 24 kilogauss.

The data are recorded in graphical form in figures 14 to 30 (appendix) in which, unless otherwise indicated, the data points have been separated in the same manner as in figure 12. Observations concerning the sources of error and the reliability of the measurements are summarized as follows.

(1) In general the data points, $\frac{2KW}{m}(\alpha_{max} - \pi/4)$ vs. H^2, for separate specimens, directions of rotation and initial positions fit straight lines very closely even though the straight lines often have distinctly different slopes and are fairly widely separated. The data points fit straight lines least well in the cases of the more weakly anisotropic substances ($\Delta X^* < 1.0 \times 10^{-6}$ cgs per mole) for which the random torques may not be expected to be negligible in comparison to the crystal-anisotropy torque (see figures 14, 19, 30). However, it may be concluded that the variation in the slopes of the straight lines and the variations in α_{max} for fixed field strength are mainly due to systematic rather than random influences; the random variations are the variations of a given set of data points about the corresponding straight line and are generally small.

(2) The straight lines do not in general extrapolate through the origin. The intercepts, $\frac{2KW}{m}(\alpha_0 - \pi/4)$, of the straight lines on the vertical coordinate axis ($H^2=0$) are regarded as a measure of the influence of ferromagnetic impurities. To obtain some idea of the magnitude of the torque due to ferromagnetic impurities, the quantity $K(\alpha_0 - \pi/4)$ for 168 such straight lines (the results of observations on 42 specimens used in this work) was calculated and the distribution of values is plotted in figure 13. To compare the ferromagnetic torques with the crystal-anisotropy torque, the largest values of α_{max} (designated α_1) obtained with each specimen (near 24 kilogauss) were taken and the corresponding torques $K(\alpha_1 - \pi/4)$ were calculated; the distribution of values is also plotted in figure 13 (this latter distribution is not regarded as significant except in regard to the present work). The distribution of ferromagnetic torques has a peak in the range $\pm 5 \times 10^{-4}$ cm-dynes, but is not quite symmetrical about zero torque; no reason is advanced to account for the lack of symmetry. In the lower half of figure 13 it

FIGURE 13

OBSERVED DISTRIBUTION OF FERROMAGNETIC TORQUES.

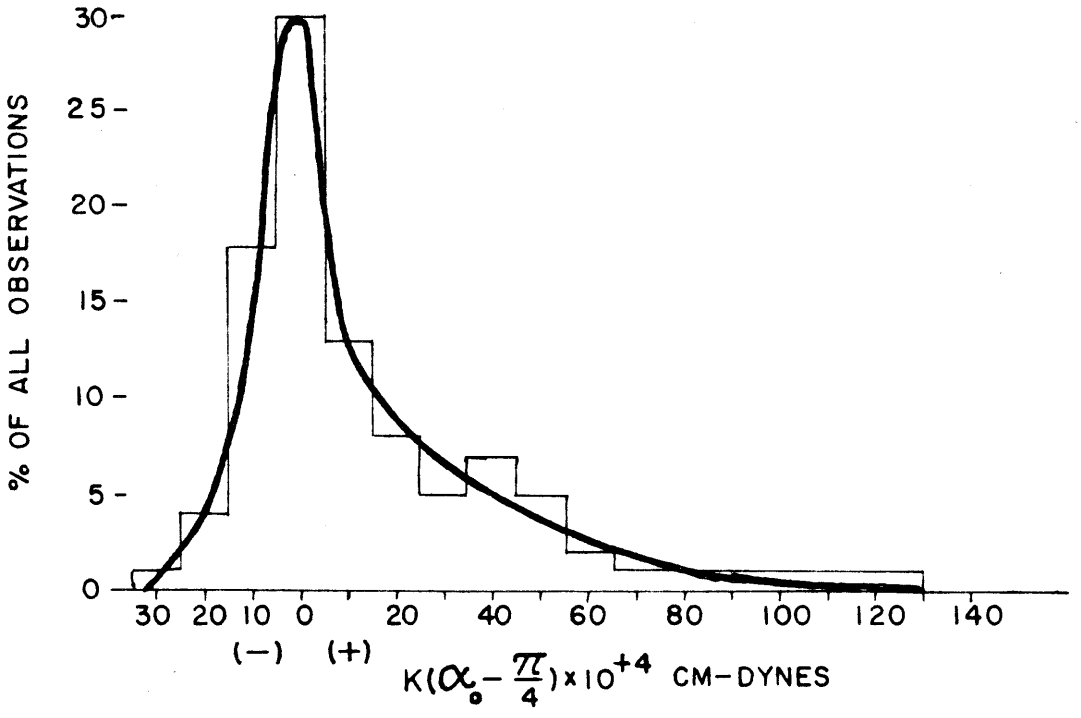

DISTRIBUTION OBSERVED IN THE PRESENT WORK OF LARGEST VALUES OF TORQUES DUE TO CRYSTAL ANISOTROPY.

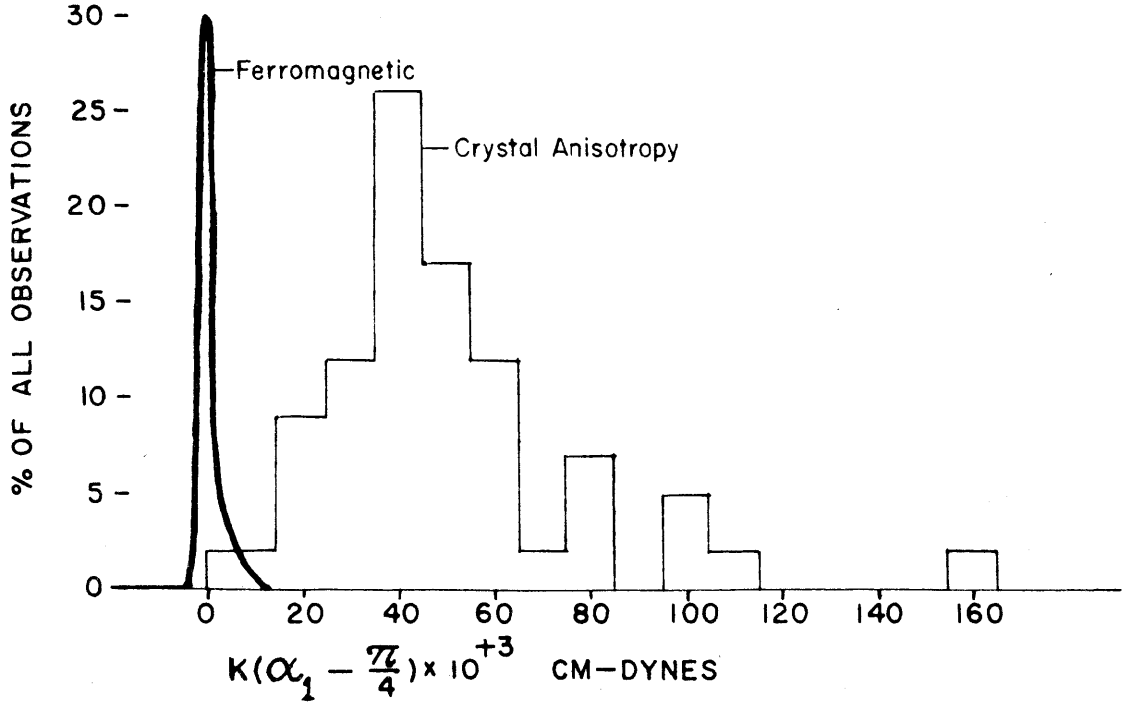

is seen that the distribution of ferromagnetic torques partially overlaps that of crystal-anisotropy torques. In general, the four values of $K(\alpha_o - \pi/4)$ obtained for a given specimen were close together and on the same size of zero.

(3) The variation in the slopes of the straight lines for a given substance and axis of rotation is generally less than $\pm 5\%$ about the average. The uncertainty in slope introduced in fitting a straight line to the data points is generally less than $\pm 1\%$. The variation in the slopes of the four straight lines obtained with a given specimen may be attributed to field inhomogeneity. Variations in average slope from sample to sample are partly due to errors in orientation.

(4) Occasionally, data points deviate more widely from the corresponding straight line than can be accounted for by uncertainty in the field strength or variations in the electrostatic torque. Attention is called to these points by circles and arrows. Whenever such deviations occurred, the discordant data points were usually reinvestigated, particularly if more than one such point occurred on a single straight line. If a more consistent value was found, the the discordant data were discarded; this was done particularly whenever it was quite clear that α_{max} had been incorrectly calculated from the final position of the torsion head and the reading on the turn counter**. However, it was sometimes found that neither could a consistent value be obtained nor could any of the original values be duplicated. In figure 26 is such a case (sample #1) for which, however, both sets of data were retained; two discordant points occurred in the first set of data and the second set of data (#1A) gave, consistently, slightly higher slopes. The change is ascribed to a change in the contribution of ferromagnetic impurities due to the chance landing of a speck of dust on the crystal or glass fiber.

(5) When the crystal begins to spin after exceeding ϑ_{cr}, it rotates so violently that there is some danger that it will be damaged by bumping into the draft shield. Such an occurrence was

**The turn counter was not synchronised with the zero on the graduated scale of the torsion head.

never evidenced either by visible fragments or by a sudden large decrease in the slopes of the straight lines.

(6) The radioactive source for the elimination of electrostatic charges was installed only late in the series of measurements and was used only during the work with monomethylurea, thiourea and anthracene. The conclusions are mainly subjective but it is felt that the torque at zero magnetic field and the average deviation of the data points about straight lines were decreased after its introduction (see figures 24-29).

(7) Cursory observations of the initial equilibrium position of the crystal and of ϑ_{cr} were made during each determination of α_{max}. For the field strengths used, and for all but the more weakly anisotropic samples, the initial position was always within $\pm 2^{\circ}$ of the position expected on the basis of a knowledge of the orientation of the principal axes, and ϑ_{cr} was always within $\pm 2^{\circ}$ of $45^{\circ}(\pm N\frac{\pi}{2})$. For the smaller of the two crystals of KNO_3 used to measure the weak anisotropy in the plane perpendicular to c (figure 14), the initial position was with the b axis about 30° from parallel to the field, and ϑ_{cr} ranged from 33° to 60°; for this crystal, the value of the largest torque was 43×10^{-4} cm-dynes, well within the range of ferromagnetic torques (figure 13). The value of $\sin 2\vartheta_{cr}$ was not used in any of the anisotropy calculations since in no case did its omission seriously affect the result.

(8) Since the average value of α_{max} for fixed field strength apparently does not have a definite value, and since the data points corresponding to particular samples, directions of rotation and equilibrium positions do fit straight lines quite closely, it seems logical to infer that the average slope is the most nearly correct measure of the anisotropy involved. This is the measure used in the next section. As conclusive proof that the measurements reported are the correct anisotropies, and not in error by a combination of other effects, is taken the fact that the results have the algebraic properties of anisotropies. That is, whenever the three principal anisotropies of a magnetically biaxial crystal were measured, the sum (or difference) of any two was equal, within the experimental error, to the third principal anisotropy, and with the cor-

rect sign. Alternatively, as in the case of glycine (monoclinic; second special case), in which the three measurements did not all correspond to principal anisotropies, the calculated orientation of the $\hat{1}$ and $\hat{2}$ principal axes with respect to the a and c crystallographic axes was equal, within experimental error, to the observed orientation.

i. Conclusion.

The following procedure is recommended for the determination of small (diamagnetic) anisotropies by the method of "maximum torque".

(1) With a given crystal sample (mass, m; formula weight, W) in a given orientation, determine the maximum torque which the crystal will sustain in a uniform magnetic field, H, against a quartz fiber of known torsion constant, K; this torque is $K(\alpha_{max} - \pi/4)$.

(2) Make the determination for both initial equilibrium positions of the crystal and for both directions of rotation. Repeat the measurements at several high field strengths, preferably above 15 kilogauss.

(3) On graph paper plot $\frac{2KW}{m}(\alpha_{max} - \pi/4)$ vs. H^2 and fit straight lines to the points corresponding to given directions of rotation and equilibrium positions and average the slopes of the four lines so obtained. It is not an acceptable substitute to average the four values of $\frac{2KW}{m}(\alpha_{max} - \pi/4)$ for a given field strength and fit a straight line to them. Repeat the measurements with other samples in the same orientation. The average of the results with the different samples is believed to be the best measure of the anisotropy involved.

D. New Measurements.

a. Introduction.

Magnetic anisotropy measurements were made on $KClO_3$, KNO_3, KHC_2O_4 (anhydrous), glycine, urea, thiourea, monomethylurea, anthracene and on two type of protein (elephant hair and silk worm gut). The magnetic anisotropies of $KClO_3$, KNO_3, urea and anthracene had been investigated by other workers; the investigations were repeated here to check the experimental procedure and to get more accurate data.

Obtaining suitable crystals of the substances presented different problems in each case. Extensive preparation was not justified in view of the seriousness of the effect of ferromagnetic impurities; until all the data had been collected and analyzed, it was quite uncertain whether meaningful results could be obtained. Consequently, experimentation was carried out only to find solvents from which the substances could be recrystallized without elaborate equipment, either by slow evaporation or by slow cooling of a solution, to yield at least a few crystals of the desired perfection and range of weight.

Since the preparation of the crystals of the individual substances is generally not concerned with the interpretation of the magnetic measurements, the preparations will be discussed in a separate sub-section.

b. Preparation of Crystals.

(1) Potassium chlorate crystallizes[46] in the monoclinic system, usually as plate-like crystals with well developed (001) faces. The (001) and (110) planes have good cleavage; the plane of the optic axes is perpendicular to b and the acute bisectrix is very nearly perpendicular to (001).

For this work, potassium chlorate was recrystallized from distilled water solutions by slow evaporation at room temperature and, alternatively, by slow cooling of a solution slightly supersaturated at room temperature. Thin plate-like crystals were invariably

formed, the majority being deformed. By cleaving some of the larger imperfect crystals to remove obvious defects, apparently perfect monocrystalline fragments suitable for magnetic anisotropy measurements were obtained. Observations of interference patterns with convergent polarized light, of morphology and of cleavage were consistent with the assumption that the specimens were monoclinic single crystals of the ordinary habit described above. Goniometric measurements on the parallelepiped-shaped fragments suggested the presence of $(00\bar{1})$ and either (110) and $(11\bar{1})$ faces but not both of the latter; the observed interfacial angles were intermediate between the values calculated** for these two habits but not in good agreement with either habit or with any other simple habit. Laue photographs revealed that the cleavage fragments were not monocrystalline but twinned, resulting in nearly perfect orthorhombic symmetry; the orthorhombic axes were the directions originally designated, on the basis of morphology etc., as the $\underset{\rightarrow}{a}$, $\underset{\rightarrow}{b}$ and $\underset{\rightarrow}{c}^*$ axes.

Potassium chlorate is known to twin on the (001) face. Introduction of a mirror plane parallel to (001) or a two-fold rotation axis normal to (001) would account for the observed orthorhombic symmetry and for the fact that interference patterns did not reveal the twinning. Cleaving the specimens parallel to the apparent (001) face did not reduce the orthorhombic symmetry revealed by the Laue photographs. Evidently the crystals were of the habit described by Groth[46] consisting of many laminar monoclinic crystals with (001) faces parallel.

Magnetic anisotropy measurements had already been made on several crystals, using the $\underset{\rightarrow}{b}$ axis (normal to plane of optic axes) as axis of rotation, before the laminar twinning was discovered and it was felt worthwhile to attempt to interpret the results in terms of orthorhombic symmetry. The corresponding calculations are set forth in table 2 and the justification of the assumptions made is further elaborated in the discussion section. Since it proved impossible to obtain truly monoclinic crystals in any of the experiments, this investigation was not pursued further.

** (001)-$(110) = 105^\circ 20'$; (001)-$(11\bar{1}) = 104^\circ 38'$; (110)-$(1\bar{1}0) = 103^\circ 50'$; $(11\bar{1})$-$(1\bar{1}\bar{1}) = 103^\circ 32'$; (110)-$(11\bar{1}) = 95^\circ 54'$. All observed interfacial angles were in the range $103\text{-}5^\circ$ or supplements thereof.

(2) Potassium nitrate crystals [47] were obtained by slow evaporation at room temperature of a saturated solution in distilled water. Large, well-formed orthorhombic crystals were obtained. Pockets of occluded solution were removed by cleaving or by heating to cause decrepitation. The crystals were initially oriented by use of goniometric measurements.

(3) Potassium binoxalate (anhydrous) crystallizes [48] in the monoclinic system. The crystals have good cleavage on (100) and (010); the plane of the optic axes is approximately perpendicular to c, and b is the obtuse bisectrix. For this work, crystals were taken directly from a stock bottle since they were in general better formed than those obtained by recrystallization from water. The crystals were identified as the particular anhydrous modification whose structure is reported in the literature[49] by comparison of Laue photographs taken parallel to the a*, b and c axes with gnomonic projections calculated from the lattice parameters**. The crystals could be easily oriented by observing the cleavage and the interference patterns; the faces were generally too poorly formed to permit goniometric observations.

(4) Glycine crystallizes in the monoclinic system[50]. The plane of the optic axes is nearly parallel to (001) and b is the acute bisectrix; the crystals have perfect cleavage on (010). Glycine crystals were obtained by slow evaporation at room temperature of solutions in distilled water. Crystals equally well developed in all directions and approximately octahedral in shape were obtained. The crystals grew to a large size and did not tend to twin or to occlude solvent; however, many crystals contained "veils", a cloudiness probably caused by misoriented micro-crystals. The veiled crystals always gave diffuse, smeared or twinned Laue diffraction spots. Specimens showing the presence of occlusions were used provided the amount of misorientation, as shown by the Laue photographs, was not

---

**This is not necessarily the best method. It was used because the gnomonic projections had already been prepared, as discussed in section B, for use in orienting the crystals precisely by means of the Laue camera. Essentially, the method verifies the crystal system, the monoclinic angle to within 10 minutes and the cell dimensions to within a few percent.

more than two degrees.

Several modifications of the crystal structure of glycine are reported[51,52,53], but the structure of only one, α-glycine, has been investigated thoroughly[54]. The faces of the available crystals were roughened by etch pits and goniometric measurements could not determine which polymorph was present. The crystals were identified as α-glycine by comparing Laue photographs taken parallel to $\underset{\sim}{a}^*$, $\underset{\sim}{b}$ and $\underset{\sim}{c}$ axes with gnomonic projections calculated from the lattice parameters of α-glycine.

Specimens used for the magnetic measurements were oriented initially by observing the morphology, cleavage and optical interference patterns.

(5) Urea crystallizes in the tetragonal system, usually forming needles elongated on the tetragonal $\underset{\sim}{c}$ axis[55]. Urea cannot be conveniently recrystallized from water since it is extremely soluble therein; its water solutions supersaturate readily and when crystallization is induced an agglomerated mass of crystals forms. Crystals of a size suitable for magnetic anisotropy measurements were obtained by recrystallization from ethanol solutions either by slow evaporation at room temperature or by slow cooling of a solution slightly supersaturated at room temperature. The crystals were of the needle-like habit and locating the four-fold axis posed no problem.

(6) Monomethylurea was recrystallized by slow evaporation at room temperature of an acetone solution. The crystals fitted the description given by Groth[56]: orthorhombic needles elongated on the $\underset{\sim}{c}$ axis and with good cleavage on (110) and (001). Pockets of occluded solvent were removed from the crystals by cleaving and by heating under vacuum to 80-90°C (M.P.=101°C) to cause decrepitation; suitable specimens were obtained from the fragments. Beeswax was used as a mounting cement because of its low melting point.

Some difficulty was encountered in using the Laue camera to orient the crystals. Since the $\underset{\sim}{a}$ and $\underset{\sim}{b}$ axial lengths differ by only one percent, these two axes could not be readily distinguished by differences in the positions of diffraction spots. Distinction was finally made by comparing the intensities of diffraction spots

on Laue photographs and on precession camera photographs with published data[57].

(7) Thiourea was recrystallized by slow evaporation at room temperature of an isobutanol solution. Water, ethanol and isopropanol were tried as recrystallization solvents but they yielded only laminated crystals which occluded solution between the laminae. The crystals from isobutanol were orthorhombic and had good cleavage on (010) and (101), as stated by Groth[58], but the faces were too rough for goniometric measurements or for observing the optical interference patterns. Locating the crystallographic axes when cleavage faces were absent was a process of trial-and-error searching with the Laue camera. Both urea and thiourea occlude certain types of organic molecules in their crystals; if this had occurred during the recrystallization of either substance it would have been evidenced by alteration of the crystal structure.

(8) Anthracene was recrystallized by slow cooling of a solution in tetrahydrofuran, slightly supersaturated at room temperature. Other methods of recrystallizing anthracene are described in the literature[59]. The crystals obtained were nearly free of the usual yellow-colored impurities found in anthracene. The crystals were monoclinic and plate-like on (001); the plane of the optic axes was perpendicular to b and one optic axis was nearly perpendicular to (001).[60] Only one specimen was used; it was oriented by means of optical interference patterns and goniometric measurements. No difficulty was encountered in the mechanics of mounting and orienting the crystal despite its small size (0.373 mg; 2x2x0.1 mm). Apiezon tar was used as a cement.

(9) The two samples of protein, namely elephant hair and silk worm gut, were obtained from Dr. Richard E. Marsh.

The weights of the crystals used for the magnetic measurements ranged from 0.3 to 40 milligrams but were usually in the range from 1 to 5 milligrams; the field strengths used were generally from 15 to 24 kilogauss. The anisotropies were determined by the new method, described on page 76, from the data recorded in figures 14-30 (appendix). In the following sub-section the magnetic anisotropies are

discussed in terms of crystal and molecular structure and specific comments on the measurements are made. The pertinent crystal and molecular data are placed in tables along with outlines of the calculations. Throughout the discussion the unit of magnetic susceptibility is 10^{-6} cgs/mole. The symbol K* will be used to distinguish the principal susceptibilities of molecules from those of the crystal (X*).

c. Discussion.

(1) Potassium Chlorate: The projection of the structure[61] onto (010) is shown in the left half of the figure (heavily outlined) accompanying table 2. The atoms marked by broken circles lie at distance $b_o/2$ below the corresponding atoms marked by full circles. The atoms K, Cl and O_1 lie on mirror planes at $y = \pm 1/4$; the atoms O_2 lie above and below the plane. The three oxygen atoms, whose plane is parallel to *b*, form very nearly an equilateral triangle; the normal to this plane is labeled *l*. The chlorine atom is very nearly equidistant from the three oxygen atoms and hence the ClO_3^- ion forms approximately a trigonal pyramid with *l* as a threefold axis. The K, Cl and O_2 atoms lie very nearly on $(20\bar{1})$. The (001) plane is a pseudo b-glide plane which fails to be a true glide mainly in that it does not reproduce the O_1 atoms.

The right half of the diagram (lightly outlined) shows how $KClO_3$ twins on the (001) face by converting (001) into a true b-glide. Because of the fortuitous value of the axial ratio a/c = 0.656 and the monoclinic angle $\beta = 109°38'$, the shorter diagonal of the parallelogram formed by the *a* and *c* axes is very nearly equal to the *c* axis length. Consequently, in the laminar twinned habit, if alternate laminae were bounded [in addition to (001)] by only (110) and only $(11\bar{1})$, the bounding faces of alternate laminae would intersect at only a small angle ($0°45'$). A crystal having such a laminar habit would, on cursory inspection, appear to be a single crystal bounded by (001) and (110) or $(11\bar{1})$, but precise goniometric measurements would give values of the interfacial angles in poor agreement

TABLE 2: POTASSIUM CHLORATE

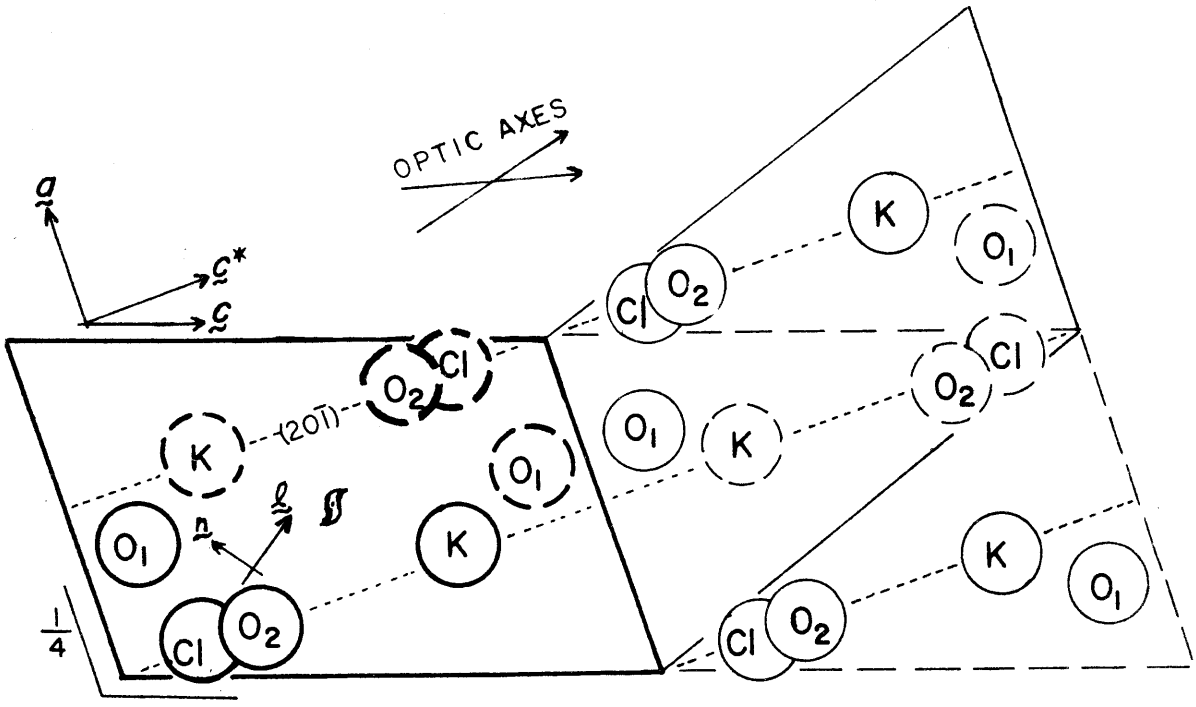

Monoclinic bimolecular unit cell; space group C_{2h}^2-$P2_1/m$

a=4.647, b=5.585, c=7.085

$\beta = 109°38'$

Unit cell reproduced by converting (001) into a b-glide plane, giving rise to orthorhombic symmetry.

Let $\underset{\sim}{\ell}$, $\underset{\sim}{m}$, $\underset{\sim}{n}$ be orthogonal axes attached to the ClO_3^- ion such that $\underset{\sim}{\ell}$ is the approximate 3-fold axis and $\underset{\sim}{m} = \underset{\sim}{b}$. The matrix, $\mathbb{S}$, transforms vectors from the a-b-c* to the ℓ-m-n coordinant system and was calculated from the oxygen parameters given in the crystal structure data (Zachariasen, 61). The matrix $\|K$ is the molecular susceptibility matrix in the ℓ-m-n coordinant system. The potassium ions are assumed magnetically isotropic; the ClO_3^- ion is assumed magnetically uniaxial with $\underset{\sim}{\ell}$ as the unique axis. The unit cell is assumed to be orthorhombic (axes $\underset{\sim}{a}$, $\underset{\sim}{b}$, $\underset{\sim}{c}^*$) with 4 molecules related by mirror and screw symmetry elements.

$$\mathbb{S} = \begin{matrix} \\ \ell \\ m \\ n \end{matrix} \begin{matrix} \begin{matrix} a & b & c^* \end{matrix} \\ \begin{Bmatrix} 0.5635 & 0.0000 & 0.8261 \\ 0.0000 & 1.0000 & 0.0000 \\ -0.8261 & 0.0000 & 0.5635 \end{Bmatrix} \end{matrix}$$

$$\|K = \begin{Bmatrix} K_\ell^* & 0 & 0 \\ 0 & K_m^* & 0 \\ 0 & 0 & K_n^* \end{Bmatrix} = \begin{Bmatrix} K_\parallel^* & 0 & 0 \\ 0 & K_\perp^* & 0 \\ 0 & 0 & K_\perp^* \end{Bmatrix}$$

$$\left.\begin{aligned} 0.3175K_\parallel^* + 0.6824K_\perp^* &= X_a^* \\ K_\perp^* &= X_b^* \\ 0.6824K_\parallel^* + 0.3175K_\perp^* &= X_{c^*}^* \end{aligned}\right\} \quad 0.3649(K_\parallel^* - K_\perp^*) = X_{c^*}^* - X_a^*$$

$$= 1.09 \pm 0.02 \quad \text{(see figure 12)}$$

$K_\parallel^* - K_\perp^* = 2.99 \pm 0.05$ (this calculation)

$= 5.9$ $[KClO_3]$

$= 5.3$ $[Ba(ClO_3)_2.2H_2O]$ } Mookherji (62)

with angles calculated for either of these habits, as in the case of the crystals actually used. Groth[46] states that each lamina is bounded by (110); if this were so, it is believed that goniometric measurements would imply the presence of $(21\bar{1})$ rather than (110). A $KClO_3$ crystal twinned in the way described and having equal amounts of each twin would be equivalent to an orthorhombic crystal having the unit cell represented by joining both halves of the figure in table 2.

From the evidence of optical interference patterns, morphology, cleavage and Laue photographs, it is clear that the crystal used for the magnetic measurements were twinned in the manner described. The treatment of the crystals as exactly orthorhombic needs some defense since there is no a priori reason why both twinned forms should be present in equal amounts: (1) It was noted that Laue photographs showed perfect orthorhombic symmetry of the diffraction spots, both in their location and intensity. (2) Further cleaving of the specimens parallel to (001) failed to reduce the orthorhombic symmetry revealed by the Laue photographs. (3) In the magnetic measurements (see figure 12), the observed anisotropy was the same, within a few percent, for each of three different crystals tested.

In table 2 the anisotropy of the chlorate ion calculated by Mookherji[62] from measurements made by Krishnan[63] on (presumably) truly monoclinic $KClO_3$ crystals and also on $Ba(ClO_3)_2 \cdot 2H_2O$ is given for comparison with the results of the new measurements. The crystal structure data for $KClO_3$ published by Zachariasen[61] were also used by Mookherji. It is noted that the value of $K^*_{\parallel} - K^*_{\perp}$ given by Mookherji is almost twice the value obtained in the present work. Since the magnetic data used by Mookherji were obtained from measurements at low field strengths, they are unreliable despite the consistency of the results for the two chlorates.

(2) Potassium Nitrate: The observed values of $X^*_a - X^*_c$ and $X^*_b - X^*_c$ were considerably larger than the values obtained by Krishnan[63] (see table 3). The older data were obtained from measurements at low field strengths and are believed to be incorrect even though the calculated anisotropy of the nitrate ion is in agreement with measurements on other nitrates using the same method and with magneto-optical measurements on melted nitrates and nitric acid[16].

TABLE 3: POTASSIUM NITRATE.

Crystal Structure[64]: orthorhombic tetramolecular unit cell, space group $V_h^{16} - P_{bnm}$

Relation of Nitrate Ion to the Crystallographic axes:

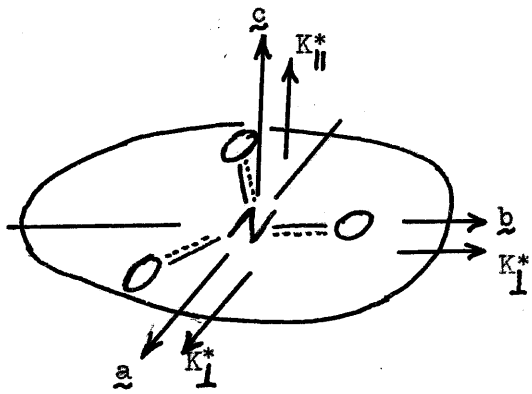

The nitrate ion is planar and perpendicular to c. The ion is magnetically uniaxial, the 3-fold axis normal to the plane being the unique axis. The crystal symmetry requires $K^*_{\parallel} = X^*_c$. If the crystal anisotropy were entirely due to isolated nitrate ions, then X^*_a, X^*_b and $K^*_{\perp}$ would be equal.

Magnetic Anisotropy (see figures 14, 15, 16):

	This Thesis	Krishnan[63]
$X^*_a - X^*_c$ =	6.98 ± 0.15	4.87
$X^*_b - X^*_a$ =	0.15 ± 0.02	0.05
$X^*_b - X^*_c$ =	7.03 ± 0.24	4.82

$\bar{X}^* = -33.0\ (\times 10^{-6})$ (International Critical Tables, 65)

$X^*_a = -49.5$, $X^*_b = -49.5$ } $= K^*_{\perp}$

$X^*_c = -56.5 = K^*_{\parallel}$

$K^*_{\perp} - K^*_{\parallel} = 7.0 \pm 0.01$ (This Thesis)

$= 4.8$ (Krishnan)

As pointed out previously (page 13), the magneto-optical measurements are based on the observation of small changes in refractive index and and on a small change in polarization of scattered polarized light and are also based on an imperfect knowledge of the dependence of the depolarization factor on other physical properties of the liquid.

The direction perpendicular to the plane of the nitrate ion is most diamagnetic. The double bond may be expected to resonate equally among the three oxygen atoms; the resulting three-fold symmetry would make the nitrate ion magnetically uniaxial. The observed anisotropy of the crystal in the plane parallel to the nitrate ion is very small and the individual measurements (figure 14) were subject to a large (percentage-wise) average deviation. As may be calculated from the data in figure 14, the largest torques involved in the two observations, 43×10^{-4} and 175×10^{-4} cm-dynes, were close to the range of torques which ferromagnetic impurities can be expected to exert (figure 13); for the smaller crystal the initial equilibrium position in the magnetic field was with the a axis 30° from parallel to the field, and φ_{cr} ranged from 33 to 60°. Nevertheless, it is felt that a small anisotropy of the order of magnitude and sign reported does exist and is probably due to polarization of the potassium and nitrate ions by the crystalline electrostatic fields.

In comparing the anisotropy of the nitrate and chlorate ions, both of which have a unique axis perpendicular to the plane of three oxygen atoms, it is noted that not only is the anisotropy $K_{\parallel}^{*} - K_{\perp}^{*}$ of the nitrate ion larger than that of the chlorate ion, it also has the opposite sign, reflecting the difference in type between the Cl-O and N-O bonds.

(3) Potassium Binoxalate: The anisotropy of the oxalate ion has been investigated by Lonsdale[66] using crystals of $H_2C_2O_4 \cdot 2H_2O$, and making the assumption that the water molecules are isotropic. To check the measurements, it was decided to use a different oxalate and in particular one having no water of crystallization. Potassium binoxalate was chosen because it is easily obtained in the anhydrous form and its crystal structure[67] is fairly well known; tests with KNO_3 indicate that the possible anisotropy of the potassium ion is negligible. The results are in table 4.

The direction perpendicular to the plane of the oxalate ion is the most diamagnetic and the plane of the ion is almost magnetically isotropic. The anisotropy in the plane is less than one sixth the value predicted by the results with glycine (table 5). Resonance

TABLE 4: POTASSIUM BINOXALATE.

Crystal Structure[67]: Monoclinic tetramolecular unit cell
space group C_{2h}^5 - $P_{2_1/c}$

Relation of Oxalate Ion to the Crystallographic Axes:

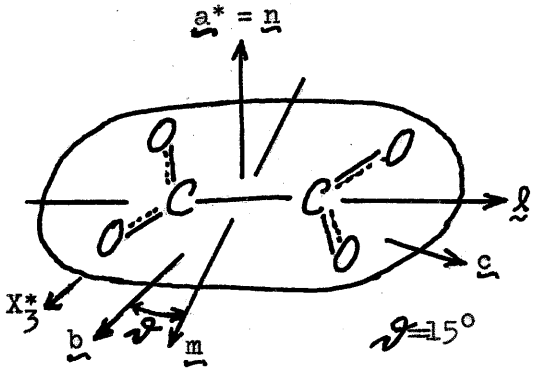

In the proposed structure, the oxalate ion has three mutually perpendicular approximate mirror planes whose intersections are $\underset{\sim}{l}$, $\underset{\sim}{m}$, and $\underset{\sim}{n}$. These vectors are assumed to be the principal magnetic axes. The plane of the ion is assumed parallel to (100), making $\underset{\sim}{a}^*$, $\underset{\sim}{b}$ and $\underset{\sim}{c}$ principal axes of the crystal.

Magnetic Anisotropy: (see figures 17, 18, 19):

$X_c^* - X_{a^*}^* = X_1^* - X_2^* = 13.05 \pm 0.10$

$X_b^* - X_{a^*}^* = X_3^* - (X_1^* \sin^2\psi + X_2^* \cos^2\psi) = 12.61 \pm 0.13$

$X_c^* - X_b^* = (X_1^* \cos^2\psi + X_2^* \sin^2\psi) - X_3^* = 0.43 \pm 0.15$

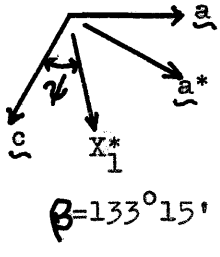

$\cos 2\psi = (0.43 + 12.61)/(13.05) = 1.000 \pm 0.02$

$\psi = 0^\circ \pm 3^\circ$ (calculated)

$\psi = 0^\circ \pm 1^\circ$ (observed)

$\overline{X}^* = -49.3$ (calcd. using Pascal constants)

$X_c^* = -44.8 = K_l^* \cos^2\vartheta + K_m^* \sin^2\vartheta$

$X_{a^*}^* = -57.9 = K_n^*$

$X_b^* = -45.3 = K_l^* \sin^2\vartheta + K_m^* \cos^2\vartheta$

$K_l^* = -44.8$
$K_m^* = -45.3$
} average $= -45.1 = K_\perp^*$

$K_n^* = K_{\parallel}^*$

$K_\perp^* - K_{\parallel}^* = 12.8$

$K_l^* - K_m^* = 0.5$

Lonsdale[66] (using oxalic acid dihydrate): $K_\perp^* - K_{\parallel}^* = 9.5$

$K_l^* - K_m^* = -0.4$

may be expected to make the C=O bonds of the oxalate ion identical; however, since the bonds make angles of 120° with each other rather than 90°, isotropy in the plane would not be expected. Possibly there is sufficient double bond character in the C-C bond to give the valence electrons of each carboxyl group nearly three-fold symmetry, causing the observed approximately uniaxial character.

The anisotropy of the nitrate and oxalate ions is assumed to be due to the non-spherical distribution of the π-electrons of the double bonds. The nitrate ion has only one double bond while the oxalate ion has two; both ions are planar. The fact that $K^*_\perp - K^*_\parallel$ for the oxalate ion has almost twice the value for the nitrate ion, and has the same sign as for the nitrate ion, strengthens this assumption.

In working out the crystal structure of potassium binoxalate, Hendricks[67] assumed that the oxalate ion was planar and parallel to (100); the molecular symmetry then required $\underset{\sim}{a}^*$ to be a principal magnetic axis. The anisotropy measurements indicate the correctness of this assumption, it being verified that a principal axis is, within 1°, parallel to $\underset{\sim}{a}^*$.

(4) Glycine: Both the oxalate ion and the bimolecular glycine group (both molecules imagined superimposed) have two coplanar carboxyl groups (see table 5). The value of $K^*_\perp - K^*_\parallel$ in both cases has the same sign and about the same magnitude. In both cases, resonance would be expected to make the C-O bonds identical. The bimolecular glycine group differs from the oxalate ion in that the principal axes $\underset{\sim}{l}$ and $\underset{\sim}{m}$ for glycine are not parallel and perpendicular to the C-C bond as in the oxalate ion and therefore the anisotropy of glycine is not due solely to the carboxyl groups. Moreover, the plane of the carboxyl groups for glycine is more anisotropic than for the oxalate ion.

From the measurements of the anisotropies in the planes perpendicular to the $\underset{\sim}{a}^*$ and to the $\underset{\sim}{c}$ axes of the glycine crystal, it should have been possible to calculate the angle ψ (table 5) with a minimum of error since $\psi \cong 45°$ (see pages 21-22). However, when the anisotropy is determined in a plane not perpendicular to a principal axis, the effect of a slight error in the orientation of the vertical axis is increased (equation 30). The actual uncertainty

TABLE 5: GLYCINE.

Crystal Structure[54]: Monoclinic tetramolecular unit cell
space group $C_{2h}^2 - P_{2_1/n}$

Relation of Glycine Molecule to the Crystallographic axes:

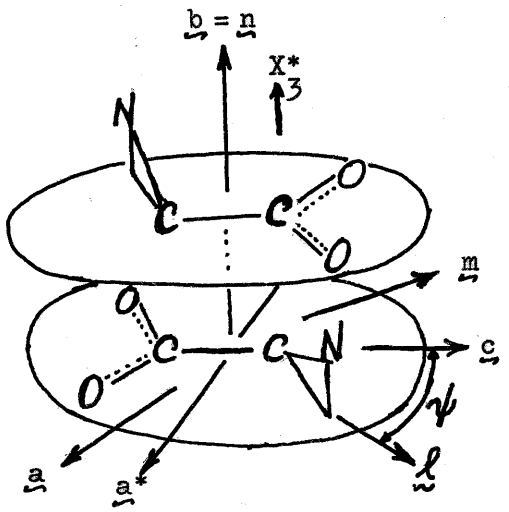

The two carbon and two oxygen atoms lie very nearly in a plane perpendicular to b. The nitrogen atom lies about 0.4 A above the plane. The molecule has no symmetry elements which determine the principal axes. Consequently, the measurements will be discussed in terms of two molecules related by a two-fold screw axis parallel to b. The principal axes ℓ, m, n of the bimolecular group are identical with those of the crystal (n = b; ℓ, m determined experimentally).

Magnetic Anisotropy (see figures 20, 21, 22):

$(X_1^* \cos^2\psi + X_2^* \sin^2\psi) - X_3^* = 5.32 \pm 0.04$ (axis of rotation = a* c parallel to H)

$X_1^* - X_2^* = 1.59 \pm 0.03$

$(X_1^* \sin^2\psi + X_2^* \cos^2\psi) - X_3^* = 5.42 \pm 0.08$ (axis of rotation = c a* parallel to H)

$\cos 2\psi = (-5.32 + 5.42)/(-1.59) = -0.063 \pm 0.04$

$2\psi = 93^\circ 36' \pm 3^\circ$

$\psi = 46^\circ 48' \pm 1\frac{1}{2}^\circ$ (calculated)

$\psi = 44^\circ \pm 1^\circ$ (observed)

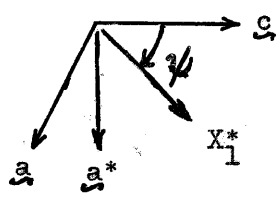

$\beta = 111^\circ 38'$

	(Per Molecule)	(Bimolecular Group)
$X_3^* - X_2^*$	$= -4.58 \pm 0.07$	$= (K_n^* - K_m^*)/2$
$X_2^* - X_1^*$	$= -1.59 \pm 0.03$	$= (K_m^* - K_\ell^*)/2$
$X_3^* - X_1^*$	$= -6.17 \pm 0.07$	$= (K_n^* - K_\ell^*)/2$

TABLE 5: (CONTINUED)

$\overline{X}^* = -80.4$ (Pascal constants; for bimolecular group)

$K_l^* = -75.2$

$K_m^* = -78.4$ } average = -76.8 = $K_\perp^*$

$K_n^* = -87.6$ = $K_\parallel^*$ } $K_\perp^* - K_\parallel^* = 10.8$

in ψ ** was found to be $\pm 1\frac{1}{2}^\circ$. In the case of potassium binoxalte the situation was reversed, the manner in which the crystals were mounted being such as to obtain the highest precision in the determination of the principal anisotropies and the minimum precision in the determination of ψ. In this case the uncertainty in the calculated value of ψ is $\pm 3^\circ$.

(5) Urea: The tetragonal symmetry of the urea crystal structure (table 6) limits the amount of information which can be obtained concerning the magnetic anisotropy of the urea molecule. One may conclude from the data that the direction of greatest diamagnetism is perpendicular to the C=O bond, as was implied by the measurements on glycine and potassium binoxalate, but cannot conclude which principal axis is least diamagnetic. Clearly, the plane of the molecule is not isotropic, as was approximately true for the oxalate ion, since this would require the crystal to be isotropic. However, the value of $K_\parallel^* - K_\perp^* = 2.5$ for urea is considerably less than the value 4.3 which would be calculated from the results with methylurea (see table 7, second structure).

Although the measurement reported by Lonsdale[68] was made at low field strengths, it agrees well with the new result.

(6) Monomethylurea: The measurements on monomethylurea (table 7) were undertaken in the hope of obtaining more information about the anisotropy of the urea group, it being assumed that the reported crystal structure[69] was reasonably correct. The principal mag-

**They symbol ψ is used here instead of φ, as in equation 30, in order to conform with the notation of Krishnan (63). It should not be confused with the Eulerian angle used in the general equation, section B.

TABLE 6: UREA.

Crystal Structure[67]: tetragonal bimolecular unit cell, space group $V_d^3 - P\bar{4}2_1m$

Relation of Urea Molecule to the Crystallographic Axes:

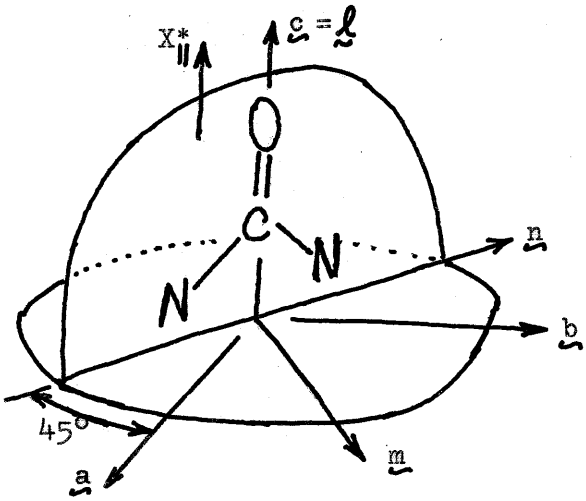

The space-group symmetry requires the molecule to lie in a plane parallel to (110), that the C=O bond be a 2-fold axis and that the molecule have a mirror plane perpendicular to the plane of the molecule and parallel to the C=O bond. The orthogonal vectors $\underset{\sim}{\ell}$, $\underset{\sim}{m}$ and $\underset{\sim}{n}$ are therefore principal molecular axes. A second molecule in the unit cell is related to this one by a 4-fold inversion axis parallel to $\underset{\sim}{c}$.

Magnetic Anisotropy (see figure 23):

	This Thesis	Lonsdale[68]
$X^*_{\parallel} - X^*_{\perp}$	2.45 ± 0.04	2.57 ($\alpha_{max} \cong 6\frac{1}{2}$ revolutions; $m \leq 5\frac{1}{2}$mg; $H \leq 7$ kilogauss)

$$X^*_{\perp} = K^*_m \mathrm{Sin}^2 45^\circ + K^*_n \mathrm{Cos}^2 45^\circ = (K^*_m + K^*_n)/2 = K^*_{\perp}$$

$$X^*_{\parallel} = K^*_{\ell} = K^*_{\parallel}$$

$$\bar{X}^* = -33.6 \quad \text{(International Critical Tables, 65)}$$

Hence: $K^*_{\perp} = -34.4$, $K^*_{\parallel} = -31.9$ $\Big\}$ $K^*_{\parallel} - K^*_{\perp} = 2.45$

netic axes of the molecule are not uniquely determined by the molecular symmetry in the case of methylurea, and making assignments of axes on the basis of symmetry in part of the molecule was proved risky in the case of glycine; however, it was felt justified to assign axes on the basis of the symmetry of the urea group and to assume the methyl group to be isotropic. Calculations based on the

TABLE 7: MONOMETHYLUREA.

Crystal Structure[69]: Orthorhombic tetramolecular unit cell, space group $V^4 - P_{2_1 2_1 2_1}$

Magnetic Anisotropy (see figures 24, 25, 26):

$X^*_a - X^*_b = 1.87 \pm 0.02$

$X^*_c - X^*_a = 3.33 \pm 0.05$

$X^*_c - X^*_b = 5.23 \pm 0.01$

$X^*_c - X^*_b = (X^*_a - X^*_b) + (X^*_c - X^*_a) = 5.20$

} average = 5.21

$\bar{X}^* \cong -40$ (three different exptl. values have been reported)[10]

Relation of the Methylurea Molecule to the Crystallographic Axes:

(Structure Proposed by Corey and Wyckoff, 69)

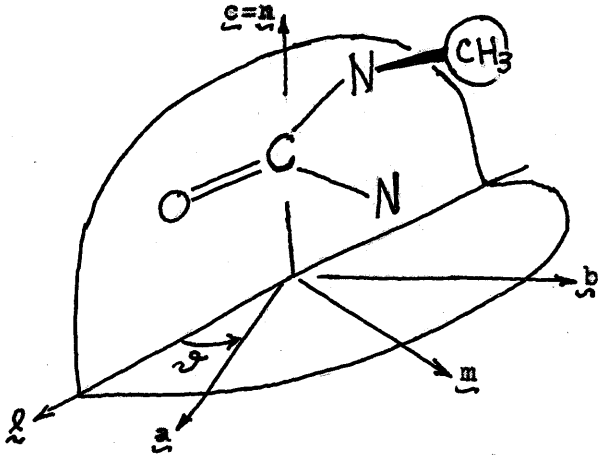

The plane of the urea group is parallel to c; The C=O bond is perpendicular to c and makes an angle of 34° with a. The principal molecular axes are assumed to be determined by the symmetry of the urea group.

$X^*_a = K^*_\ell \cos^2\vartheta + K^*_m \sin^2\vartheta$

$X^*_b = K^*_\ell \sin^2\vartheta + K^*_m \cos^2\vartheta$

$X^*_c = K^*_n \qquad \vartheta \cong 34^\circ$

$K^*_\ell - K^*_m = 5.00$

$K^*_n - K^*_\ell = 1.80 \qquad K^*_n > K^*_\ell > K^*_m$

$K^*_n - K^*_m = 6.80$

(Newly Proposed Structure, see part II)

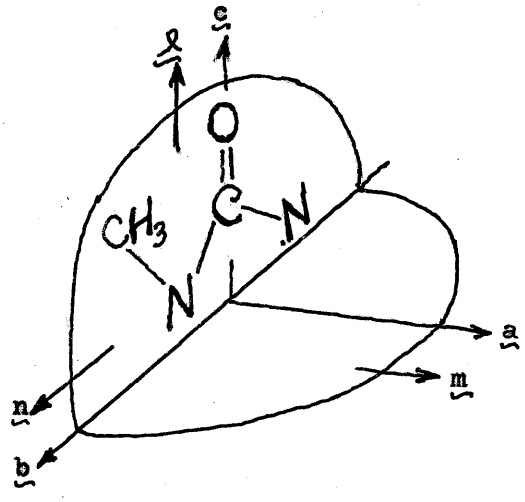

The plane of the urea group is nearly perpendicular to a and the C=O bond is nearly parallel to c.

$K^*_\ell - K^*_n \cong X^*_c - X^*_b = 5.21$

$K^*_\ell - K^*_m \cong X^*_c - X^*_a = 3.33$

$K^*_m - K^*_n \cong X^*_a - X^*_b = 1.87$

$K^*_\ell > K^*_m > K^*_n$

crystal structure proposed by Corey and Wyckoff[69] would require the direction of least diamagnetism (largest algebraic susceptibility), K_n^*, to be perpendicular to the C=O bond and parallel to the plane of the urea group.

It had been expected that the direction of minimum diamagnetism would be parallel to the C=O bond and that the molecule would be nearly magnetically isotropic in the plane perpendicular to the C=O bond. This expectation was based on the following considerations: (1) The anisotropy was assumed to be associated mainly with the special distribution of the two π-electrons of the four shared electrons in the C=O double bond. (2) The probability distribution assigned to the π-electrons by the molecular orbital approximation is such that they are mainly in two nearly cylindrical regions elongated parallel to the C=O bond and symmetrical about the plane of the urea group. This being true, the mean square radius of the electrons projected onto a plane, and hence the diamagnetism perpendicular to the plane, would be least for a plane perpendicular to the C=O bond and would be constant for planes parallel to the bond.

An investigation was begun to determine whether a crystal structure in agreement with these expectations and in agreement with the diffraction data recorded in the literature[69] is possible. The work is described in part II of this thesis. The results, although incomplete, show conclusively that the originally proposed structure is incorrect and strongly indicate that the molecules are oriented as shown in table 7. In the newly proposed structure, the direction of minimum molecular diamagnetism is parallel to the C=O bond and the smallest principal anisotropy is in the plane perpendicular to this bond.

(7) Thiourea: The thiourea molecule may be expected to have the same symmetry as the urea molecule. In the reported crystal structure[70], however, the carbon atom is slightly out of the plane formed by the two nitrogen atoms and the sulfur atom (see table 8); the C=S bond makes an angle of about 25½° with the a axis. A refinement of the crystal structure might change this angle by a few degrees, causing the sign of the calculated value of $K_m^* - K_l^*$ (table 8) to change. However, to make the direction of the C=S bond the direc-

TABLE 8: THIOUREA.

Crystal Structure[70]: Orthorhombic tetramolecular unit cell
space group V_h^{16} - P_{bnm}

Relation of the Thiourea Molecule to the Crystallographic Axes:

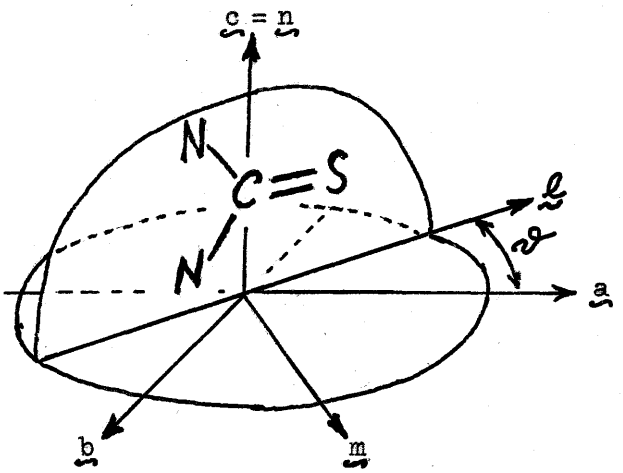

The crystal symmetry requires the molecule to have a plane of symmetry parallel to (001). Hence the plane of the two nitrogen atoms and the sulfur atom is parallel to c and the C=S bond is perpendicular to c. For the purpose of this calculation, the molecule will be assumed exactly planar; the molecular symmetry then requires the vectors ℓ, m and n to be principal axes.

Magnetic Anisotropy (see figures 27, 28):

$X_c^* - X_b^* = 2.52 \pm 0.02$
$X_c^* - X_a^* = 2.75 \pm 0.04$
$\Big\}$ $X_b^* - X_a^* = 0.23$ (calculated)

$\overline{X}^* = -43.8$ (Pascal constants)

$X_a^* = -44.8 = K_\ell^* \cos^2\vartheta + K_m^* \sin^2\vartheta$

$X_b^* = -44.5 = K_\ell^* \sin^2\vartheta + K_m^* \cos^2\vartheta$

$X_c^* = -42.0 = K_n^*$

$K_\ell^* = -44.9$
$K_m^* = -44.4$
$\Big\}$ average $= -44.6$

$K_m^* - K_\ell^* = 0.5$ $\qquad K_n^* > K_m^* > K_\ell^*$

tion of minimum molecular diamagnetism, this angle would have to be increased to slightly over 45°, an improbable situation. Hence, the direction of minimum diamagnetism is in the plane of the thiourea

molecule and perpendicular to the C=S bond. This difference from monomethylurea may be attributed to the fact that the radius of the sulfur atom is larger than that of an oxygen atom, to the fact that the electronegativity of the sulfur atom is less than that of the oxygen atom so that the C-N bonds have greater double-bond character, or to both.

(8) Anthracene: The molecular anisotropies of naphthalene and of anthracene calculated by Pauling[12] were in considerable disagreement with the experimental values reported by Krishnan[63]. The discrepancy was due to an error in the original measurements which was later corrected[36]**. It was decided to make a single measurement of the largest anisotropy of one of these two compounds in order to judge the correctness of Krishnan's values of the crystal anisotropies***.

Anthracene was chosen because it is readily crystallized and because it is non-volatile. The anisotropy in the plane perpendicular to the b axis was measured. Even though the crystal used in this experiment weighed only 0.373 mg, the largest torque obtained was 750×10^{-4} cm-dynes, well above the range of torques with ferromagnetic impurities may be expected to exert (figure 13). It may be noted that the average deviation of the slopes of the four straight lines $\frac{2KW}{m}(\alpha_{max} - \pi/4)$ vs. H^2 (figure 29), namely $\pm 1 \times 10^{-6}$ cgs per mole, while percentage-wise the same as the average deviation observed in other experiments, is numerically 3 to 100 times greater than in the other experiments. This is attributed to: (1) the uncertainty in the slope of each line (in this case, less than $\pm$½%) due to scatter in the data (uncertainty in H^2); (2) to the larger average susceptibility of anthracene in the plane perpendicular to b, about 3 times greater than the average susceptibility of any of the other substances investigated, which made the effect of field

---

**Selwood[71], in his book on magnetochemistry, has recalculated the molecular susceptibilities of anthracene and naphthalene on the basis of Krishnan's later results. However, there is apparently a mistake in his calculation for anthracene.

***His measurements on anthracene were absolute susceptibility measurements parallel to the X_1^* direction, X_2^* direction and c* direction using the method of Rabi(page 13) rather than anisotropy measurements by the method of maximum torque.

TABLE 9: ANTHRACENE.

Crystal Structure[72]: Monoclinic bimolecular unit cell

space group $C_{2h}^5 - P2_1/a$

Crystal and Molecular Principal Axes:

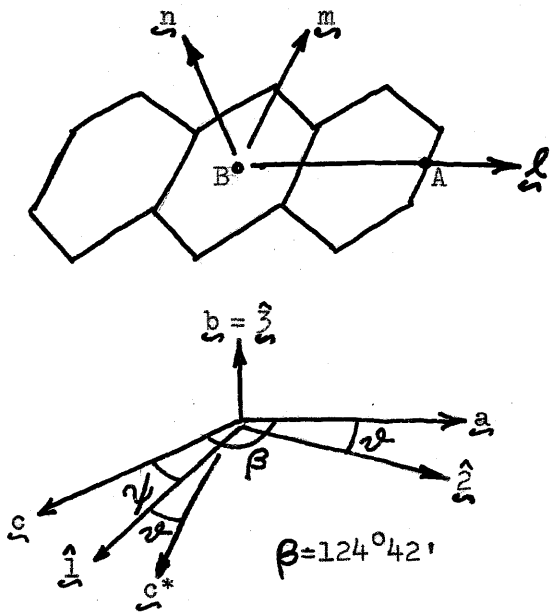

The molecule is centrosymmetric and the centers of the carbon atoms deviate from the mean plane by ≤ 0.012 A.

$\underset{\sim}{n}$ = normal to mean plane

B = molecular center

A = projection onto mean plane of mid-point between two carbon atoms.

$\underset{\sim}{\ell}$ = $\underset{\sim}{AB}$

$\underset{\sim}{m}$ = perpendicular to $\underset{\sim}{\ell}$ and $\underset{\sim}{n}$.

Vectors $\underset{\sim}{\ell}$, $\underset{\sim}{m}$ and $\underset{\sim}{n}$ are each normal to approximate mirror planes and hence are very probably the true principal molecular axes.

Magnetic Anisotropy:

$$\mathbb{X}^* = \begin{Bmatrix} X_1^* & 0 & 0 \\ 0 & X_2^* & 0 \\ 0 & 0 & X_3^* \end{Bmatrix}$$

Crystal magnetic susceptibility matrix in principal axis coordinates 1-2-3.

$$\mathbb{K}^* = \begin{Bmatrix} K_\ell^* & 0 & 0 \\ 0 & K_m^* & 0 \\ 0 & 0 & K_n^* \end{Bmatrix}$$

Molecular magnetic susceptibility matrix in principal axis coordinates ℓ-m-n.

$$\mathbb{C} = \begin{matrix} a & b & c^* \\ \begin{Bmatrix} -\mathrm{Sin}\vartheta & 0 & \mathrm{Cos}\vartheta \\ \mathrm{Cos}\vartheta & 0 & \mathrm{Sin}\vartheta \\ 0 & 1 & 0 \end{Bmatrix} & \begin{matrix} 1 \\ 2 \\ 3 \end{matrix} \end{matrix}$$

Matrix for transforming from a-b-c* coordinate axes to 1-2-3 axes.

$$\mathbb{S} = \begin{matrix} \begin{Bmatrix} -0.4960 & -0.1248 & 0.8593 \\ -0.3234 & -0.8919 & -0.3162 \\ 0.8059 & -0.4347 & 0.4020 \end{Bmatrix} & \begin{matrix} \ell \\ m \\ n \end{matrix} \\ a \quad b \quad c^* \end{matrix}$$

Matrix for transforming from a-b-c* coordinate axes to ℓ-m-n axes. (72)

TABLE 9: (CONTINUED)

$$\mathbb{A} = \begin{Bmatrix} -1 & 0 & 0 \\ 0 & 1 & 0 \\ 0 & 0 & -1 \end{Bmatrix}$$

Transformation of a-b-c* coordinate axes corresponding to a 2-fold axis parallel to $\underset{\sim}{b}$

$$\mathbb{B} = \left\{ b_{ij} \right\} = \frac{1}{2}\left[\mathbb{S}^{-1} \mathbb{K} \mathbb{S} \right]$$

$$\underset{\sim}{M}(a\text{-}b\text{-}c^*) = \mathbb{C}^{-1} \mathbb{K} \mathbb{C}\, \underset{\sim}{H}(a\text{-}b\text{-}c^*) = \left[\mathbb{B} + \mathbb{A}^{-1}\mathbb{B}\mathbb{A} \right] \underset{\sim}{H}(a\text{-}b\text{-}c^*) =$$

$$\begin{Bmatrix} b_{11} & 0 & b_{13} \\ 0 & b_{22} & 0 \\ b_{13} & 0 & b_{33} \end{Bmatrix} \cdot \underset{\sim}{H}(a\text{-}b\text{-}c^*)$$

Equate corresponding non-zero matrix elements to obtain four equations involving X_i^*, X_j^*, X_k^*, K_ℓ^*, K_m^*, K_n^* and ϑ. Solve the equations obtained by equating diagonal elements for K_ℓ^*, K_m^*, K_n^*.

$$-K_\ell^*/0.3392 = X_2^*(0.1097\cos^2\vartheta - 0.4969\sin^2\vartheta) + X_1^*(0.1097\sin^2\vartheta - 0.4969\cos^2\vartheta) + 0.0480X_3^*$$

$$-K_m^*/0.3392 = X_2^*(0.1370\cos^2\vartheta - 0.0364\sin^2\vartheta) + X_1^*(0.1370\sin^2\vartheta - 0.0364\cos^2\vartheta) - 0.4398X_3^*$$

$$-K_n^*/0.3392 = X_2^*(-0.5858\cos^2\vartheta + 0.1941\sin^2\vartheta) + X_1^*(-0.5858\sin^2\vartheta + 0.1941\cos^2\vartheta) + 0.0526X_3^*$$

$$X_2^*(-0.2225\cos^2\vartheta + 0.2709\sin^2\vartheta + 0.3392\sin\vartheta\cos\vartheta) + X_1^*(0.2709\cos^2\vartheta - 0.2225\sin^2\vartheta - 0.3392\sin\vartheta\cos\vartheta) - 0.0484X_3^* = 0$$

The fourth equation was obtained by equating the off-diagonal elements.

Results of Present Work:

$X_1^* - X_2^* = 138.7 \pm 0.9$ $\qquad \vartheta = 25^\circ \pm 1^\circ$ (observed)

$\overline{X}^* = \frac{1}{3}(X_1^* + X_2^* + X_3^*) = -129.3$ (Internat. Crit. Tables, 65)

$-0.0045X_2^* + 0.0539X_1^* - 0.00484X_3^* = 0$ (From fourth equation using observed value of ϑ)

Solving these three equations yields:

$X_2^* = -226$; $X_1^* = -87$; $X_3^* = -74$

TABLE 9: (CONTINUED)

Krishnan's Results[36]:

$X_2^* = -211.8$

$X_1^* = -75.5$

$X_3^* = -102.9$

$X_1^* - X_2^* = 136.3$

$\vartheta = 25^\circ$ (observed), $\vartheta = 26^\circ 22'$ (calculated from fourth equation using X_1^*, X_2^* and X_3^*)

Molecular Susceptibilities:

	Using Krishnan's values of $X_{1,2,3}^*$ and calculated value of ϑ.		Pauling's Calculation (12)
K_l^* =	-75.6	average = -72.5	-83
K_m^* =	-69.3	$= K_\perp^*$	
K_n^* =	-244.6	$= K_\parallel^*$	-242
$K_\perp^* - K_\parallel^*$ =	172.1		159

inhomogeneity greater for anthracene than for other substances.

As shown in table 9, it is possible to calculate the three crystal and molecular susceptibilities from this single measurement and a knowledge of the average susceptibility; the results are not reliable, however, because of the poor precision in the determination of the initial equilibrium position of the crystal in the magnetic field.

With some reservations concerning the accuracy of the measurements, Krishnan's values of the principal susceptibilities of the anthracene crystal were used in connection with the latest refinement of the crystal structure[72] to calculate the molecular susceptibilities. The result was that the molecular susceptibilities so obtained

were in good agreement with the values calculated by Pauling, the value of $K_{\perp}^{*} - K_{\parallel}^{*}$ being within 10% of that proposed by Pauling.

(9) Proteins: The two samples of protein tested, unstretched elephant hair (α-keratin) and silk worm gut (silk fibroin; β-keratin), were rather weakly anisotropic and appeared to be strongly influenced by electrostatic forces. These forces were strong enough that there was some uncertainty (one or two turns) whether or not the quartz fiber was unwound at the beginning of each measurement and the suspended samples were influenced by objects outside the draft shield (for example, a finger). The average deviation of the results (figure 30) ranged from $\pm$10 to $\pm$20%. Both specimens were cylindrical or fiber-like in shape and both were magnetically uniaxial, the axis of the cylinder being the unique axis and the direction of least diamagnetism in both cases.

The anisotropy values in figure 30 are given in terms of susceptibilities per gram since the average residue molecular weights were uncertain. Using an average residue weight of 120 for elephant hair and 85 for silk worm gut, the anisotropy of elephant hair becomes $X_{\parallel}^{*} - X_{\perp}^{*} = 1.4$ cgs/residue and for silk worm gut becomes $X_{\parallel}^{*} - X_{\perp}^{*} = 0.7$ cgs/residue.

The structure of elephant hair is believed to be based on a helical configuration; that of silk worm gut is believed to be based on a "pleated sheet"[21,73]. The six atoms in the amide group, C-CO-NH-C, all lie in a single plane. In the helical structure, each amide nitrogen is hydrogen-bonded to the third or possibly the fifth carbonyl oxygen atom beyond it in the helix. The planes of the amide groups are parallel to the helix axis and the C=O double bonds are nearly so. Assuming the side groups to be isotropic or randomly oriented, the anisotropy may then be related to the anisotropy of the amide group. The helices are magnetically uniaxial because of the many-fold rotational symmetry about the helix axis. The pleated sheet consists of uncoiled peptide chains with the C=O bonds of the amide groups perpendicular to the chains; separate chains are held together by hydrogen bonds between the carbonyl oxygen atoms and the amide nitrogen atoms. In silk worm gut the peptide chains are parallel to the axis of the cylinder or fiber; the pleated sheets are

randomly oriented about this axis, making the sample magnetically uniaxial.

The observed anisotropy of the elephant hair is consistent with the present belief that the direction of minimum susceptibility of the amide group should be parallel to the C=O double bond. For silk worm gut, the unique axis would have been predicted to be the direction of greatest diamagnetism but this was not found to be true experimentally.

E. Conclusion.

The measurement of magnetic anisotropy in single crystals by the "maximum torque" method, developed by Krishnan, has been investigated. It was found that when measuring small (necessarily diamagnetic) anisotropies, of the order of 1×10^{-6} cgs/mole, ferromagnetic impurities were a considerable source of error. It was found that this error could be eliminated by using high field strengths.

A systematic method of orienting crystal specimens before attaching them to the quartz torsion fiber has been devised. This process was formerly dependent on trial and error. The use of X-ray diffraction techniques to determine accurately the orientation of the crystals has been described.

The determination of torsion constants of quartz fibers, in the range 10^{-5} to 10^{-3} cm-dynes/radian, from the period of oscillation of a torsion pendulum has been investigated. A pendulum with a moment of inertia of about 10^{-2} cgs, accurate to $\pm 0.2\%$, was constructed. The technique of accurately determining the period of oscillation of this pendulum has been described.

A decrease in the torsion constants of thin quartz fibers as they age was definitely established. This decrease is probably due to elongation of the fibers by plastic flow under tension. Accurate measurements of magnetic anisotropy require that the torsion constants of the fibers be rechecked periodically.

Some measurements of diamagnetic anisotropy were made to test the new experimental procedure and to obtain new data. In particular, simple molecules containing N=O, C=O and C=S double bonds were investigated . A small amount of work was done on anthracene to check the reliability of older measurements and to check Pauling's theory of the anisotropy of aromatic and conjugated polynuclear hydrocarbons.

II. THE CRYSTAL STRUCTURE OF MONOMETHYLUREA.

A. Introduction.

The measurement of the magnetic anisotropy of monomethylurea discussed in Part I was carried out under the assumption that the crystal structure was known with sufficient accuracy to permit the interpretation of the magnetic anisotropy in terms of the molecular structure. Some work on the crystal structure was done in 1933 by Corey and Wyckoff[1]. They found that the structure was based on an orthorhombic tetramolecular unit cell with space group V^4 - $P_{2_1 2_1 2_1}$ and having dimensions a_o=6.89 A, b_o=6.95 A, c_o=8.45 A. They also

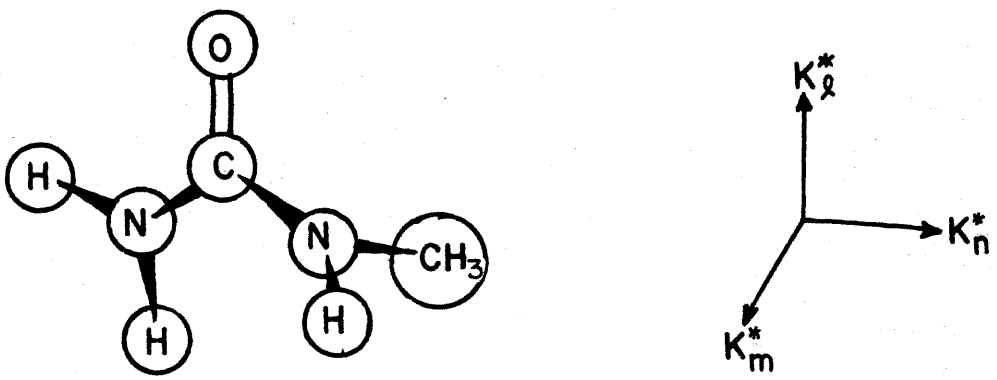

FIGURE 1. DIAGRAM OF THE METHYLUREA MOLECULE.

proposed atomic parameters on the basis of Fourier analyses and comparisons of calculated and observed values of low-order hk0 and h0ℓ structure factors. In their proposed structure, the plane of the urea group was nearly perpendicular to the a-b plane, making an angle of 34° with the a axis, and the C=O bond was nearly perpendicular to the c axis. The methyl group lay considerably outside the plane. The agreement of observed and calculated structure factors, particularly for the h0ℓ reflections of higher order, was not entirely satisfactory, however, and the authors were prompted to suggest that the proposed structure was probably not the correct one.

The magnetic measurements gave the following principal anisotropies for the methylurea crystal: $X^*_a - X^*_b = 1.87$, $X^*_c - X^*_a = 3.33$, and

$X^*_c - X^*_b = 5.21$ ($\times 10^{-6}$ cgs/mole); $X^*_c > X^*_a > X^*_b$ algebraically. Assuming the principal molecular axes to be determined by the symmetry of the urea group and hence to have the simple orientation shown in figure 1, the principal molecular anisotropies calculated for molecules oriented as in the proposed structure are: $K^*_\ell - K^*_m = 5.0$, $K^*_n - K^*_\ell = 1.8$, $K^*_n - K^*_m = 6.8$; $K^*_n > K^*_\ell > K^*_m$. This calculation would require the direction of minimum molecular diamagnetism (algebraically largest susceptibility) to be perpendicular to the C=O bond.

The anisotropy of methylurea was believed to be due to the non-spherical distribution of the π-electrons in the C=O double bond. Since the probability distribution assigned to these electrons by the molecular orbital approximation is such that they are mainly in two nearly cylindrical regions, elongated parallel to the C=O bond and symmetric about the urea group, it was believed that the direction of the C=O bond should be least diamagnetic and that the plane perpendicular to this bond should be nearly isotropic. It was therefore concluded that the structure proposed by Corey and Wyckoff was indeed not correct, and that the true structure was a radically different one.

B. Discussion of the Trial Structures.

An effort was made to determine the correct crystal structure of monomethylurea with the aid of the structure factors published by Corey and Wyckoff and the aid of the knowledge of the magnetic anisotropy of the crystal.

It was presumed that the principal molecular axes bore the simple relation to the urea group shown in figure 1, and that the direction of the C=O double bond was the principal axis of minimum diamagnetism. This being the case, the molecules must be oriented in the unit cell with the C=O bonds nearly parallel to the c axis, the direction of minimum crystal diamagnetism. It was then noted that the relative structure factor for the plane 200 was one of the two largest of the hk0 and h0ℓ reflections reported by Corey and Wyckoff;

its value was 48% of the maximum possible value which would occur if all the atoms were in phase. This fact suggested that the molecules lie nearly in planes which are perpendcular to the a axis and are separated by $a_o/2$. Finally, it was presumed that separate molecules in the crystal would be held together by hydrogen bonds between the oxygen atom of one molecule and a nitrogen atom of another.

Tests with scale models of the methylurea molecule showed that the molecules could be arranged in accordance with the first two conditions and in accordance with the symmetry of the space group $V^4 - P_{2_1 2_1 2_1}$, to which methylurea is known to belong, and that it could indeed be possible for separate molecules to be held together by hydrogen bonds as suggested, the molecules forming chains lying along the two-fold screw axes parallel to the c axis. By slight tilting of the plane of the urea group, a structure in agreement with the known dimensions of the unit cell could be possible. By turning the plane of the three atoms $H\text{-}N\text{-}C_{(methyl)}$ perpendicular to the plane of the urea group, as shown in figure 1, the scale models further suggested the possibility of a second hydrogen bond between the oxygen atom of one molecule and the secondary amide nitrogen atom of a molecule in a neighboring chain (see figure 2). The molecules could then be tied together into a three-dimensional network by hydrogen bonds. Although the bond between the carbonyl carbon atom and the nitrogen atom in the secondary amide group, $H\text{-}N\text{-}C_{(methyl)}$, would not have double bond character if the plane of this group were perpendicular to the plane of the urea group, it was felt that the corresponding decrease in resonance stabilization of the molecule would be offset by the increased stability of the crystal structure. For simplicity in the following calculation, the three bonds of the secondary amide nitrogen were made planar (actually corresponding to some double bond character in one of the bonds) rather than tetrahedral as in amines (the difference in the bond angles is only about 10^o).

The existence of a three-dimensional network of hydrogen bonds would mean that the dimensions and orientation of a single molecule, plus the hydrogen bond lengths, determine the unit cell dimensions. Using reasonable values of the interatomic distances[2], a system of

simultaneous equations was set up satisfying the above conditions and relating the unit cell dimensions to Eulerian angles defining the orientation of one molecule with respect to the crystallographic axes. The system of equations was solved graphically and it was found that only two orientations of the molecule were consistent with the observed unit cell parameters. For each orientation the coordinates of the atoms were then calculated with respect to an origin at the center of one oxygen atom. Thereafter, the origin was translated to the canonical origin for the particular space group (mid-way between three sets of mutually perpendicular non-intersecting 2-fold screw axes). The a-c and b-c projections of the trial

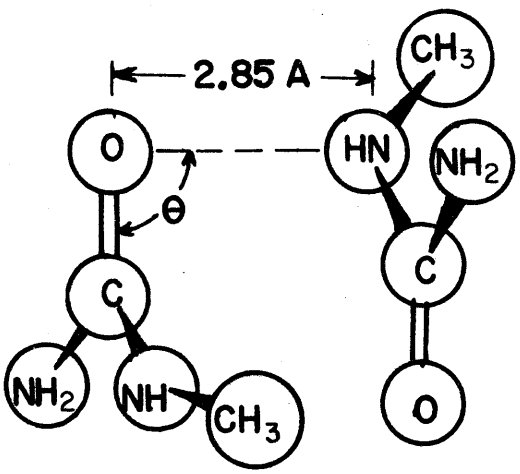

FIGURE 2. LINKING OF NEIGHBORING CHAINS.

structure corresponding to one of the allowed orientations of the molecule are shown in figures 3 and 4. The principal molecular anisotropies calculated for this structure, $K_{\ell}^{*}-K_{m}^{*}=6.6$, $K_{\ell}^{*}-K_{n}^{*}=6.9$, and $K_{m}^{*}-K_{n}^{*}=0.3$ ($\times 10^{-6}$ cgs/mole) ($K_{\ell}^{*}>K_{m}^{*}>K_{n}^{*}$) were in agreement with predictions. The trial structure corresponding to the second allowed orientation was rejected because the angle θ (see figure 2) was only 94°, a value which was felt to be too small for good hydrogen bonding.

Although the proposed trial structure was in general agreement with Patterson vector maps calculated for the a-c and a-b projections,

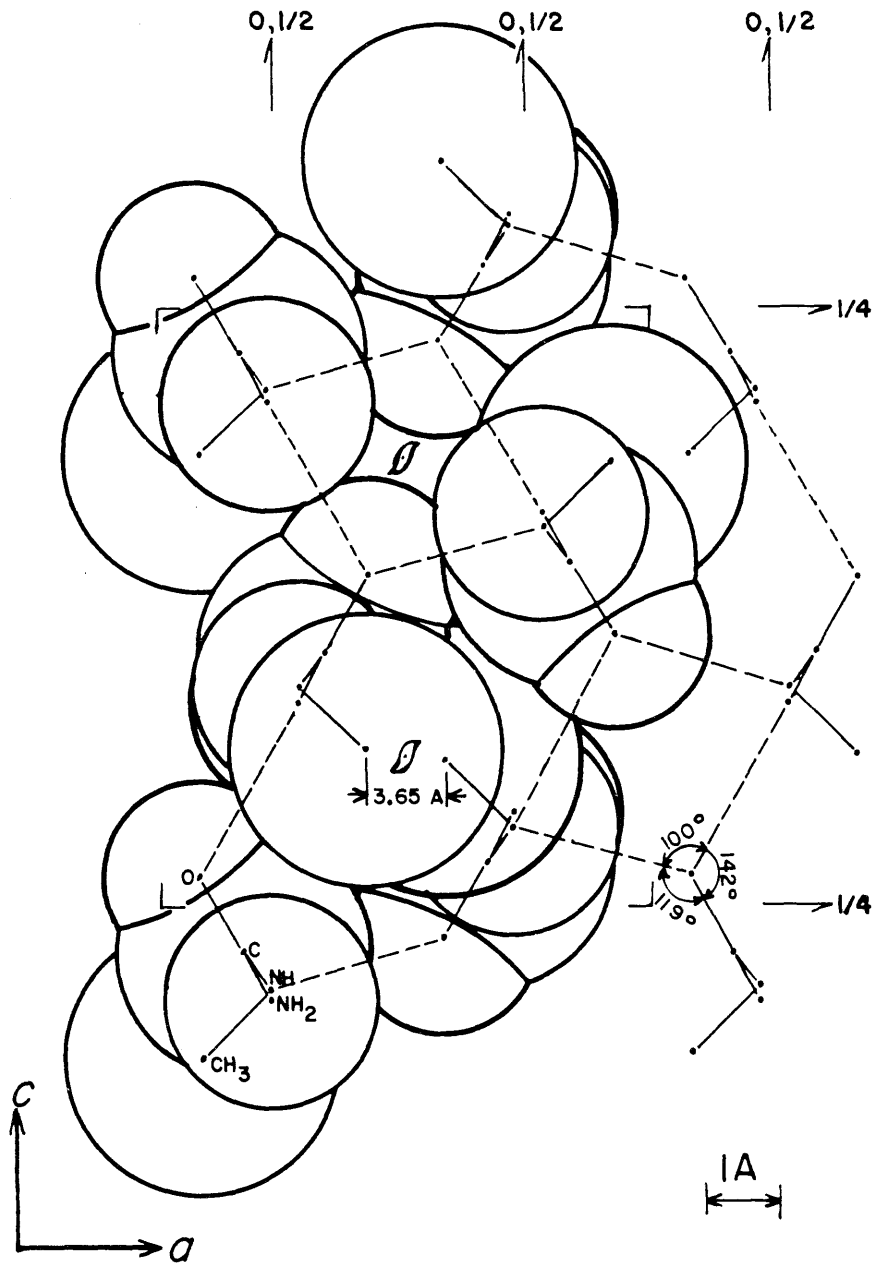

FIG. 3

METHYLUREA. *a-c* PROJECTION OF TRIAL STRUCTURE.

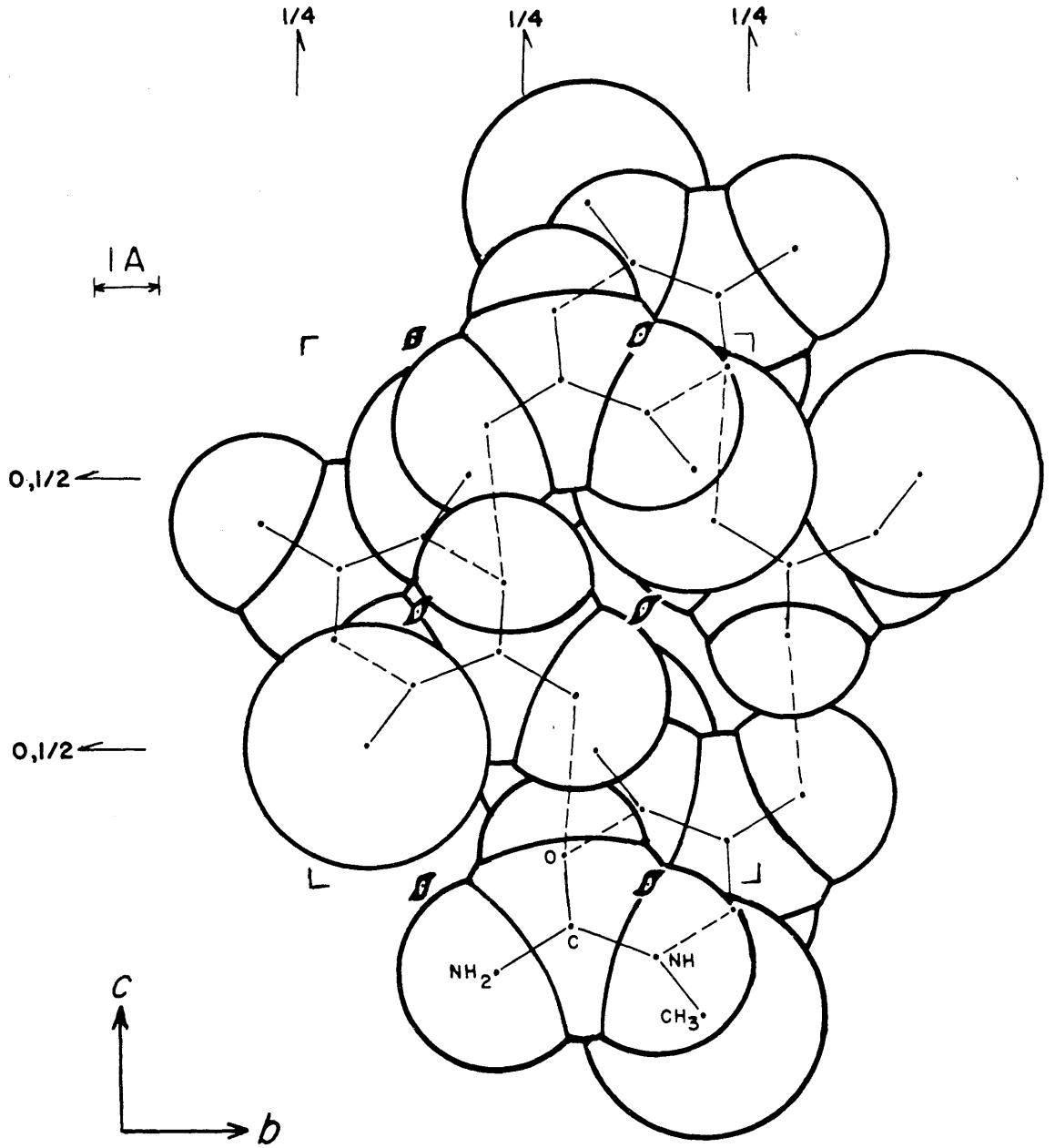

FIG. 4

METHYLUREA. *b-c* PROJECTION OF TRIAL STRUCTURE.

it did not give good agreement with the observed relative structure factors recorded by Corey and Wyckoff. Two-dimensional Fourier syntheses of the electron density, and corresponding difference maps, for the a-c and a-b projections were used to decide on atomic shifts. After four months work a structure was found which gave reasonable-appearing electron density maps for both the a-b and a-c projections. In this refined structure the center of gravity of the molecules had been shifted about one-half angstrom along the c-axis (closer to the centers of symmetry in figure 3) from the positions assigned in the original trial structure, the methyl group had been changed from one end of the molecule to the other (losing the hydrogen bonds between chains), the C=O bonds had been made more nearly parallel to the c axis, and the molecules had been rotated slightly around the c axis making the urea group less nearly perpendicular to the a axis.

Since the agreement of the observed and calculated structure factors was not satisfactory, it was decided to check the structure by obtaining 0kℓ diffraction data which were recorded only qualitatively by Corey and Wyckoff. In the process of collecting the 0kℓ data, the h0ℓ data were also collected for comparison with those of Corey and Wyckoff. It was immediately seen that their value of $|F_{102}|$ was in serious error. Instead of being one of the weakest reflections, the 102 reflection was the third strongest and almost as strong as the 200 reflection. Examination of the original report revealed that the 102 and 012 reflections had been confused. This was easily possible because the data were obtained from rotation photographs and because the a and b axis unit cell dimensions are almost equal. Also, because of this near equality, the 102 and 012 reflections are indistinguishable on the powder spectrogram reproduced by Corey and Wyckoff in their figure 1. As a consequence of this error, neither the structure proposed by Corey and Wyckoff, nor the newly proposed structure** was correct.

Some time was spent in trying to find a new trial structure to fit the data. The problem was first attacked by calculating Patterson vector maps for the three projections (figures 5,6,7). Then Fourier syntheses of the electron density in the a-b and a-c projec-

**Nor the rejected trial structure based on the second allowed orientation.

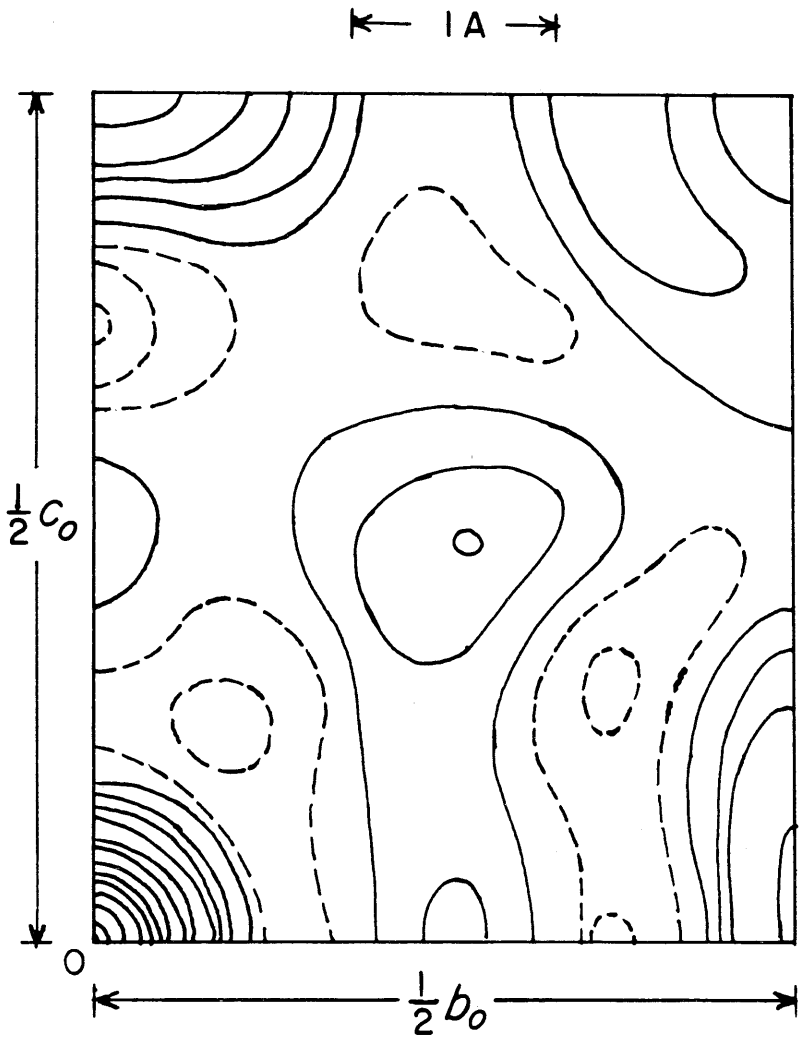

FIG. 5 (1 0 0) PATTERSON PROJECTION.

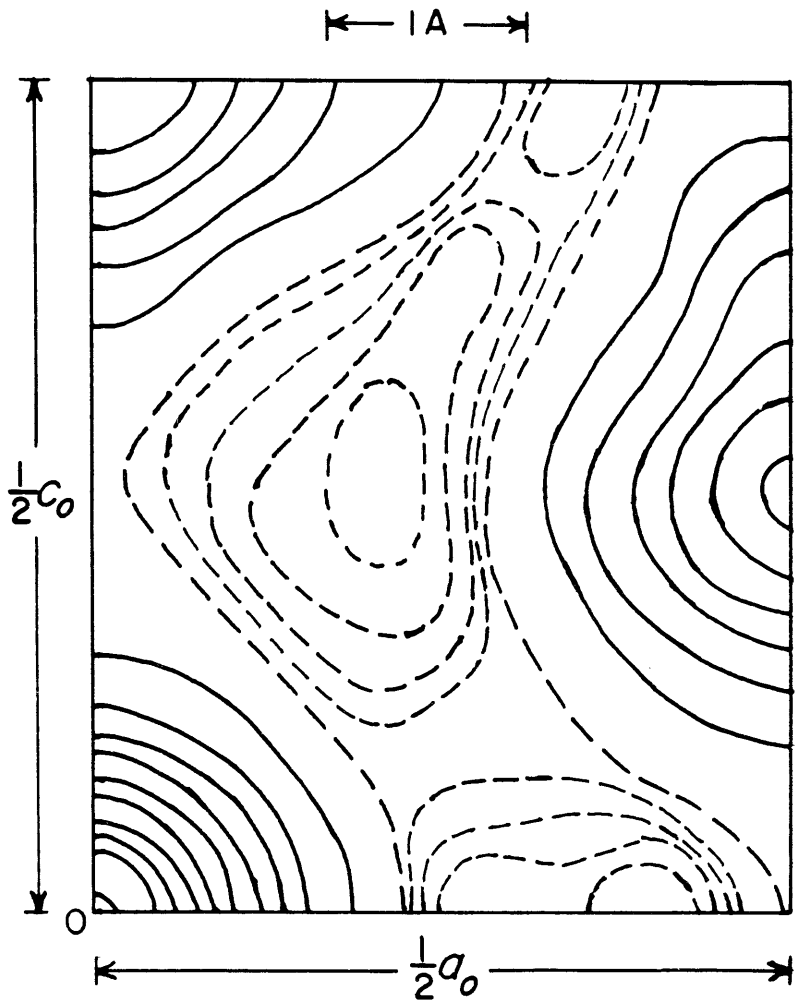

FIG. 6 (0 1 0) PATTERSON PROJECTION.

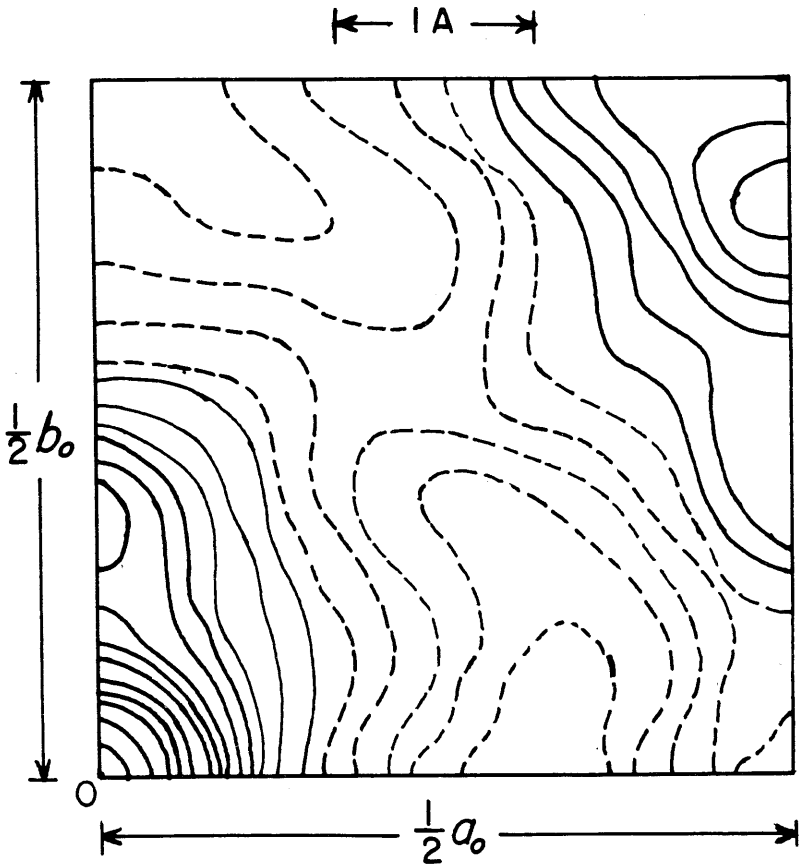

FIG. 7 (0 0 1) PATTERSON PROJECTION.

tions were made using for each only the three largest structure factors with signs arbitrarily assigned. Only one distinct synthesis for each projection was possible, the effect of changing signs being only to shift the origin or to change the sign of the electron density. The two Fourier syntheses are reproduced in figures 8 and 9 in which the electron density is on an arbitrary scale and the first unbroken contour is the zero contour. Since all other structure factors were smaller than the smallest used in figures 8 and 9, and therefore less than half the size of the largest, these two Fourier syntheses determine some of the essential features of the crystal structure.

The following conclusions were drawn: (1) The shape of the solid contours suggests that they outline the region of high (positive) electron density. (2) At $x = \frac{1}{4}$, $y = \frac{1}{2}$ in the a-b projection and at $x = \frac{1}{4}$, $z = \frac{3}{8}$ in the a-c projection the electron density is very large because many atoms overlap in projection. (3) The stretching out parallel to the b axis of the electron density in the a-b projection suggests that the molecules lie very nearly in planes perpendicular to the a axis and that the C=O bond is nearly parallel to the c axis. Two molecules related by the 2-fold screw axis parallel to the c axis and passing through $x = \frac{1}{4}$, $y = \frac{1}{2}$ are in the projection, figure 8. (4) The localization of the electron density near $x = \frac{1}{4}$, $z = \frac{3}{8}$ in the a-c projection and the prominence of the peaks in the a-c Patterson projection strengthen the previous conclusion and, further, suggest that the oxygen atom and methyl group are in cis configuration, a configuration which would increase the overlapping of atoms, in projection, if the conclusion were correct. (5) If the previous two conclusions are correct then in the b-c projection few atoms will greatly overlap. The facts that no $0k\ell$ structure factor (table 1) is especially large and that the peaks on the b-c Patterson projection are smaller than those in the a-c and a-b projections indicate that such is the case.

A trial structure with the following general features was then proposed. The molecules lie nearly in planes perpendicular to the a axis and the C=O bonds are nearly parallel to the c axis. The oxygen atom and the methyl group are in cis configuration. The

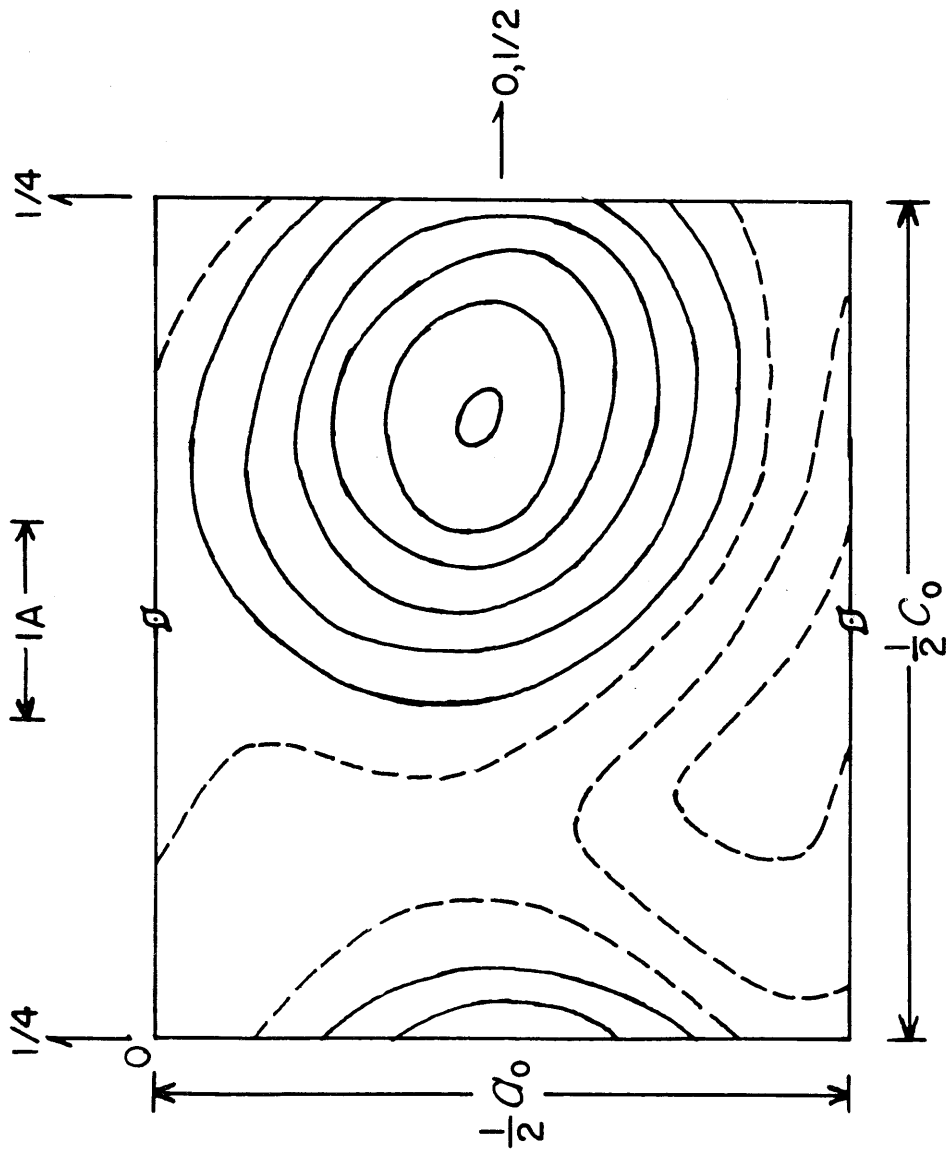

FIG. 8 (010) FOURIER PROJECTION USING ONLY THE THREE LARGEST STRUCTURE FACTORS : $F_{ho\ell} = A_{ho\ell} + B_{ho\ell}\sqrt{-1}$
$A_{200} = -72$, $B_{200} = 0$; $A_{102} = +64$, $B_{102} = 0$; $A_{101} = 0$, $B_{101} = +25$

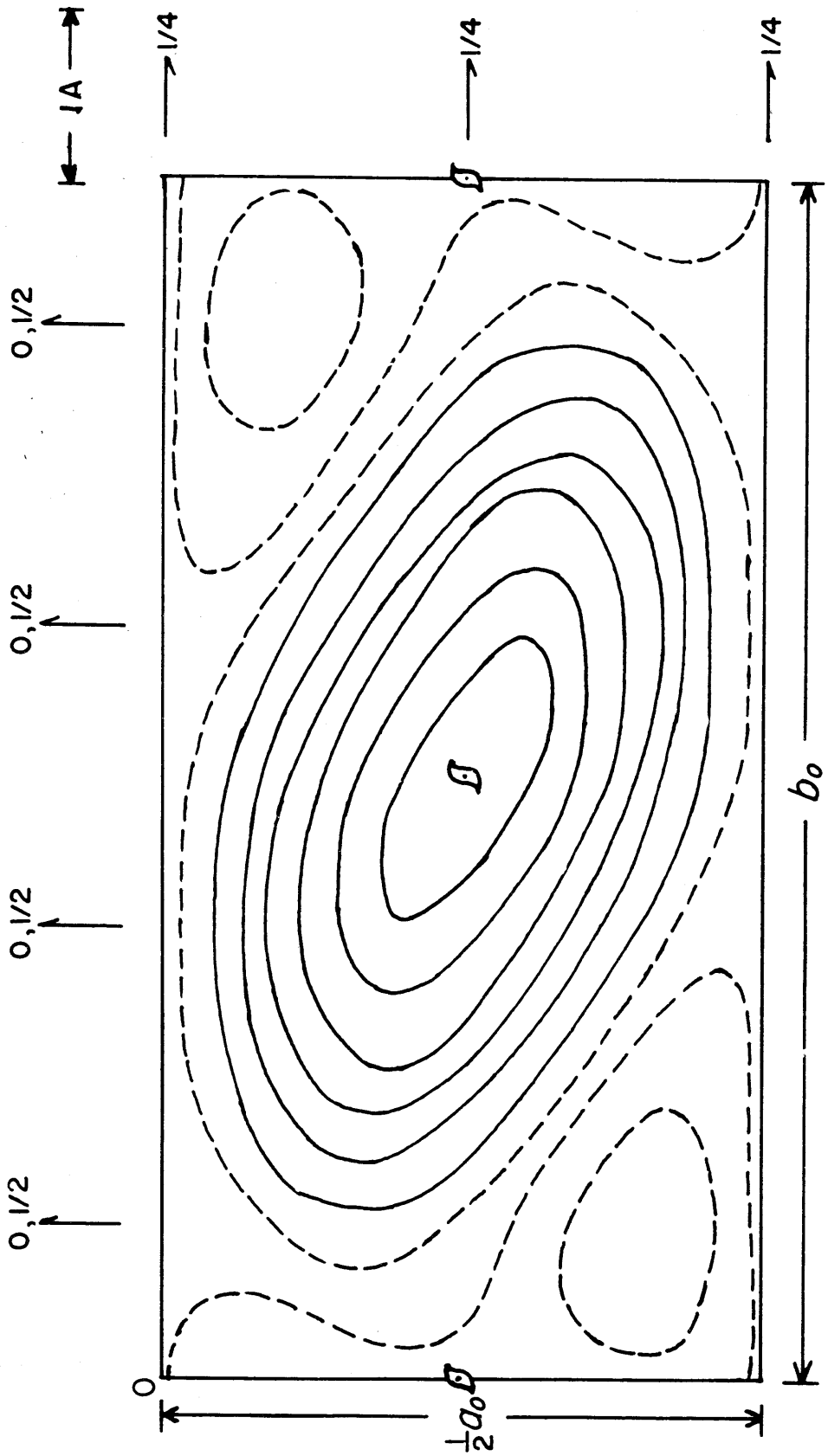

FIG. 9 (001) FOURIER PROJECTION USING ONLY THE THREE LARGEST STRUCTURE FACTORS: $F_{hko} = A_{hko} + B_{hko}\sqrt{-1}$
$A_{200} = -72$, $B_{200} = 0$; $A_{110} = 0$, $B_{110} = -77$; $A_{210} = -42$, $B_{210} = 0$

centers of gravity of the molecules are near $x = \frac{1}{4}$, $z = \frac{3}{8}$ and equivalent positions. As in the previous trial structure, hydrogen bonds hold the molecules together in chains which lie along the 2-fold screw axis parallel to c. Such a structure can best account for the greater length of the c axis and for the cleavage parallel to (110). Absence of cross-linking of the chains by hydrogen bonds would be consistent with the low melting point (101°C) of the crystal and with the (110) cleavage. The systematic weakness of the 0kℓ reflections for ℓ odd indicates a pseudo unit cell in the b-c projection with one-half the true c axis length. Such a pseudo unit cell exists in this trial structure if the centers of gravity of the molecules are near $y = 0$ or $y = \frac{1}{2}$.

Other structure factors of low order were added to the syntheses in figures 8 and 9 and their signs were varied in an attempt to deduce more detail, but without success. Because of the overlapping of the atoms in the a-b and a-c projections, it would be impossible to assign parameters to atoms with any certainty on the basis of two-dimensional Fourier syntheses or two-dimensional least-square refinements of these two projections. Indeed, it had been possible to obtain reasonable agreement between the refined first trial structure and the hk0 structure factors (which contained no error) and to obtain reasonable appearing electron density maps of the a-b projection even though the structure was incorrect. So long as two-dimensional data alone are available, this trial structure for methylurea can be confirmed in detail only in the b-c projection. Some work has been done to solve the structure by making Fourier syntheses of the b-c projection in which only the lower order and stronger reflections were used, their signs being varied judiciously. Several variations of the above trial structure which were in agreement with simple Fourier syntheses were tested by calculating the 0kℓ structure factors in order to determine more signs for the preparation of more complete Fourier syntheses and difference maps. So far, this process has not met with success.

C. Structure Factors for Methylurea.

The Buerger[3] precession camera was used to obtain the diffraction data listed in table 1. The precession angle used was $\mu = 30^\circ$, and the crystal-to-film distance was F = 90 mm. The radiation used was Mo-K_α. Only one hundred thirty of the 301 zero layer reflections possible (for $\mu = 30^\circ$ and Mo-K_α) were recorded since the film holder was not large enough. Reflections of the type hk0, h0ℓ and 0kℓ were recorded with h and k up to 6 and ℓ up to 7 plus 008. Fourteen more hk0 and h0ℓ reflections were observed than were observed by Corey and Wyckoff.

The intensities of the diffraction maxima were recorded photographically and estimated visually by comparison with a standard intensity strip. The intensity strip had 12 spots with relative darkness ranging from 1 to 40 (barely visible to near maximum darkness) and successive spots differed in darkness by somewhat more than the least amount detectable by the eye. The size of the spots on the intensity strip was about the same as that of the spots being measured. The precision with which the intensities could be measured was estimated to be $\pm 5\%$. The diffraction maxima from each reciprocal net investigated were recorded several times for different lengths of time in order to extend the range of observable intensities. To compare diffraction maxima recorded on two different films for different lengths of time, the ratios of intensities of corresponding spots on the two films were averaged for many spots in the moderate intensity range in order to get the most reliable ratio.

Lorentz and polarization factors (L and P) for the precession camera for $\mu = 30^\circ$, for the zeroth layer, and as a function of position on the film were calculated by Waser[4] who put the data in the form of a map on which level curves of 1/LP were drawn at intervals of 5% of the maximum value. A positive transparency of the map was made photographically and enlarged to correspond to a crystal-to-film distance of F=90 mm. There is a slight distortion in the shape of the map as reproduced in the literature but this error had negligible effect on the structure factors. The transparency was placed over the X-ray photographs and the factor 1/LP for each diffraction maximum was read directly.

Relative structure factors were then calculated. To make the relative structure factors for any two of the three different reciprocal nets comparable, the structure factors were multiplied by the average ratio of values of corresponding $h00$, $0k0$ and 00ℓ structure factors which they had in common. Since the data for any one of the reciprocal nets had only 3 or 4 relative structure factors in common with the data for any other net, this procedure was not completely reliable. When comparable relative structure factors had been computed for the three reciprocal nets, they were multiplied by a factor to make them comparable with those of Corey and Wyckoff which, in turn, probably do not differ greatly from the absolute structure factors.

The largest structure factors, those for the 110, 200 and 102 reflections, were corrected for extinction using the powder spectrogram given by Corey and Wyckoff in their figure 1. The corresponding Lorentz and Polarization factor (1/LP) for the 102 reflection was obtained by graphical interpolation of the factors in a table accompanying the reproduction of the spectrogram.

In addition to the change in the value of $|F_{102}|$, the value of $|F_{204}|$ given by Corey and Wyckoff was also noticeably changed, but the change was less serious than that in $|F_{102}|$.

The following criticisms of the experimental technique by which the diffraction data were obtained may be made. First, the crystals were larger in cross section than the X-ray beam and not spherical so that the amount of scattering matter in the X-ray beam varied as the crystals moved. Second, the crystals were large enough so that absorption effects might have to be considered.

Counter arguments are the following; (1) The crystal used to obtain the $hk0$ data was a one-millimeter cube with the c-axis perpendicular to a face. The variation of scattering matter for a precession angle of 30° was negligible. The crystal used to obtain the $h0\ell$ and $0k\ell$ data was a prism with square cross section, 4x1x1 mm. The c axis was parallel to the long direction and the long faces, (110), made angles of 45° with the a and b axes. For 30° precession angle and an X-ray beam one-half millimeter in cross section, a variation of $\pm 14\%$ in scattering matter was estimated. The corresponding

error in the relative structure factors is ±7%. (2) Using the atomic absorption coefficients, μ/ρ, given by Compton and Allison[5], the absorption coefficient per unit volume, μ, for methylurea is 0.99. The effect of absorption on intensity of X-rays scattered by a cylindrical powder specimen of radius r has been calculated[6] as a function of r and of ϑ, the scattering angle (plane of incident and scattered rays perpendicular to axis of cylinder). For μ=0.99 and r = 0.1 cm, the intensity of the scattered ray is reduced to 85% of the value in absence of absorption, but the reduction is practically independent of ϑ. (3) No unexplainable variations of intensities of corresponding diffraction spots in the four quadrants of any precession photograph were observed. (4) Corey and Wyckoff obtained their data from rotation photographs using a cylindrical crystal small enough to need no absorption correction with Cu-K_α radiation and, except for errors in indexing, their data are presumably more accurate than the new data. Seventeen h0ℓ relative structure factors greater than 9 (excluding 200, 102 and 204) were compared with the corresponding values given by Corey and Wyckoff and found to differ by amounts in the range +19% to -12% (average, ±6%). The geometry of crystal and X-ray beam was the same during the recording of both the h0ℓ and the 0kℓ data. It is therefore inferred that the range of errors in the 0kℓ data is not greater than the range, above, for the h0ℓ data.

It is concluded that the data are sufficiently accurate for their intended purposes of detecting errors in indexing of the older data and of checking the proposed trial structure.

In table 1 the relative structure factors for the observed h0ℓ, hk0 and 0kℓ reflections are recorded. The data published by Corey and Wyckoff for the h0ℓ and hk0 reflections are given for comparison.

TABLE 1. OBSERVED RELATIVE STRUCTURE FACTORS FOR MONOMETHYLUREA.

	$F_{h0\ell}$			F_{hk0}			$F_{0k\ell}$
	This	Wyckoff		This	Wyckoff		This
h ℓ	Thesis	& Corey	h k	Thesis	& Corey	k ℓ	Thesis
2 0	70.9	60.5	2 0	71.1	60.5	2 0	17.5
4 0	24.8	22.3	4 0	26.4	22.3	4 0	29.3
6 0	12.7	10.7	6 0	11.3	10.7	6 0	11.1
0 2	27.6	25.4	0 2	18.5	14.7	0 2	25.8
0 4	31.8	30.6	0 4	29.3	23.8	0 4	32.6
0 6	<3.0	2.7	0 6	10.0	10.3	0 6	≤4.2
0 8	5.5	6.7	2 2	≤2.7	0.0	0 8	6.4
2 2	7.1	7.7	2 4	11.4	10.0	2 2	30.1
2 4	18.7	1.6	2 6	10.7	8.7	2 4	9.8
2 6	<3.0	0.0	4 2	5.7	5.7	2 6	12.6
4 2	13.3	13.5	4 4	5.1	4.7	4 2	10.1
4 4	<3.0	2.8	4 6	<1.0	---	4 4	10.1
4 6	<3.0	0.0	6 2	<1.0	0.0	4 6	11.1
6 2	<3.0	0.0	6 4	4.0	---	6 2	5.4
6 4	6.8	---	6 6	3.8	---	6 4	10.3
6 6	<3.0	---	2 1	42.3	33.7	6 6	2.3
1 2	64.1	4.3	2 3	13.0	11.2	2 1	7.7
1 4	16.6	18.6	2 5	32.6	26.1	2 3	16.1
1 6	17.7	17.5	4 1	23.7	19.8	2 5	7.4
3 2	20.2	20.7	4 3	4.7	3.6	2 7	7.2
3 4	9.4	9.7	4 5	15.4	14.3	4 1	31.8
3 6	5.2	0.0	6 1	4.9	4.9	4 3	11.7
5 2	8.6	7.7	6 3	3.0	3.4	4 5	10.6
5 4	3.7	5.2	6 5	<1.0	---	4 7	8.0
5 6	5.6	---	1 2	12.1	9.9	6 1	11.6
1 1	25.4	24.5	1 4	16.1	14.7	6 3	<2.0
1 3	11.3	12.0	1 6	7.7	6.6	6 5	4.1
1 5	<3.0	0.0	3 2	6.8	6.5	6 7	2.3
1 7	<3.0	3.6	3 4	18.0	16.0	1 2	19.5
3 1	19.2	19.7	3 6	9.7	8.6	1 4	27.9
3 3	9.7	10.4	5 2	12.8	11.7	1 6	15.3
3 5	<3.0	3.3	5 4	4.3	0.0	3 2	16.1
3 7	5.3	---	5 6	<1.0	---	3 4	23.4
5 1	3.4	2.8	1 1	77.1	60.6	3 6	2.2
5 3	<3.0	0.0	1 3	8.1	7.0	5 2	7.7
5 5	6.6	6.4	1 5	<1.0	0.0	5 4	7.8
5 7	<3.0	---	3 1	2.4	0.0	5 6	2.3
2 1	12.7	13.5	3 3	12.1	9.3	1 1	13.2
2 3	15.4	17.5	3 5	8.6	6.8	1 3	2.2
2 5	14.5	15.0	5 1	9.4	9.1	1 5	5.6
2 7	5.3	6.4	5 3	1.7	2.8	1 7	3.2
4 1	<3.0	0.0	5 5	3.2	---	3 1	3.1
4 3	8.2	7.6				3 3	8.4
4 5	5.2	6.2				3 5	8.8
4 7	<3.0	---				3 7	7.2
6 1	<3.0	0.0				5 1	4.0
6 3	10.8	11.2				5 3	5.9
6 5	9.7	---				5 5	4.4
6 7	<3.0	---				5 7	3.3

III. REFERENCES.

Part I.

(1) G.H.Livens, The Theory of Electricity, Cambridge University Press, London (1926).

(2) J.H.Van Vleck, The Theory of Electric and Magnetic Susceptibilities, Oxford University Press, London (1932).

(3) P.W.Selwood, Magnetochemistry, Interscience Publishers Inc., New York (1956).

(4) L.F.Bates, Modern Magnetism, Cambridge University Press, London (1951).

(5) I.S.Sokolnikoff, Tensor Analysis, John Wiley & Sons Inc., New York (1951), chapter 1.

(6) W.A.Wooster, Crystal Physics, Cambridge University Press, London (1938), chapter 1.

(7) F.Bitter, Introduction to Ferromagnetism, McGraw-Hill Book Co. Inc., New York (1937), chapter 6.

(8) L.Page and N.I.Adams, Principles of Electricity, D.Van Nostrand Co. Inc., New York, Ed.2 (1949), pages 90-4.

(9) See, for example, reference 3, pages 91-103.

(10) A.Clow, Trans. Faraday Soc. (1937), 33, 381-8.

(11) Reference 3, pages 119-22.

(12) L.Pauling, J.Chem.Physics, (1936), 4,673-7.

(13) Reference 8, pages 166-70.

(14) Reference 8, pages 237-44.

(15) C.V.Raman and K.S.Krishnan, Proc.Roy.Soc.London (1927), 113A, 511-19.

(16) C.V.Raman and K.S.Krishan, ibid., (1927), 115A,549-54.

(17) M.B.Vol'kenshtein and L.A.Borovinsky, Doklady Akad. Nauk SSSR, (1952), 85,977-80 (see Chem.Abstr. 47,1445D).

(18) K.Lonsdale, Proc.Roy.Soc.London (1939), 171A,541-67.

(19) K.Lonsdale, Reports on Progress in Physics, (1937), 4,368-89.

(20) Reference 3, chapter 7.

(21) L.Pauling, R.B.Corey and H.R.Branson, a series of papers in Proc. Nat. Acad. Sci., (1951), 37, 205-11 and 235-85.

(22) L.C.Jackson, Proc.Roy.Soc.London, (1933), 140A,695-

(23) I.I.Rabi, Phys.Rev. (1927), 29,174-85.

(24) See for example, reference 4, pages 115-18.

(25) K.S.Krishnan et.al., a series of papers in Phil.Trans.Roy.Soc. London between 1933 and 1939, especially:(1933),231A,235-262; (1933),232A,99-115; (1935), 234A,265-98.

(26) H.W.Hoyer, M.S. Thesis, California Institute of Technology (1948),

(27) See for example, reference 8, pages 394-402.

(28) See for example, reference 3, chapter 4.

(29) R.W.G.Wyckoff, The Structure of Crystals, Chemical Catalog Co., New York,(1924), pages 123-40

(30) N.J.Tighe, Fused-Quartz Fibers, National Bureau of Standards circular #569 (U.S.Department of Commerce, $0.50)

(31) O.Reinkober, Physik. Z., (1931), 32, 243-50.

(32) O.Reinkober, ibid., (1932), 33,32-38.

(33) O.Reinkober, ibid., (1937), 38,112-22.

(34) J.Strong, Procedures in Experimental Physics, Prentice-Hall Inc., Englewood Cliffs, N.J., (1938), chapter 5.

(35) M.T.Rogers, Ph.D. Thesis, California Institute of Technology, (1941), pages 64 and 70.

(36) K.S.Krishnan, B.C.Guha, S.Banerjee, Phil.Trans.Roy.Soc.London (1936), 235A,343 (footnote)

(37) Reference 26, page 12.

(38) Reference 34, chapter 3.

(39) K.Iokibe, S.Sakai, Phil.Mag. (1921), 42,397-418.

(40) Reference 4, page 194.

(41) F.W.Constant and J.M.Formwalt, Phys.Rev. (1939), 56,373-7; (1938), 53,432 ; (1945), 63,441-5; and Rev.Mod.Phys. (1945), 17,81-6.

(42) Reference 4, page 133.

(43) Reference 3, pages 189-92

(44) Reference 18, pages 544-5

(45) W.R.Smythe, Static and Dynamic Electricity, McGraw-Hill Book Co. Inc., New York (1939), pages 205-6 (problems 80-84)

(46) P.Groth, Chemische Krystallographie, W.Englemann, Leipzig (1908), Volume 2, pages 90-92.

(47) Reference 46, volume 2, pages 59-62 and 74-75

(48) Reference 46, volume 3, pages 143-4

(49) S.B.Hencricks, Z.Krist., (1935), 91, 48-64

(50) Reference 46, volume 3, page 98.

(51) J.D.Bernal, Z.Krist., (1931), 78, 363-9

(52) C.J.Ksanda and G.Tunell, Am.J.Sci., (1938), 35A, 173-8 (see Chem.Abstr. 33, 2787(9))

(53) Yoichi Iitaka, Proc. Japan Acad., (1954), 30, 109-12

(54) G.Albrecht and R.B.Corey, J.Am.Chem.Soc. (1939), 61, 1087-1103

(55) Reference 46, volume 3, pages 539-40

(56) Reference 46, volume 3, page 550

(57) R.B.Corey and R.W.G.Wyckoff, Z.Krist. (1932), 81, 386-95

(58) Reference 46, volume 3, page 555.

(59) F.R.Lipsett, Can.J.Phys. (1957), 35, 284-98.

(60) Reference 46, volume 5, pages 437-8.

(61) W.H.Zachariasen, Z.Krist. (1929), 71, 501-12.

(62) A.Mookherji, Acta.Cryst., (1957), 10, 25-6.

(63) K.S.Krishnan, B.C.Guha and S.Banerjee, Phil.Trans.Roy.Soc. London, (1933), 231A, 235-62.

(64) D.A.Edwards, Z.Krist., (1931), 80, 154-63

(65) International Critical Tables, McGraw-Hill Book Co, Inc. New York (1929), volume 6, pages 354-64.

(66) K.Lonsdale, J.Chem.Soc., (1938), 364-8.

(67) R.B.Corey and R.W.G.Wyckoff, Z.Krist., (1934), 89, 462-8.

(68) K.Lonsdale, Proc.Roy.Soc.London, (1941), 177A, 272-80.

(69) R.B.Corey and R.W.G.Wyckoff, Z.Krist., (1933), 85, 132-42.

(70) R.B.Corey and R.W.G.Wyckoff, Z.Krist., (1932), 81, 386-95.

(71) Reference 3, page 111.

(72) D.W.J.Curickshank, Acta.Cryst., (1956), 9, 915-23.

(73) R.E.Marsh, R.B.Corey and L.Pauling, Biochimica et Biophysica Acta, (1955), 16, 1-34.

Part II

(1) R.B.Corey and R.W.G.Wyckoff, Z.Krist., (1933), 85, 132-42.

(2) L.Pauling, The Nature of the Chemical Bond, Cornell University Press, Ithaca, New York (1948), Chapter 5.

(3) M.J.Buerger, The Photography of the Reciprocal Lattice, American Society for X-ray and Electron Diffraction, monograph, The Murray Printing Co., Cambridge, Mass.(1944)

(4) J.Waser, Rev.Sci.Instr., (1951), 22, 563-8.

(5) A.H.Compton and S.K.Allison, X-rays in Theory and Experiment, D.Van Nostrand Co., New York (1946), page 800.

(6) International Tables for Determination of Crystal Structures, Gebr. Borntraeger, Berlin (1935), volume 2, page 583.

IV. APPENDIX.

FIGURE 14. MAGNETIC ANISOTROPY DATA FOR KNO_3.

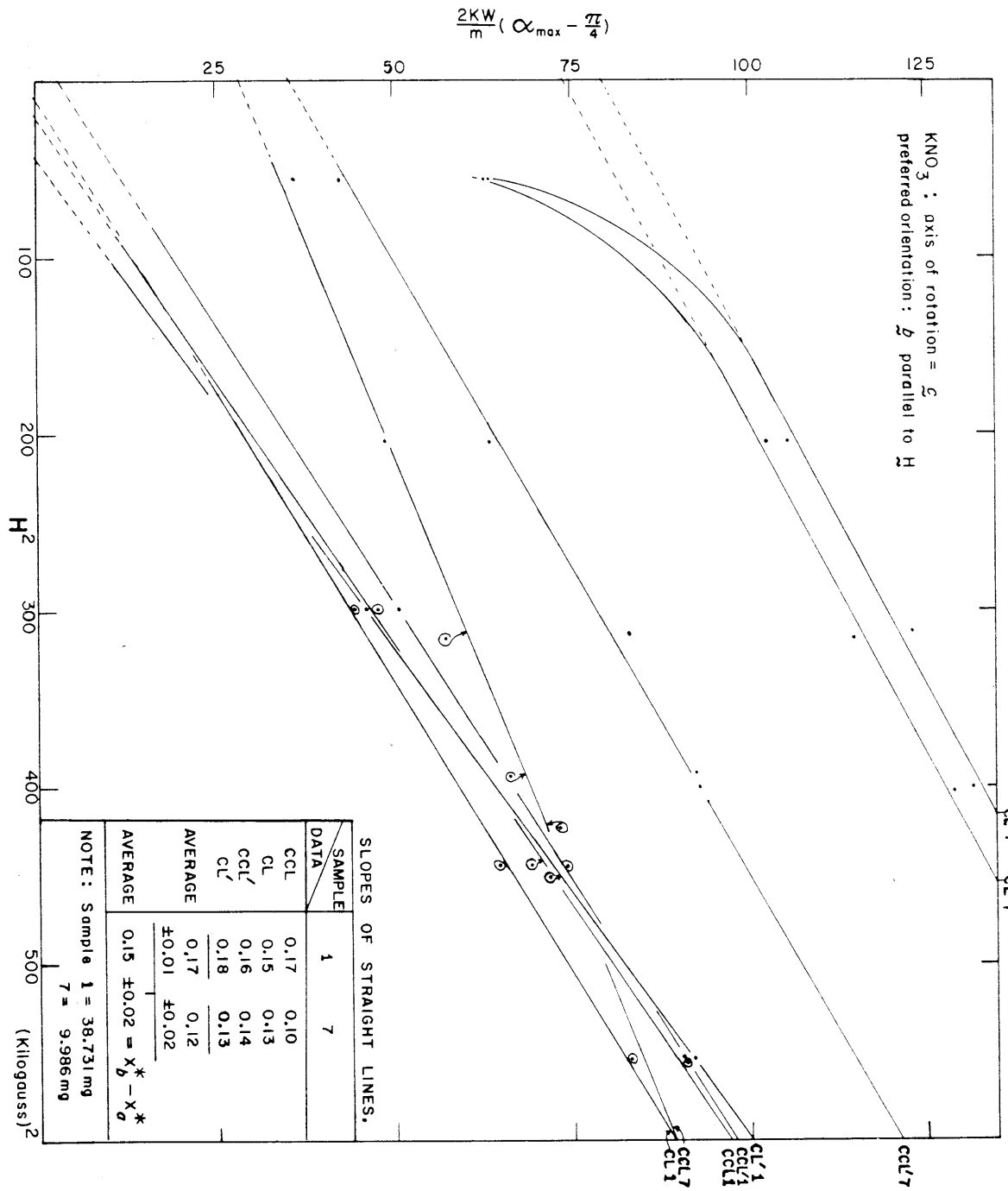

SLOPES OF STRAIGHT LINES.

DATA \ SAMPLE	1	7
CCL	0.17	0.10
CL	0.15	0.13
CCL′	0.16	0.14
CL′	0.18	0.13
AVERAGE	0.17 ±0.01	0.12 ±0.02
AVERAGE	0.15 ±0.02 = $\chi_b^* - \chi_a^*$	

NOTE: Sample 1 = 38.731 mg
7 = 9.986 mg

FIGURE 15. MAGNETIC ANISOTROPY DATA FOR KNO_3.

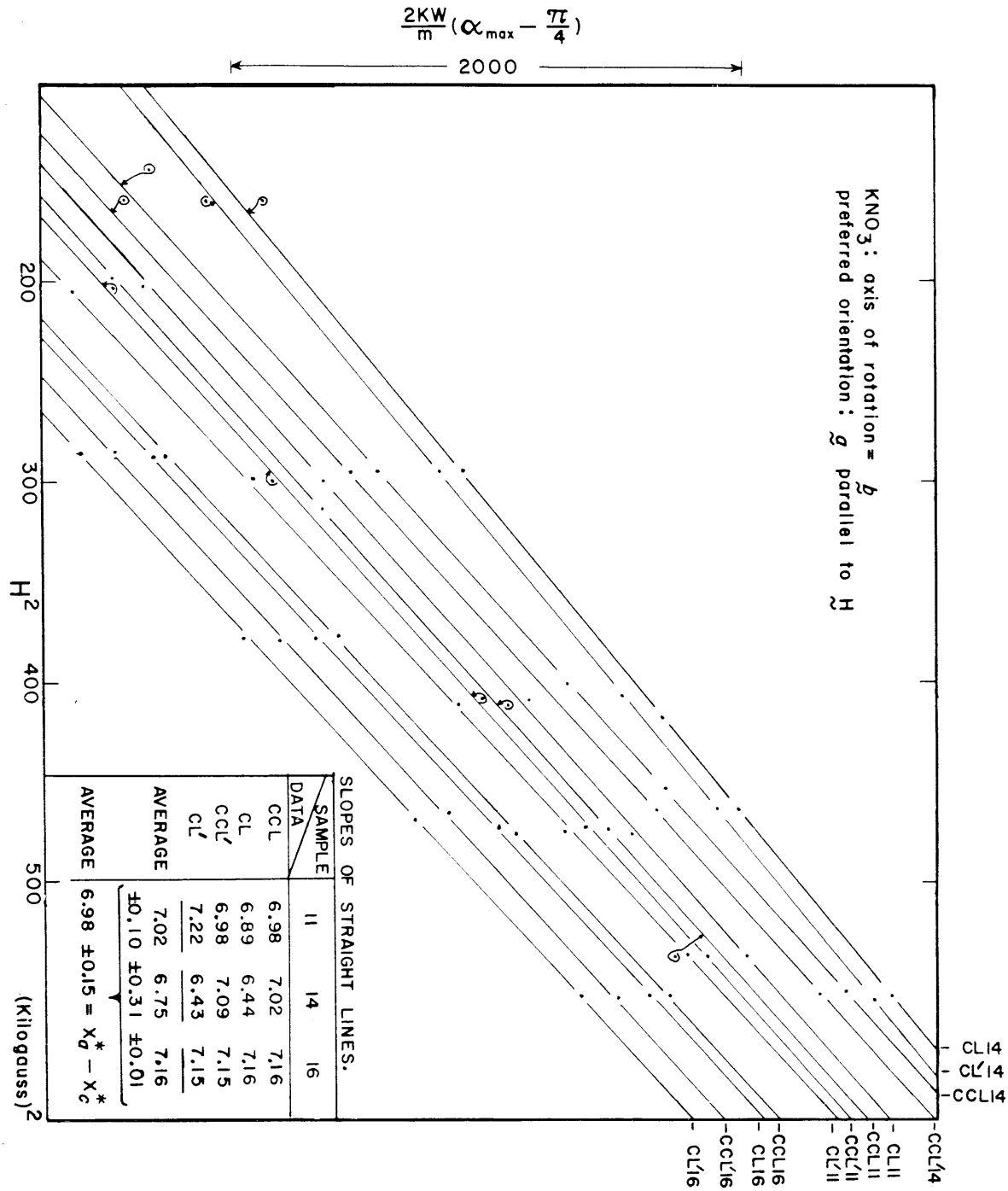

SLOPES OF STRAIGHT LINES.

DATA \ SAMPLE	11	14	16
CCL	6.98	7.02	7.16
CL	6.89	6.44	7.16
CCL'	6.98	7.09	7.15
CL'	7.22	6.43	7.15
AVERAGE	7.02	6.75	7.16
	±0.10	±0.31	±0.01

AVERAGE $6.98 \pm 0.15 = X_a^* - X_c^*$

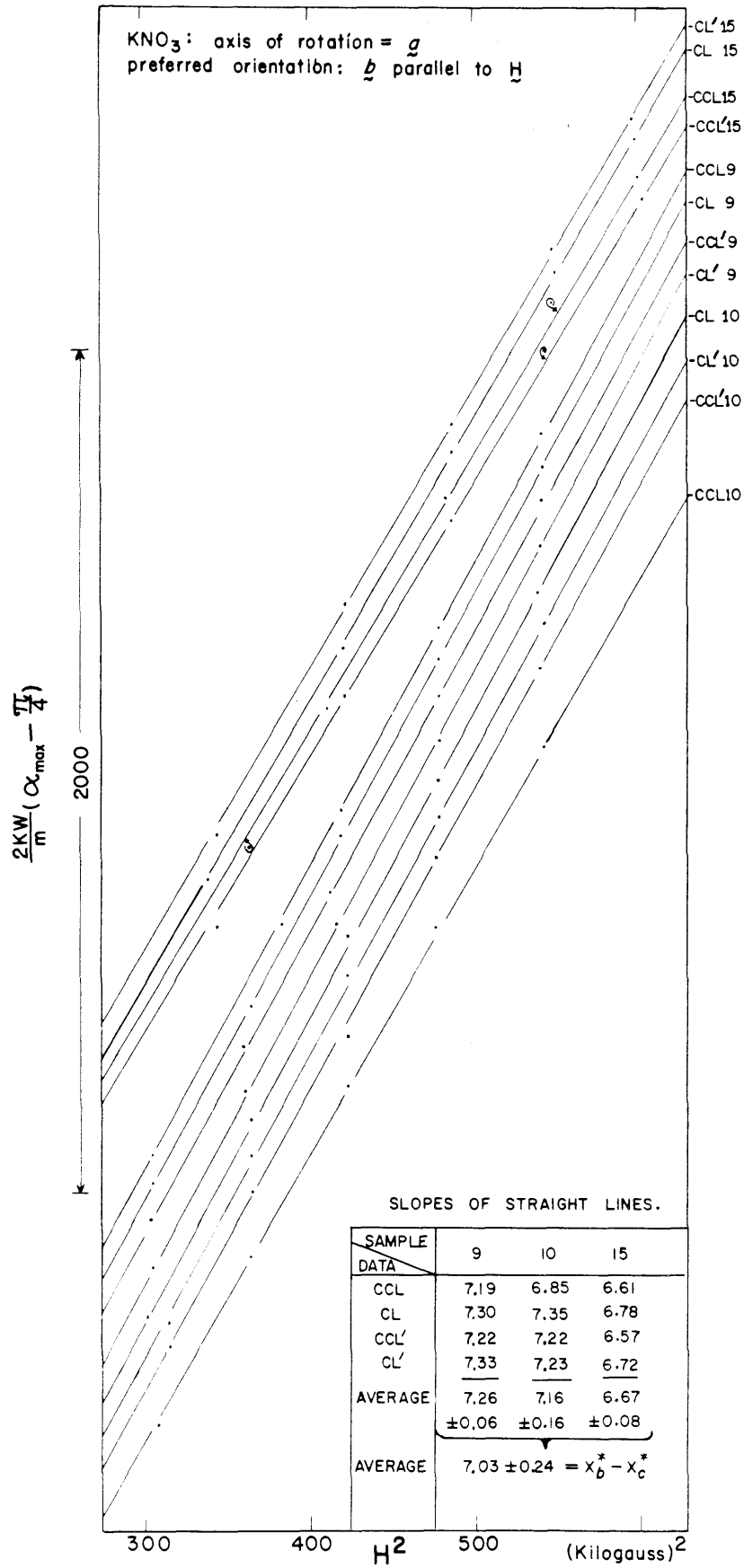

SLOPES OF STRAIGHT LINES.

SAMPLE / DATA	9	10	15
CCL	7.19	6.85	6.61
CL	7.30	7.35	6.78
CCL'	7.22	7.22	6.57
CL'	7.33	7.23	6.72
AVERAGE	7.26	7.16	6.67
	±0.06	±0.16	±0.08
AVERAGE	7.03 ±0.24 $= x_b^* - x_c^*$		

FIGURE 16. MAGNETIC ANISOTROPY DATA FOR KNO_3.

FIGURE 17. MAGNETIC ANISOTROPY DATA FOR KHC_2O_4.

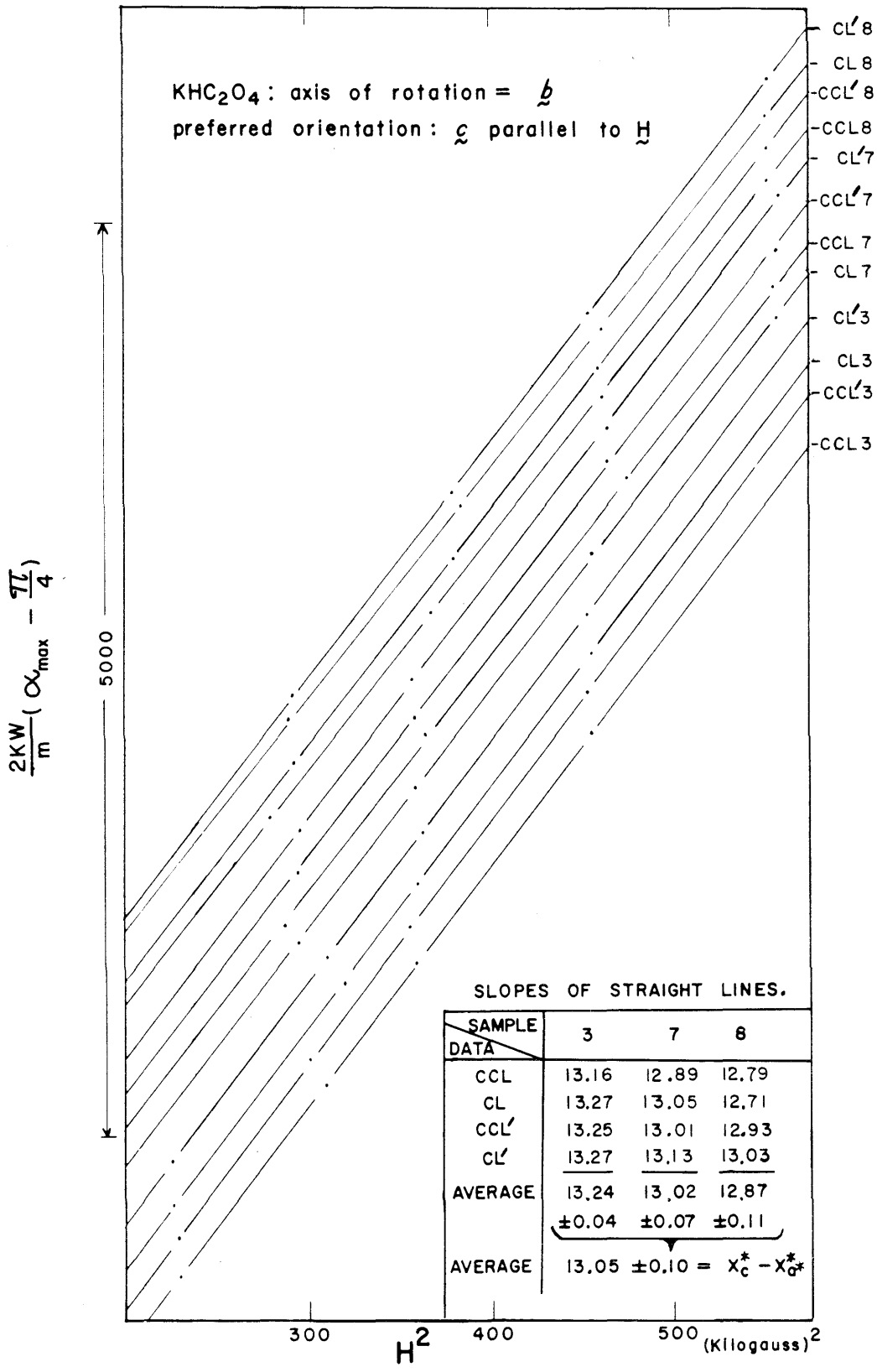

FIGURE 18. MAGNETIC ANISOTROPY DATA FOR KHC_2O_4.

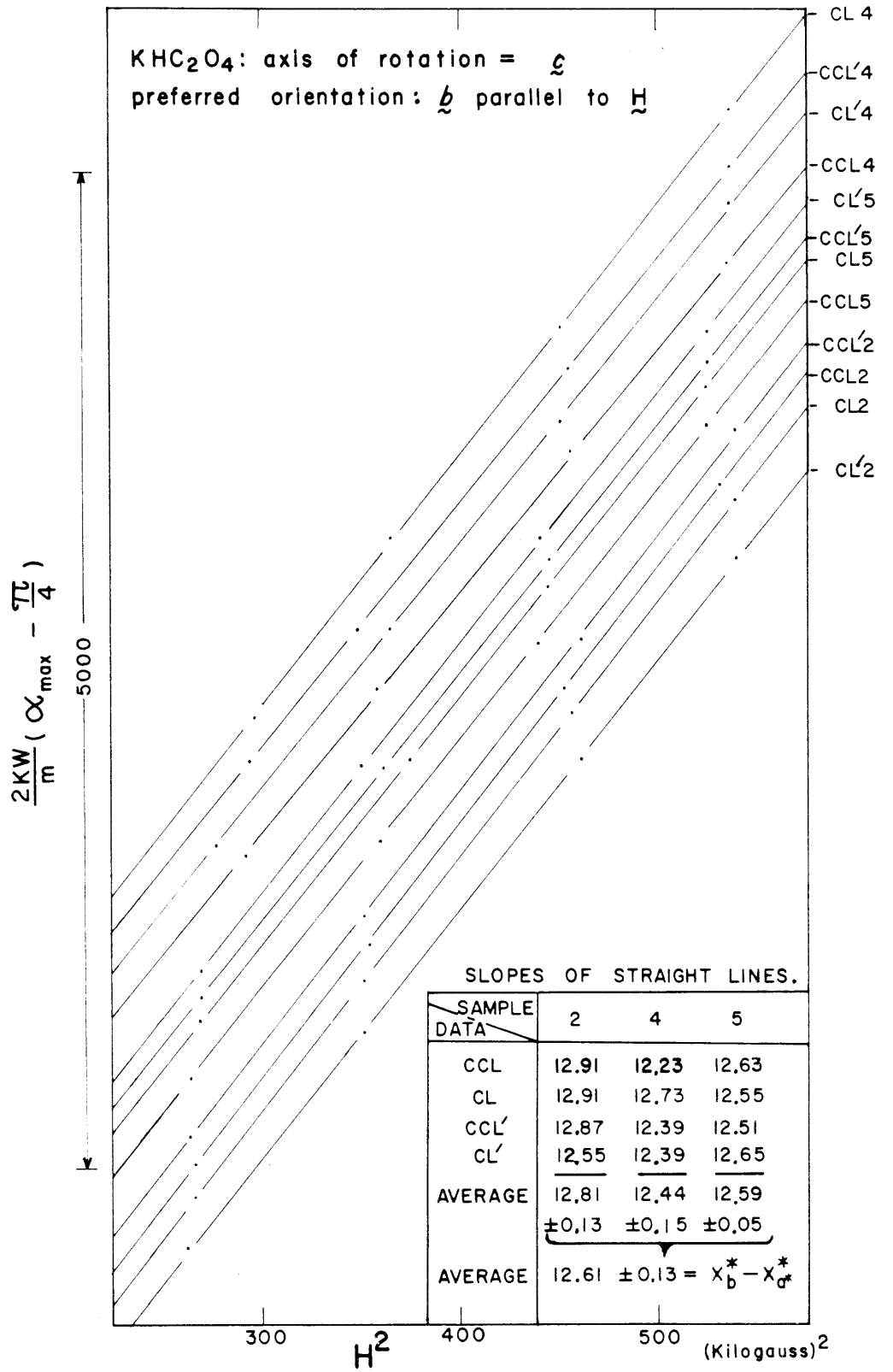

SLOPES OF STRAIGHT LINES.

SAMPLE / DATA	2	4	5
CCL	12.91	12.23	12.63
CL	12.91	12.73	12.55
CCL'	12.87	12.39	12.51
CL'	12.55	12.39	12.65
AVERAGE	12.81	12.44	12.59
	±0.13	±0.15	±0.05
AVERAGE	12.61 ±0.13 = $X_b^* - X_{a^*}^*$		

FIG. 19 MAGNETIC ANISOTROPY DATA FOR KHC_2O_4.

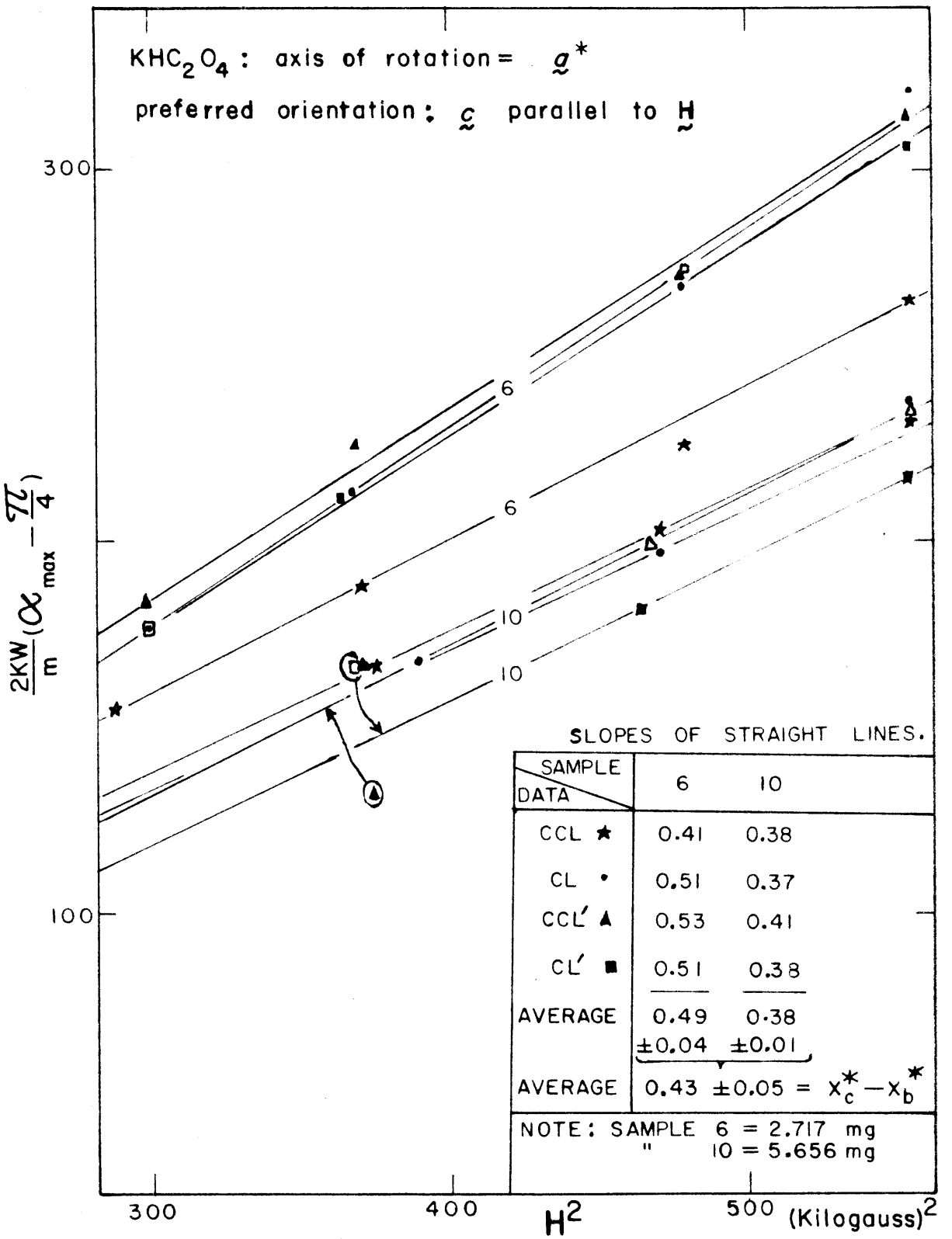

SLOPES OF STRAIGHT LINES.

SAMPLE / DATA	6	10
CCL ★	0.41	0.38
CL •	0.51	0.37
CCL′ ▲	0.53	0.41
CL′ ■	0.51	0.38
AVERAGE	0.49 ±0.04	0.38 ±0.01
AVERAGE	0.43 ±0.05 = $x_c^* - x_b^*$	

NOTE: SAMPLE 6 = 2.717 mg
" 10 = 5.656 mg

FIGURE 20. MAGNETIC ANISOTROPY DATA FOR GLYCINE.

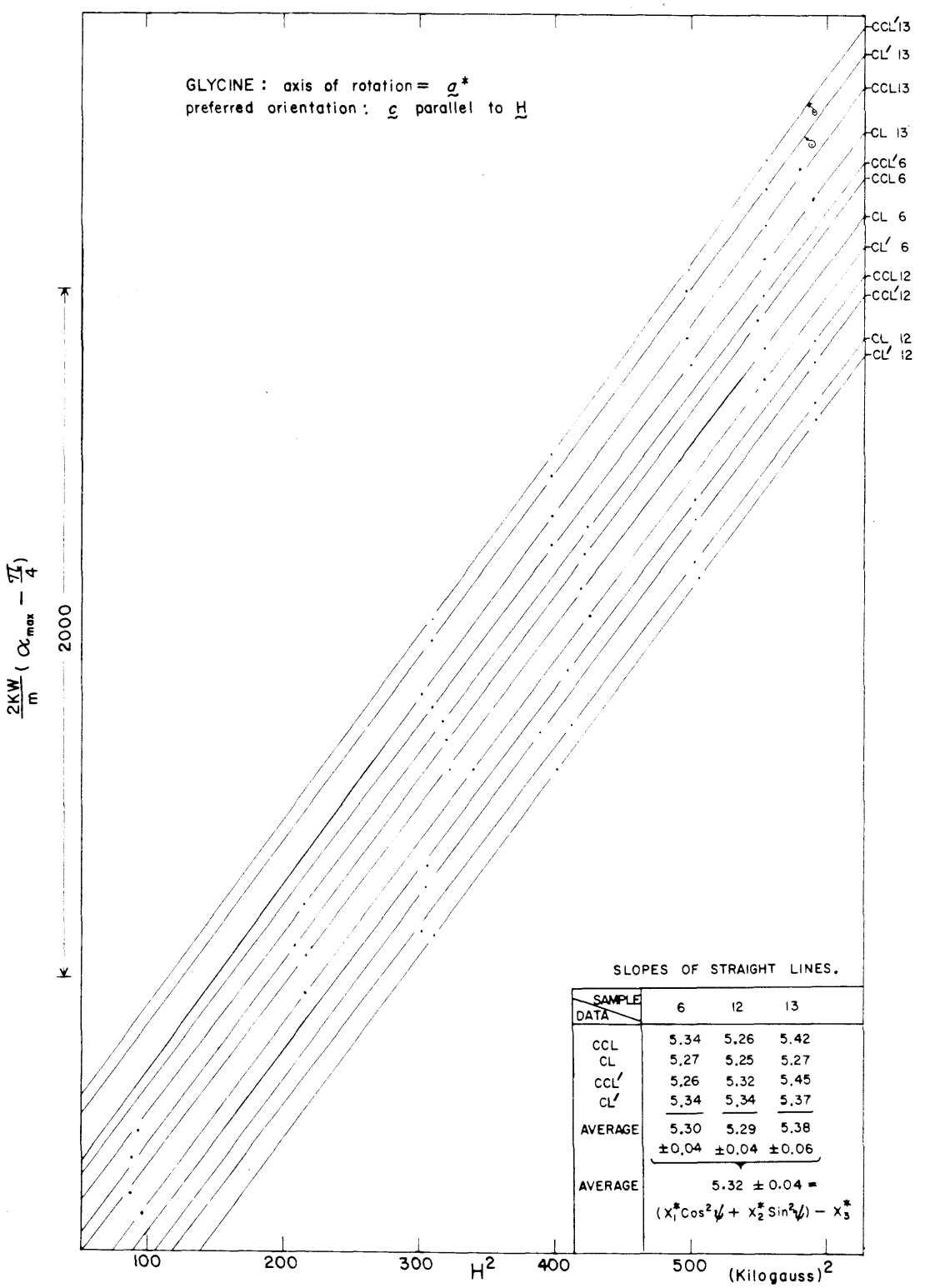

$\frac{2KW}{m}(\alpha_{max} - \frac{\pi}{4})$

SLOPES OF STRAIGHT LINES.

DATA \ SAMPLE	6	12	13
CCL	5.34	5.26	5.42
CL	5.27	5.25	5.27
CCL'	5.26	5.32	5.45
CL'	5.34	5.34	5.37
AVERAGE	5.30 ±0.04	5.29 ±0.04	5.38 ±0.06
AVERAGE	5.32 ± 0.04 = $(X_1^* \cos^2\psi + X_2^* \sin^2\psi) - X_3^*$		

FIGURE 21. MAGNETIC ANISOTROPY DATA FOR GLYCINE.

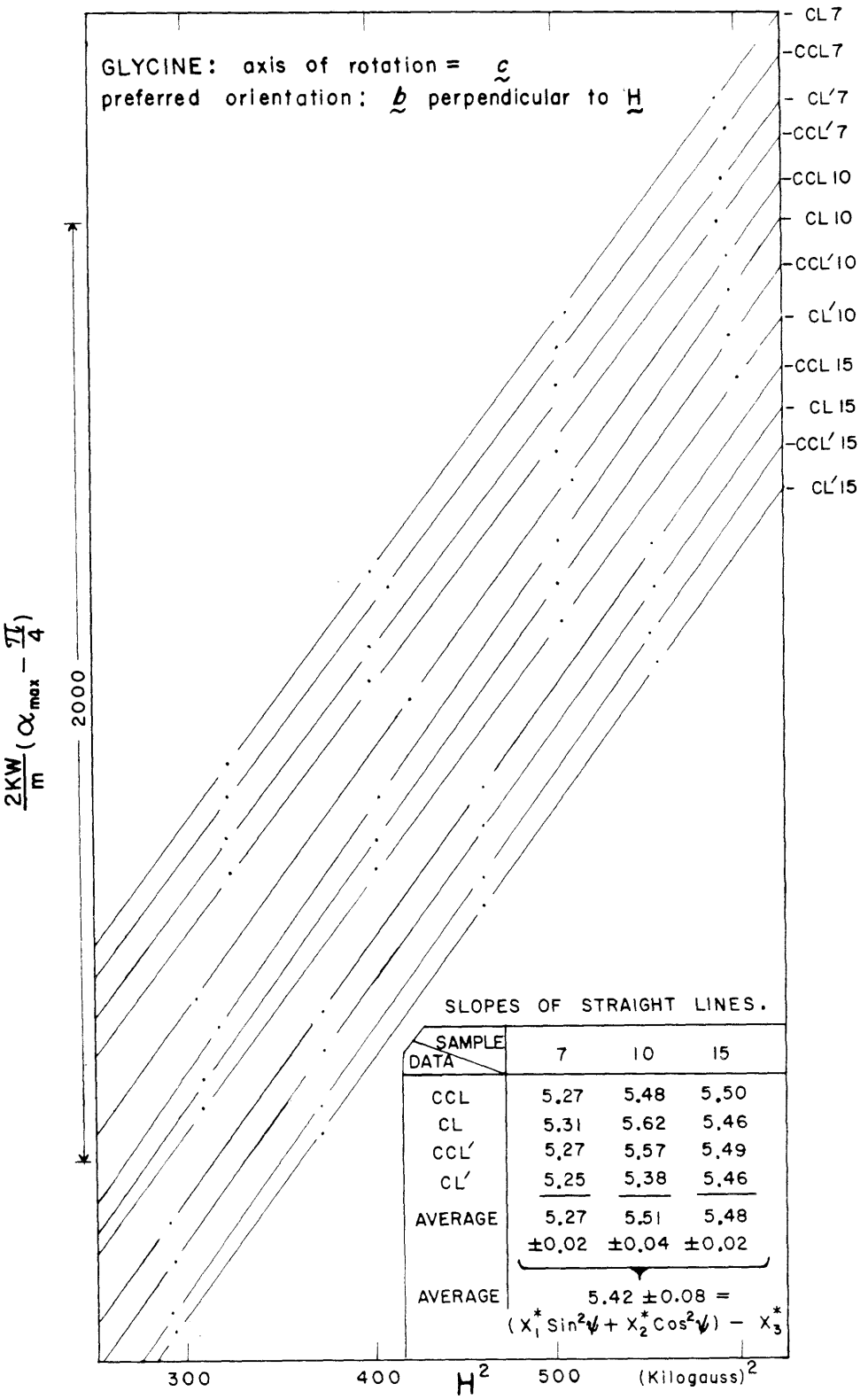

FIGURE 22. MAGNETIC ANISOTROPY DATA FOR GLYCINE.

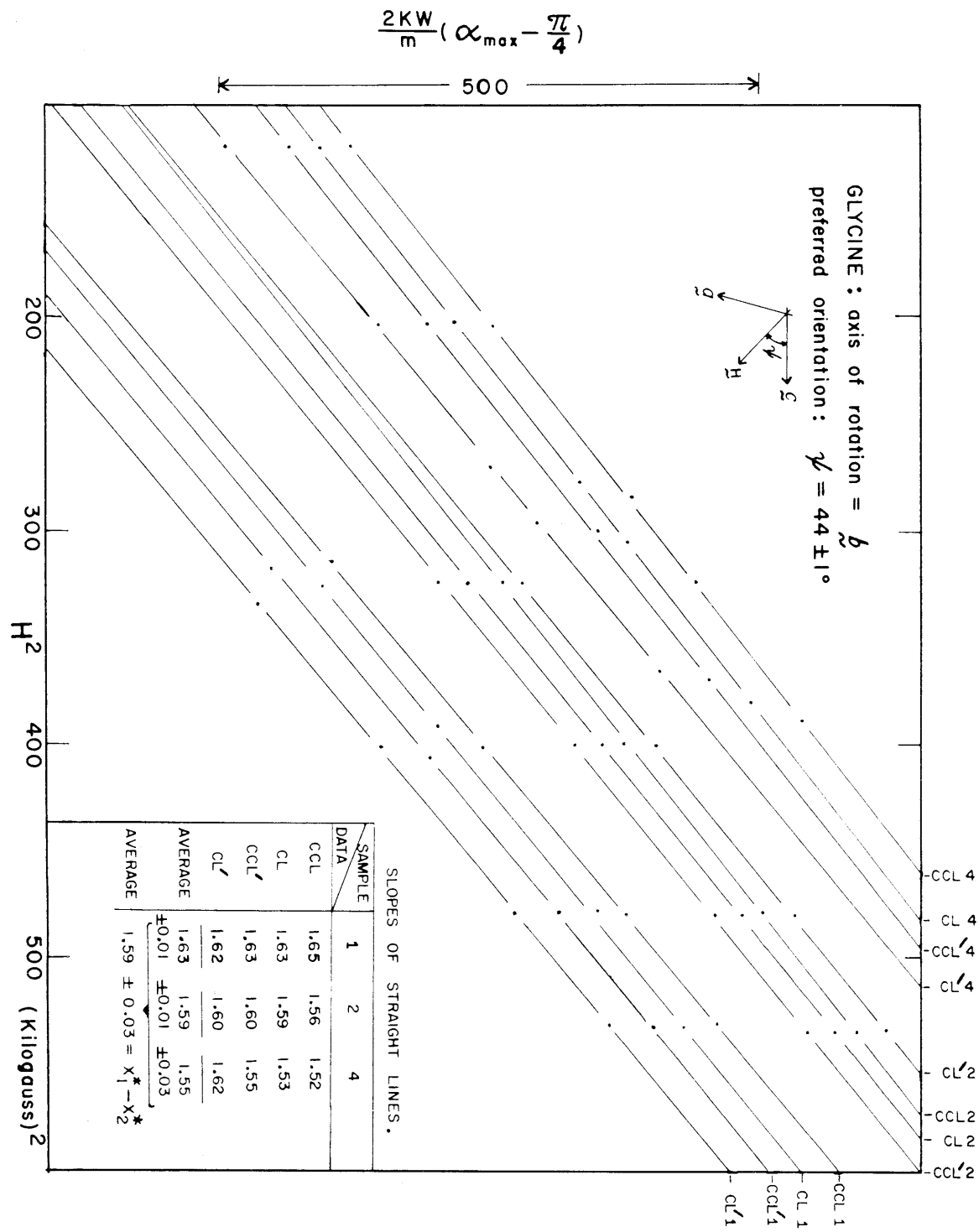

SLOPES OF STRAIGHT LINES.

DATA \ SAMPLE	1	2	4
CCL	1.65	1.56	1.52
CL	1.63	1.59	1.53
CCL'	1.63	1.60	1.55
CL'	1.62	1.60	1.62
AVERAGE	1.63 ±0.01	1.59 ±0.01	1.55 ±0.03

AVERAGE $1.59 \pm 0.03 = X_1^* - X_2^*$

FIGURE 23. MAGNETIC ANISOTROPY DATA FOR UREA.

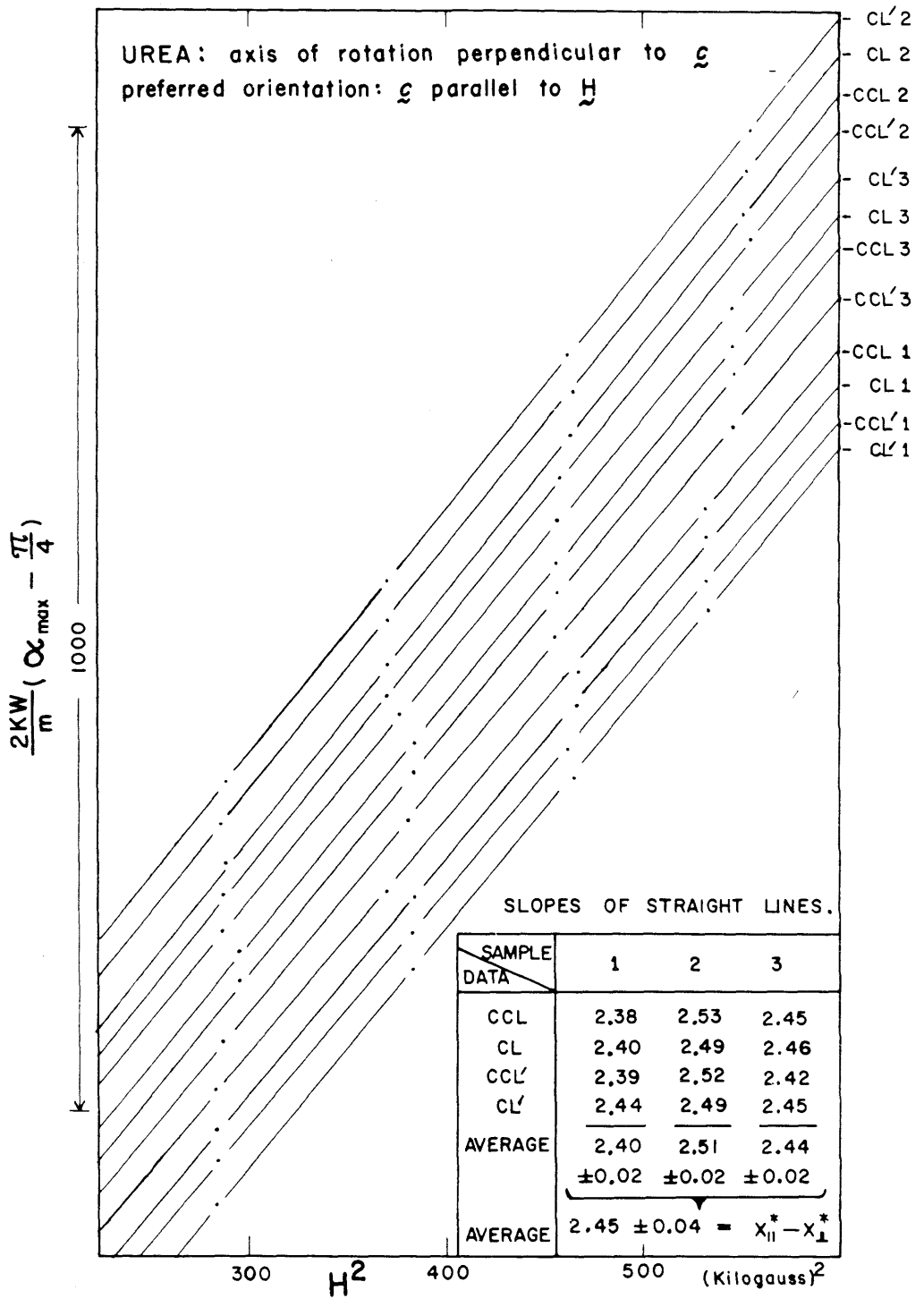

SLOPES OF STRAIGHT LINES.

SAMPLE / DATA	1	2	3
CCL	2.38	2.53	2.45
CL	2.40	2.49	2.46
CCL'	2.39	2.52	2.42
CL'	2.44	2.49	2.45
AVERAGE	2.40	2.51	2.44
	±0.02	±0.02	±0.02
AVERAGE	2.45 ±0.04 = $\chi_{\parallel}^{*} - \chi_{\perp}^{*}$		

FIG. 24 MAGNETIC ANISOTROPY DATA FOR MONOMETHYLUREA.

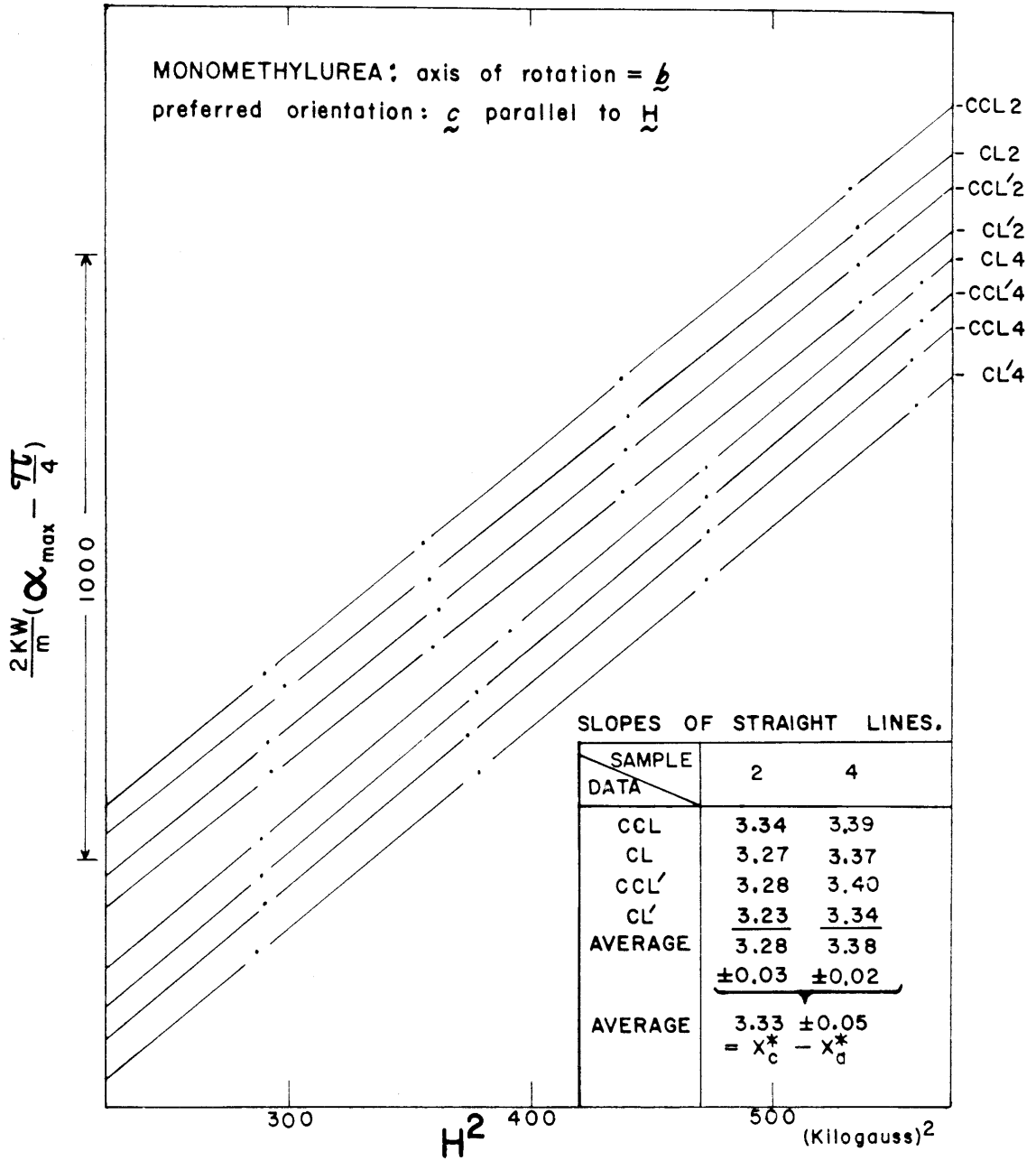

FIG. 25 MAGNETIC ANISOTROPY DATA FOR METHYLUREA.

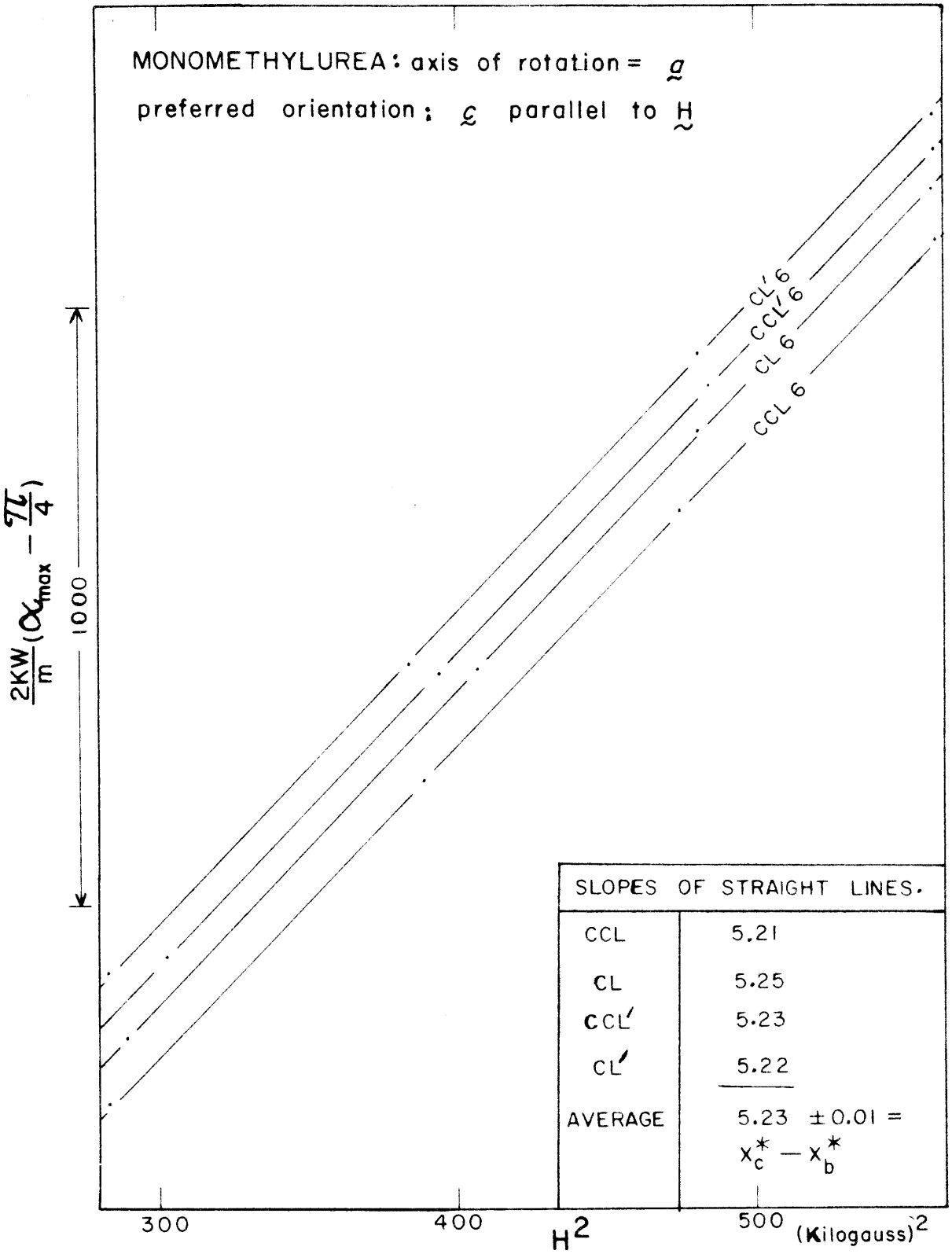

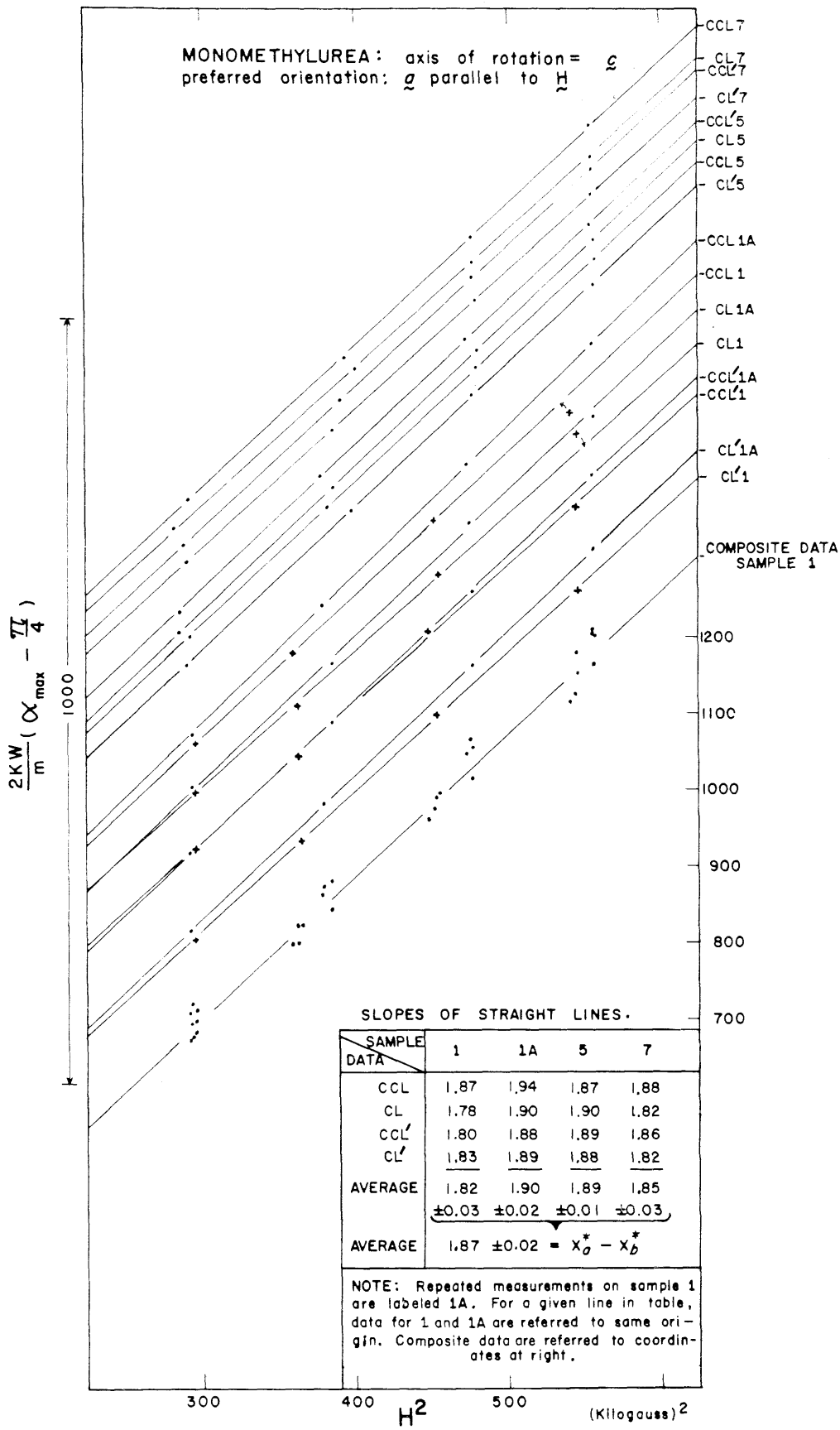

SLOPES OF STRAIGHT LINES.

SAMPLE / DATA	1	1A	5	7
CCL	1.87	1.94	1.87	1.88
CL	1.78	1.90	1.90	1.82
CCL'	1.80	1.88	1.89	1.86
CL'	1.83	1.89	1.88	1.82
AVERAGE	1.82	1.90	1.89	1.85
	±0.03	±0.02	±0.01	±0.03
AVERAGE	1.87 ±0.02 = $X_a^* - X_b^*$			

NOTE: Repeated measurements on sample 1 are labeled 1A. For a given line in table, data for 1 and 1A are referred to same origin. Composite data are referred to coordinates at right.

FIGURE 26. MAGNETIC ANISOTROPY DATA FOR MONOMETHYLUREA.

FIGURE 27. MAGNETIC ANISOTROPY DATA FOR THIOUREA.

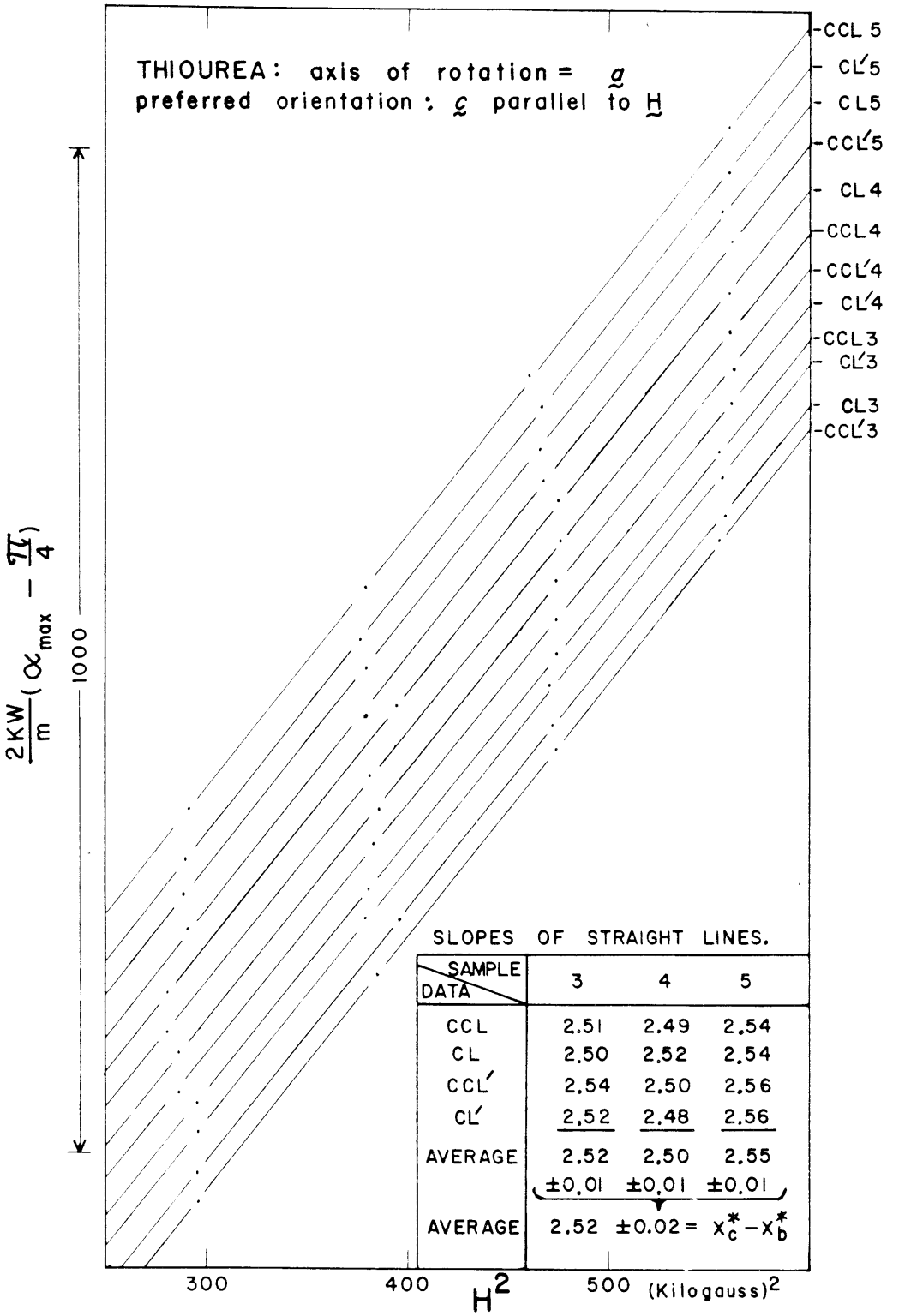

SLOPES OF STRAIGHT LINES.

SAMPLE / DATA	3	4	5
CCL	2.51	2.49	2.54
CL	2.50	2.52	2.54
CCL′	2.54	2.50	2.56
CL′	2.52	2.48	2.56
AVERAGE	2.52	2.50	2.55
	±0.01	±0.01	±0.01
AVERAGE	2.52 ±0.02 = $X_c^* - X_b^*$		

FIGURE 28. MAGNETIC ANISOTROPY DATA FOR THIOUREA.

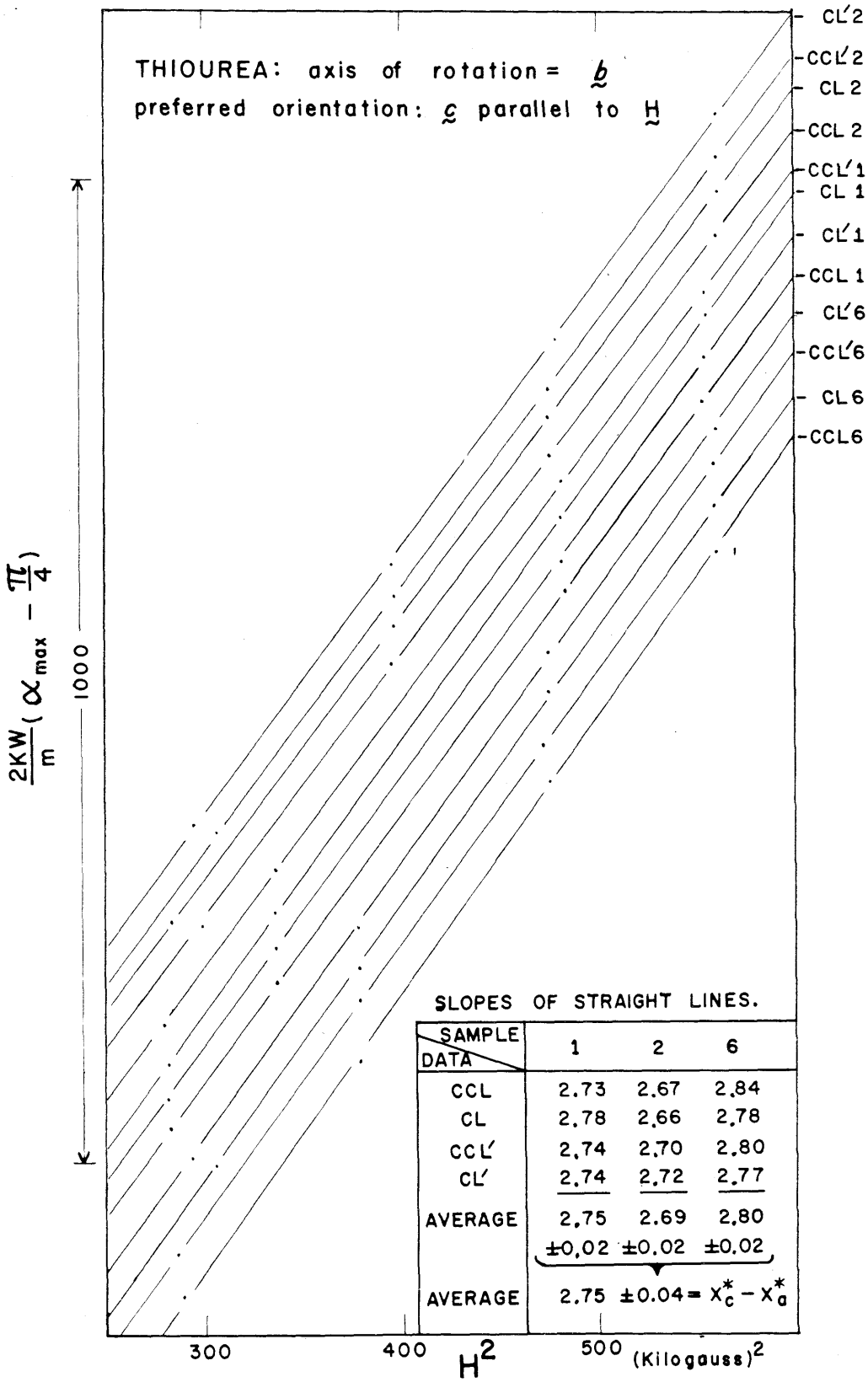

SLOPES OF STRAIGHT LINES.

SAMPLE / DATA	1	2	6
CCL	2.73	2.67	2.84
CL	2.78	2.66	2.78
CCL'	2.74	2.70	2.80
CL'	2.74	2.72	2.77
AVERAGE	2.75 ±0.02	2.69 ±0.02	2.80 ±0.02
AVERAGE	2.75 ±0.04 = $X_c^* - X_a^*$		

FIG. 29 MAGNETIC ANISOTROPY DATA FOR ANTHRACENE.

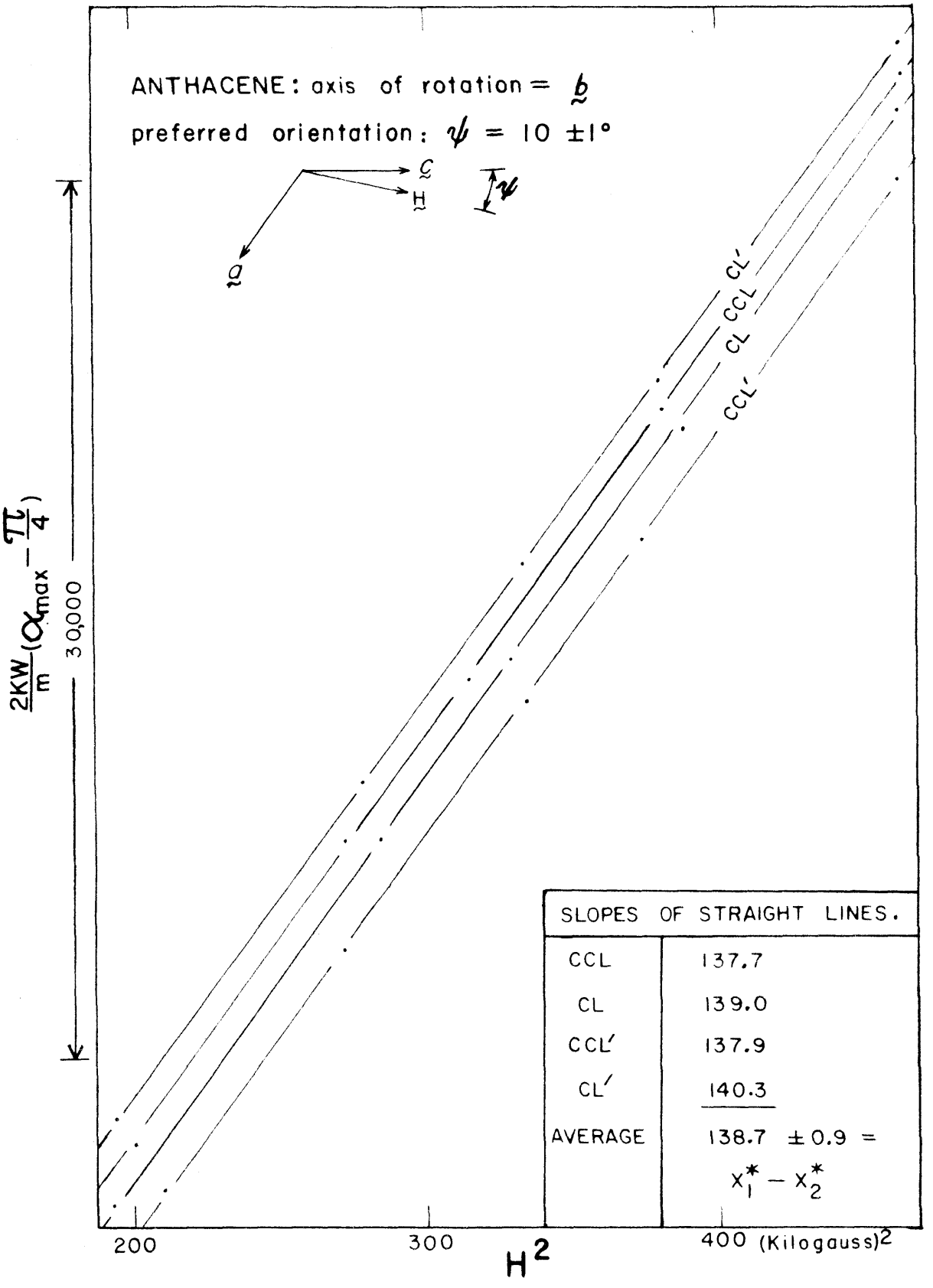

SLOPES OF STRAIGHT LINES.	
CCL	137.7
CL	139.0
CCL′	137.9
CL′	140.3
AVERAGE	138.7 ±0.9 = $X_1^* - X_2^*$

FIGURE 30.

MAGNETIC ANISOTROPY DATA FOR PROTEIN FIBERS.

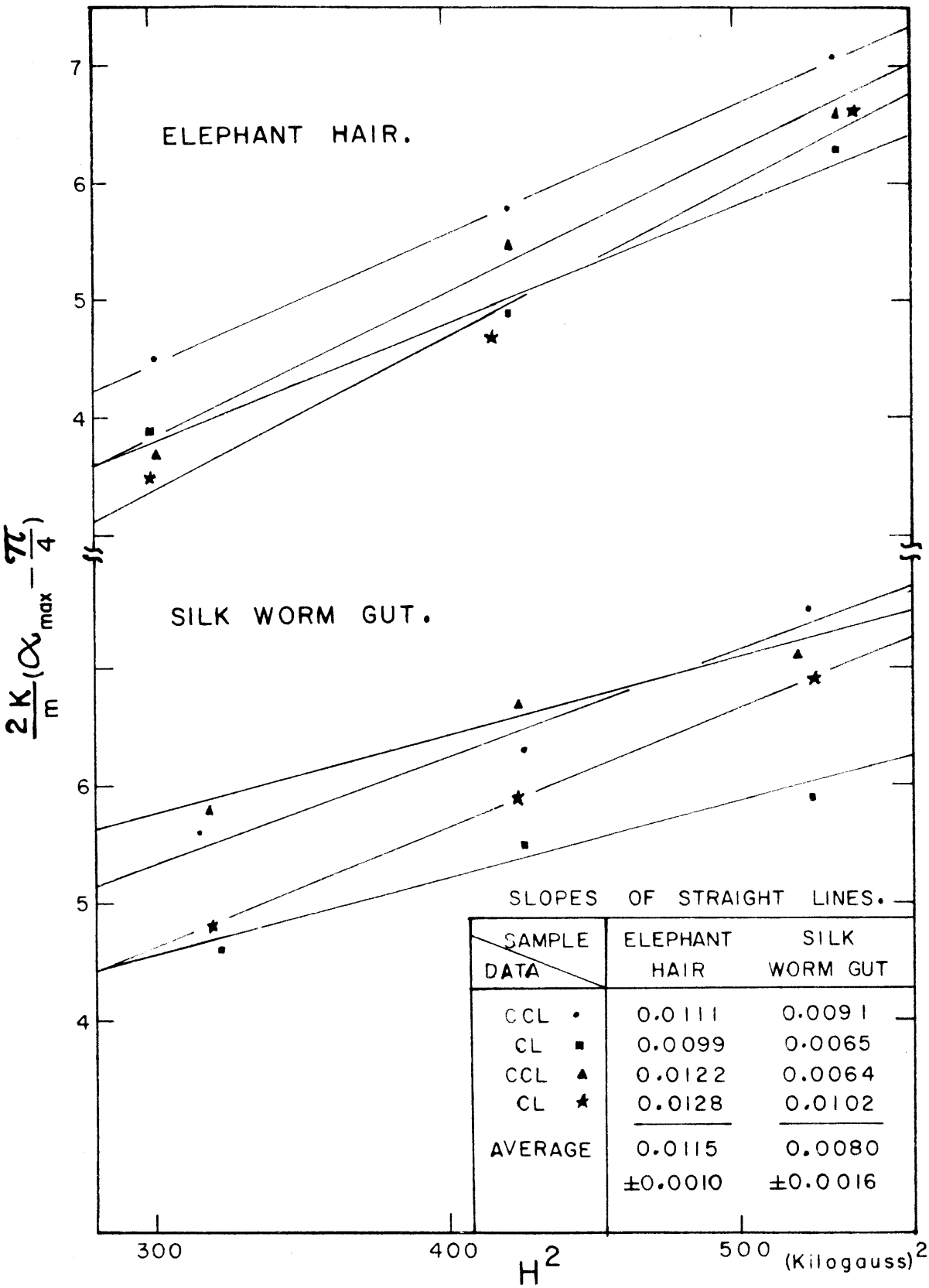

SLOPES OF STRAIGHT LINES.

SAMPLE / DATA	ELEPHANT HAIR	SILK WORM GUT
CCL •	0.0111	0.0091
CL ■	0.0099	0.0065
CCL ▲	0.0122	0.0064
CL ★	0.0128	0.0102
AVERAGE	0.0115	0.0080
	±0.0010	±0.0016

V. PROPOSITIONS.

(1) The equation $\nabla^2\psi + \left(\frac{2\pi}{\nu}\right)^2 F(\underset{\sim}{r})\,\psi = 0$, where $F(\underset{\sim}{r}) = \sum_{\substack{hk\ell \\ -\infty}}^{+\infty} A_{hk\ell}\,\mathrm{EXP}\left\{2\pi i(hx+ky+\ell z)\right\}$ is a triply periodic function of position, arises in the study of the propagation of waves in a crystal. The waves may be mechanical vibrations or electromagnetic disturbances, or may be of quantum-mechanical origin. The general solution is $\psi = \sum_{\substack{hk\ell \\ -\infty}}^{+\infty} C_{hk\ell}\,\mathrm{EXP}\left\{2\pi i\left[(h-\alpha)x+(k-\beta)y+(\ell-\gamma)z\right]\right\}$ where α,β and γ are arbitrary parameters. The coefficients $C_{hk\ell}$ may, in principle, be evaluated by substituting the solution into the differential equation to obtain a system of infinitely-many linear homogeneous simultaneous equations. For the one-dimensional case, the system of equations is $\sum_{h\ -\infty}^{+\infty}\left\{\delta_{h,m} - \frac{\nu^2 C_{m-h}}{(m-\alpha)^2}\right\} A_h = 0 \Big|_{m=0,\ \pm 1,\ldots}$ In order to solve this system of equations, it is necessary that the values of ν and α be such that the determinant of the system of equations is zero. For the three-dimensional case the indices m, h and m-h are each replaced by a set of three indices; nevertheless, it is proposed that the treatment of the three-dimensional case is not more difficult than for the one-dimensional case.

(2) For a chemical reaction involving a gain or loss of heat energy, Einstein's equation, $\Delta E = \Delta m C^2$, predicts that the mass of the products should be slightly different from that of the reactants. It is proposed that this may be verified experimentally by a practical method.

(3) Great difficulty is often encountered in trying to locate the crystallographic axes of an irregular crystal fragment by use of the Laue camera. In principle, one must take Laue photographs parallel to a great many directions until an axis is come upon by

accident. It is proposed that the amount of work involved may be greatly reduced by an alternate method using equipment presently available in the X-ray laboratory.

(4) Ferromagnetic impurities cause a small error in measurements of the average susceptibilities of diamagnetic substances made by the Gouy method. It is proposed that this error can be eliminated by the use of a specially designed magnet and a modification in the experimental procedure similar to the modification made in Part I of this thesis for the elimination of the analogous error in measurements of diamagnetic anisotropy.

(5) Anisotropic crystals give, as is well known, optical interference patterns of a special kind when observed in convergen polarized light. These patterns are sharpest when observed in monochromatic light; in white light, they are blurred and indistinct. If one wanted to study the change in the location of the optic axes with changing wave-lengths of light, or merely wanted to see how nice the patterns look in color, a light source having several fairly sharply defined wave lengths of about equal intensity could be used. It is proposed that a very simple light source of this type is readily available.

(6) It is proposed that the value of the magnetic susceptibility of methane recorded in the International Critical Tables[1] is too high by a factor of 3.

(7) Pencil notations on X-ray photographic films remain after the films have been developed and fixed. It has been suggested that the pressure of the pencil point "exposes" the silver emulsion. This is incorrect.

(8) An anisotropic diamagnetic molecule in a liquid or gas should tend to orient itself in a magnetic field with the direction of minimum diamagnetism parallel to the field. Collisions with other molecules would oppose the tendency to orient. Hence, a liquid or

gas containing anisotropic diamagnetic molecules should have an average susceptibility which is slightly dependent both on field strength and on temperature. It is proposed that the following equation describes the dependence to good approximation:

$$\overline{X}^*(T,H) = \overline{X}^*_o + \frac{2H^2}{45RT}\left[X_1^{*2}+X_2^{*2}+X_3^{*2} - X_1^*X_2^* - X_1^*X_3^* - X_2^*X_3^*\right] .$$

(9) A qualitative discussion of ionic conductances involving an idealized conductance cell divided into a number of compartments can be found in many texts on Physical Chemistry. When the migration of the ions in the idealized cell is treated quantitatively, a useful mathematical relation between concentrations, velocities of ions and the current conducted by the electrolyte is obtained.

(10) In organic preparations, it is occasionally necessary to carry out a distillation of a two-phase liquid for the purpose of separating only one phase, the second phase being returned to the kettle. A compact distillation-head with small liquid hold-up which would automatically separate the phases without the attention of an operator and without moving parts would be convenient for large scale preparations. It is proposed that such a distillation-head may be constructed which, in addition, will separate liquids, such as sec-butyl alcohol and water, which are fairly miscible when hot.**

REFERENCES.

(1) International Critical Tables, McGraw-Hill Book Co. Inc., New York (1929), volume 6, pages 354-64.

**It was pointed out by a member of the examining committee, Dr.E.R. Buchman, that the principle involved had already been employed in an apparatus described by H.T.Clarke, J.A.C.S. (1921),43,366-70.